

Determination of LTPP Properties of Asphalt Materials on Concrete Bridges and in Pavements

by

Manfred N. Partl

Adj. Prof. Carleton, Ottawa,CN

Swiss Federal Laboratories for Materials Testing and Research,
EMPA Center Road Engineering/Sealing Components
Dübendorf, www.empa.ch/Abt113

COE Intensive Course, 17 Feb 2005
Graduate School of Engineering, Hokkaido University

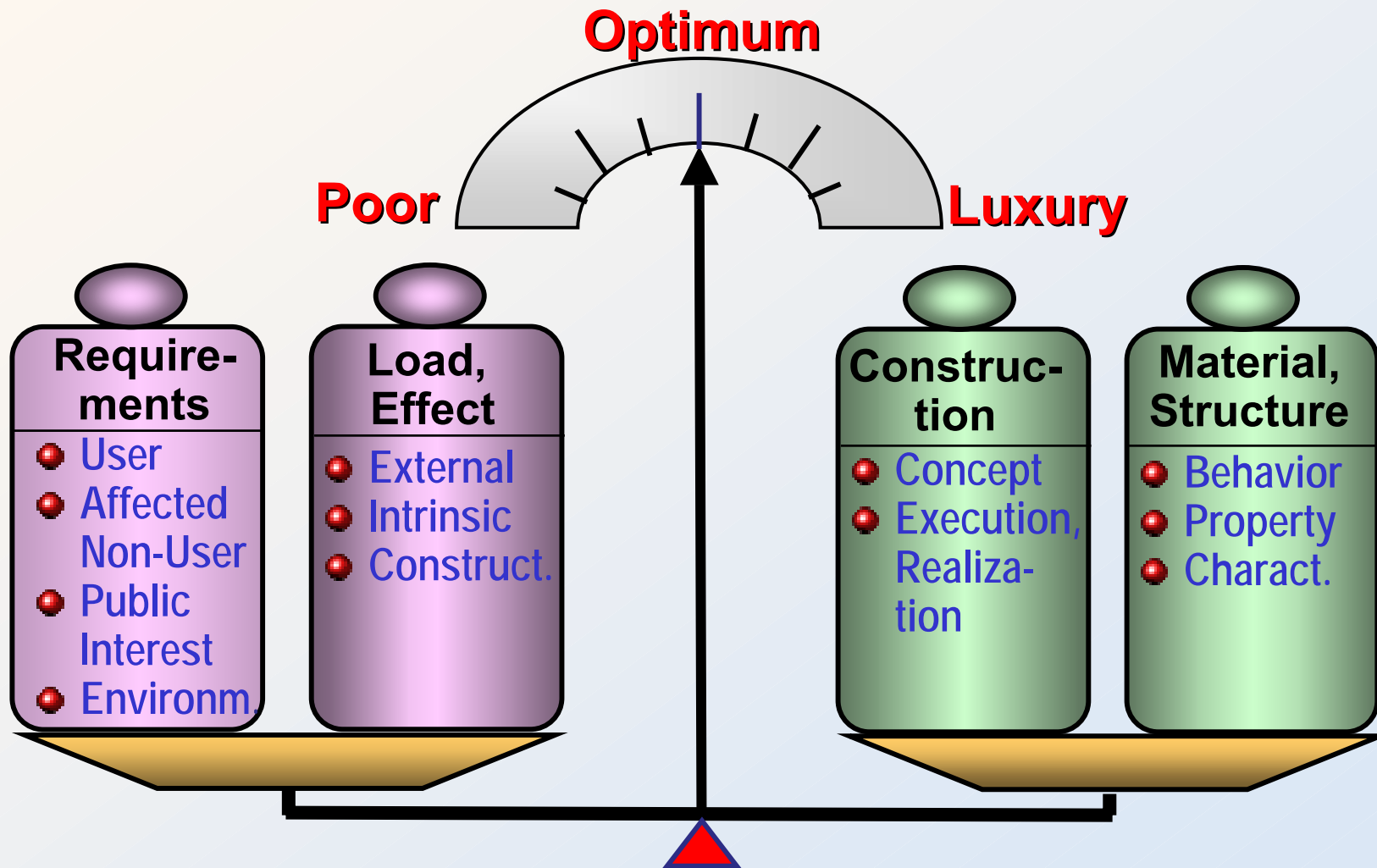


Content

- Introduction
- Compaction
 - Field compaction
 - Lab compaction of test specimens
- Aging and durability
 - Binder-Polymers
 - Artificial Aging
- Water susceptibility evaluation of Mixes
- Inlayer and interlayer bond
- Accelerated pavement testing APT
- Asphaltic plug joints for large movements
- Joints

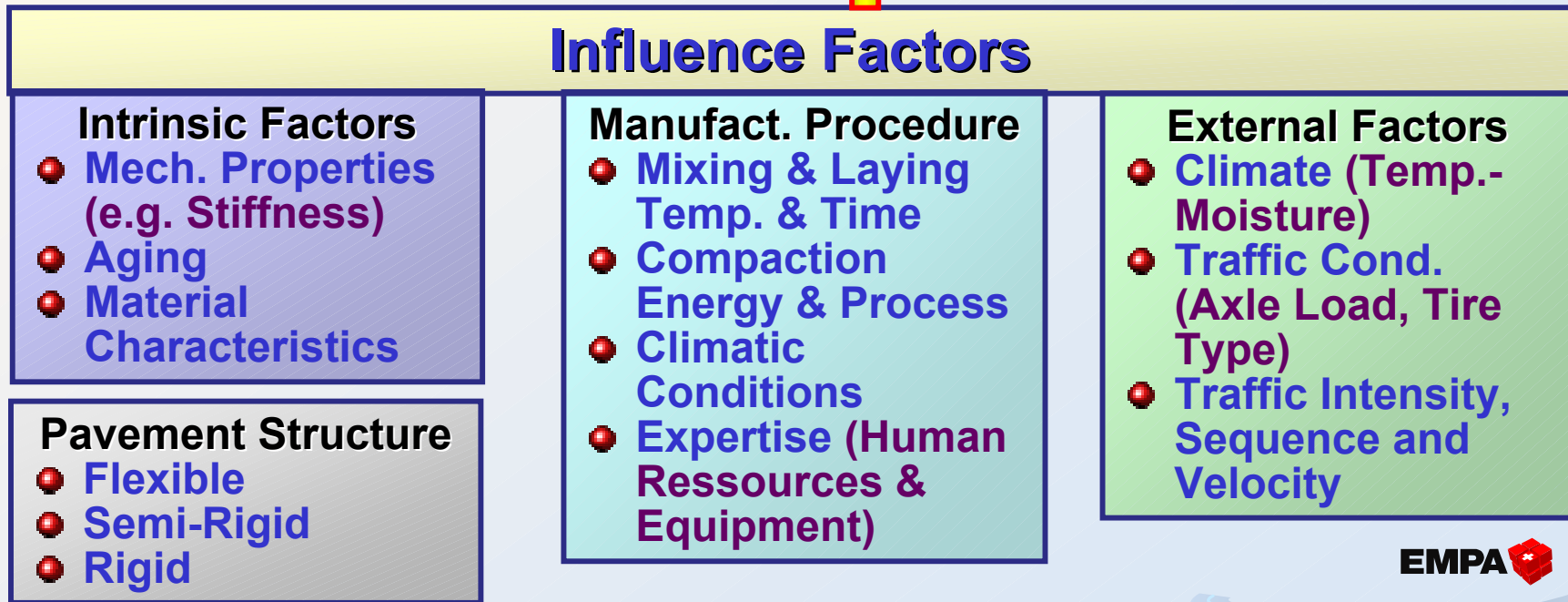
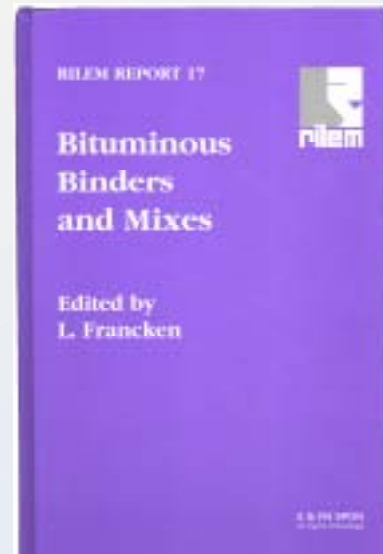
Introduction

Optimization Scale



Pav. Perform. Mechanisms

Part I et Francken in RILEM Report 17 (1998), ISBN 0 419 22870 5



Types of Distress (1)

● Cracks

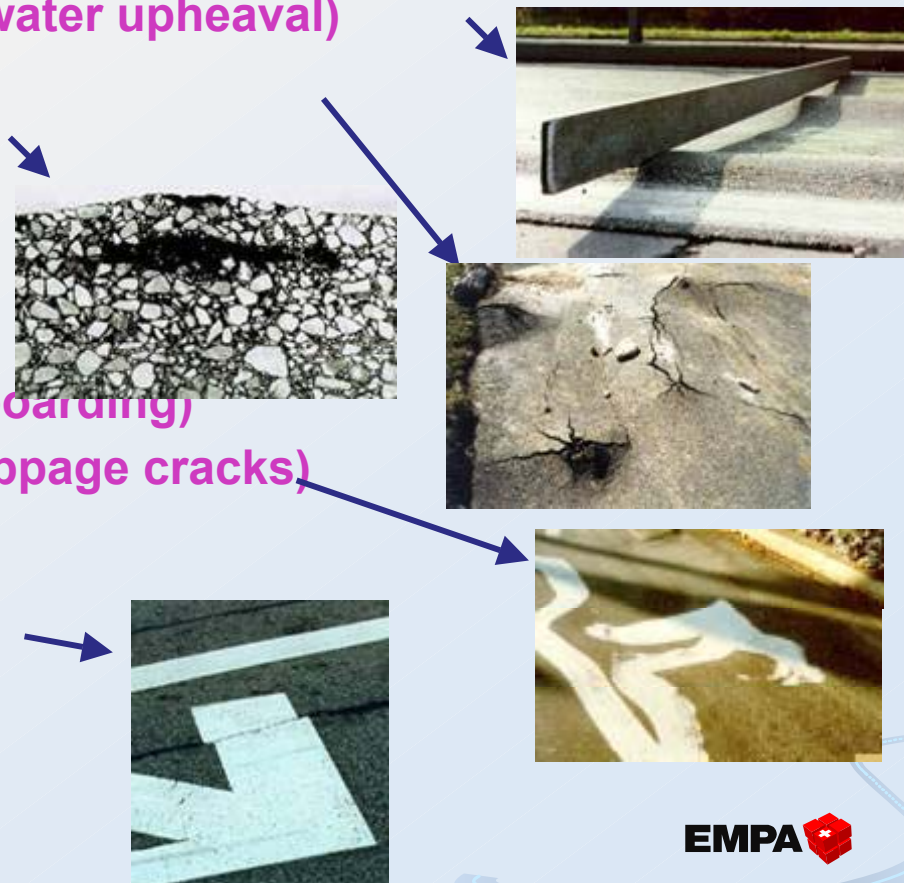
- Temperature Induced
 - Temp. cycles (fatigue)
 - Extreme cooling (thermal contract.)
- Compaction and construction induced
 - Surface cracks (compactor)
 - Longitudinal cracks (paver)
 - Delamination & interlayer de-bonding
- Traffic induced (fatigue)
 - Top-Down (e.g. from tire-surface interaction)
 - Bottom-Up (e.g reflective cracking)
- Consolidation & sliding
 - Transverse border cracks
 - Longitudinal border cracks
 - Kerbstone cracking



Types of Distress (2)

● Permanent Deformation

- Vertical layer deformation (material problem, traffic induced)
- Structural vertical deformation (design problem)
 - Traffic induced ruts (poor fundation, consolidation)
 - Climate induced (frost & water upheaval)
 - In & Inter-layer Blisters
- Compaction induced (unevenness)
- Shear
 - in layer (shoving & washboarding)
 - Inter-layer (can lead to slippage cracks)
 - longitudinal/transversal



Types of Distress (3)

● Material Desintegration

- Material incompatibility (stripping, bad additives)
- Leaching



HRA



Mastic

● Surface Defects

- Raveling, loss of aggregates →
- Polishing
- Wear (ruts, e.g. studded tires)
- Aging of binder (hardening or softening) →
- Bleeding and pumping
- Catastrophy (e.g. Fire) →
- Blisters →

SMA
Airfield

St.Gotthard 2001



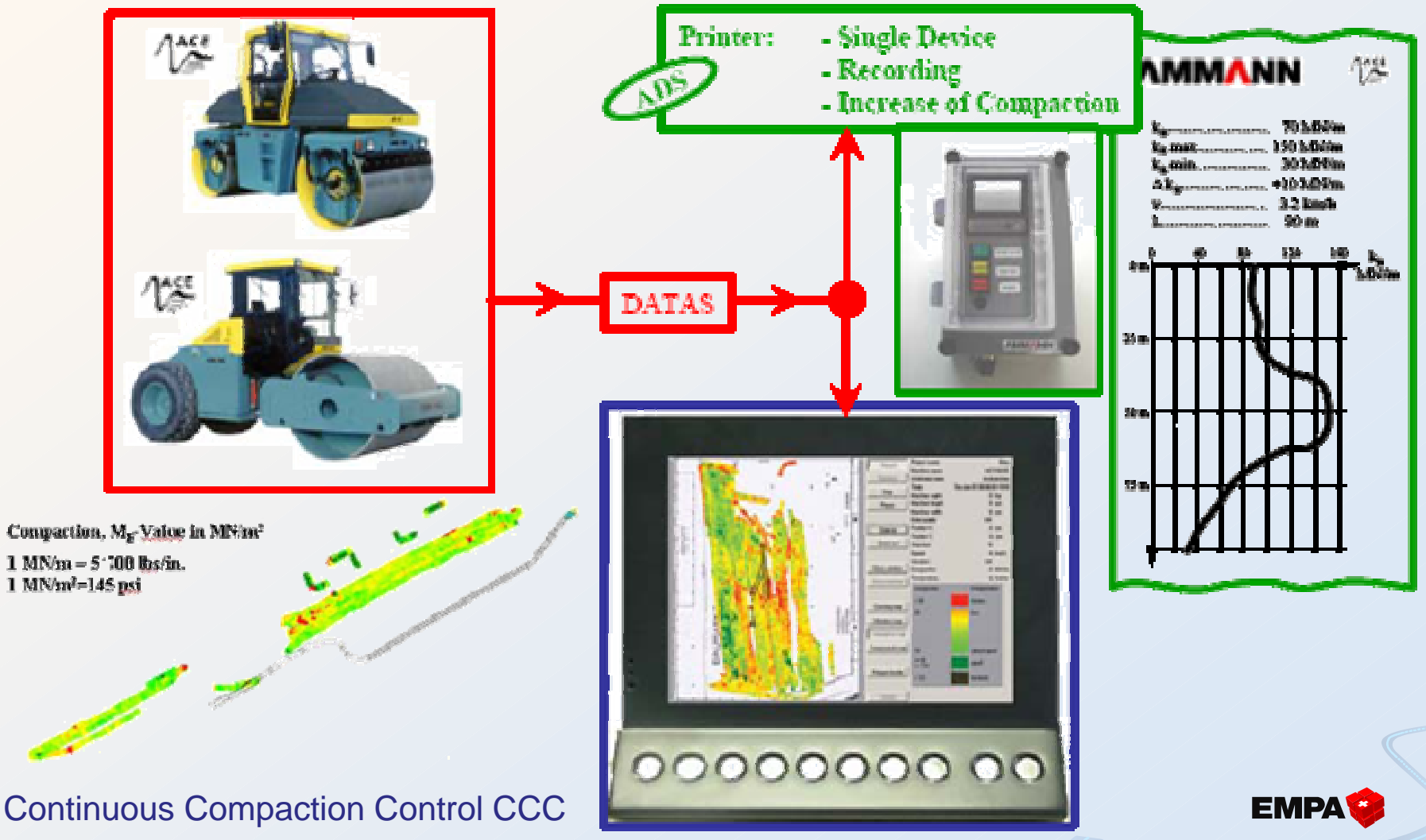
EMPA

Compaction

Field Compaction

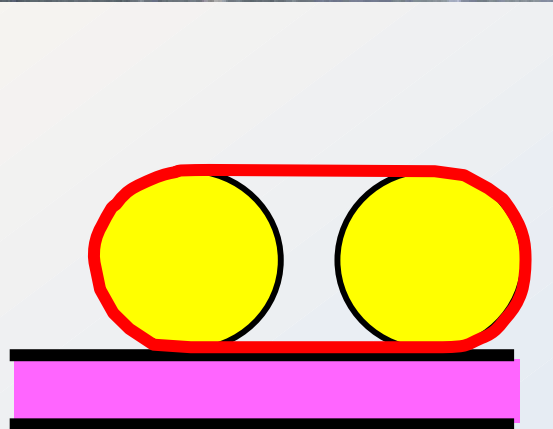
New Developments

- Intelligent Compaction (e.g. ACE Ammann Compaction Expert)



Surface Cracks due to Compaction

A. O. Abd El Halim, Carleton University, Ottawa, CN

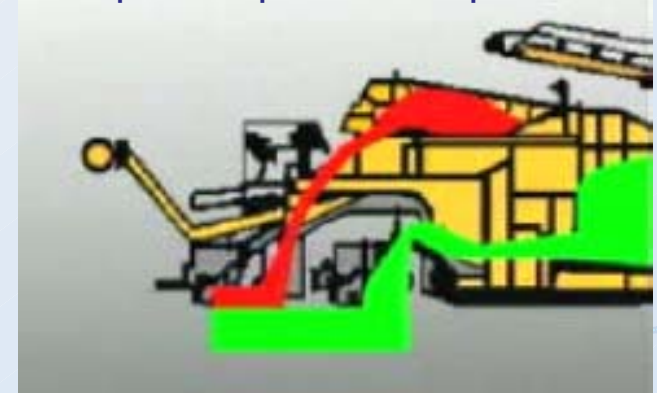


Compaction Main Issues

- Examine & Review **compact. mechanisms**; with steel roller drums higher risk of **crack initiation at surface**; consider alternatives → 
- Pay more attention to **construction** not only on mix design
- Any special problems when compacting **cold or warm** mixes?
- Use **computer** controlled technologies (e.g. cont. comp. control)
- How to compact **as deep as** possible without crushing the surface and the aggregates?
- Face new compaction challenges, like **compact asphalt** pavements hot/hot Germany



Compact Asphalt Principle

**EMPA**

Lab Compaction of Test Specimens

Compaction Devices

M. Jönsson, M.N. Partl



Marshall
Hammer

Gyratory
Comp.



LCPC
Rolling
Wheel
Comp.



Compaction Methods

M. Jönsson, M.N. Partl

- Changes in homogeneity and isotropy in AB11S asphalt concrete specimens during compaction with Marshall-, Gyratory- and LCPC Rolling-Wheel-Compactor
- Tools: Standard air-void content determination (AV) and X-ray computer tomography (CT).

Compaction Method @ 145C	Compaction Level					Compaction Counter	Type of Investigation	
	Initial	Slight	Medium	Strong	Final		AV	CT
Marshall	5	-	20	-	50	Double Blows	X	X
Gyratory #1	0	5	20	50	200	Gyratory Cycles	X	X
Gyratory #2		-	20	-	200	Gyratory Cycles	-	X
Rolling-Wheel	0-0-0	-	8-4-8	-	32-16-32	Wheel Passes	X	X

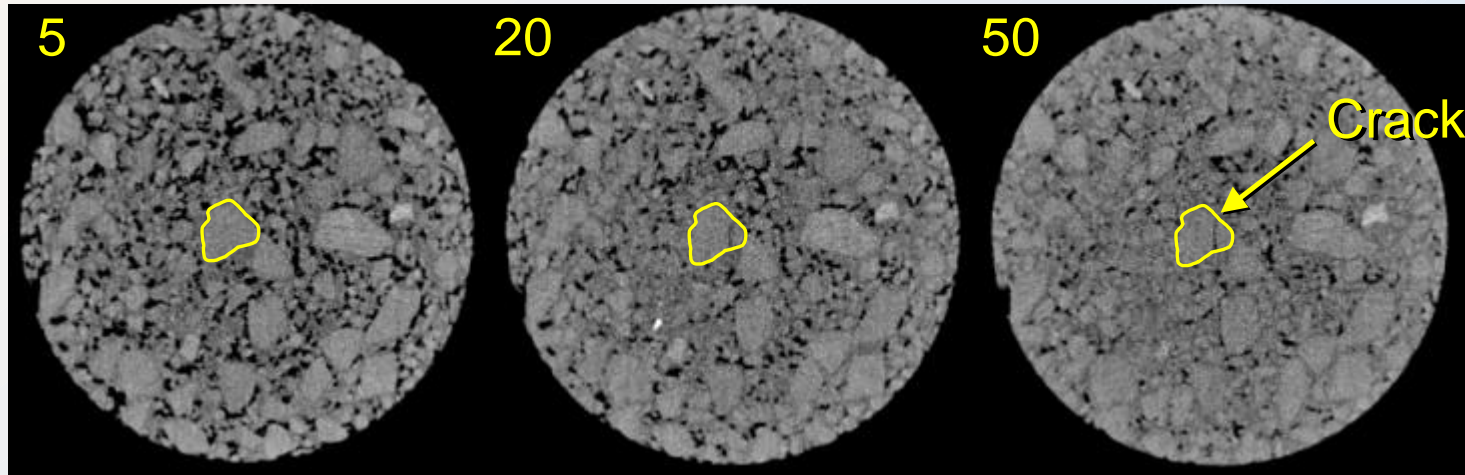
Gyratory #2: three planes

X-Ray CT: Marshall @58% Height

M. Jönsson, A. Flisch, M.N. Partl

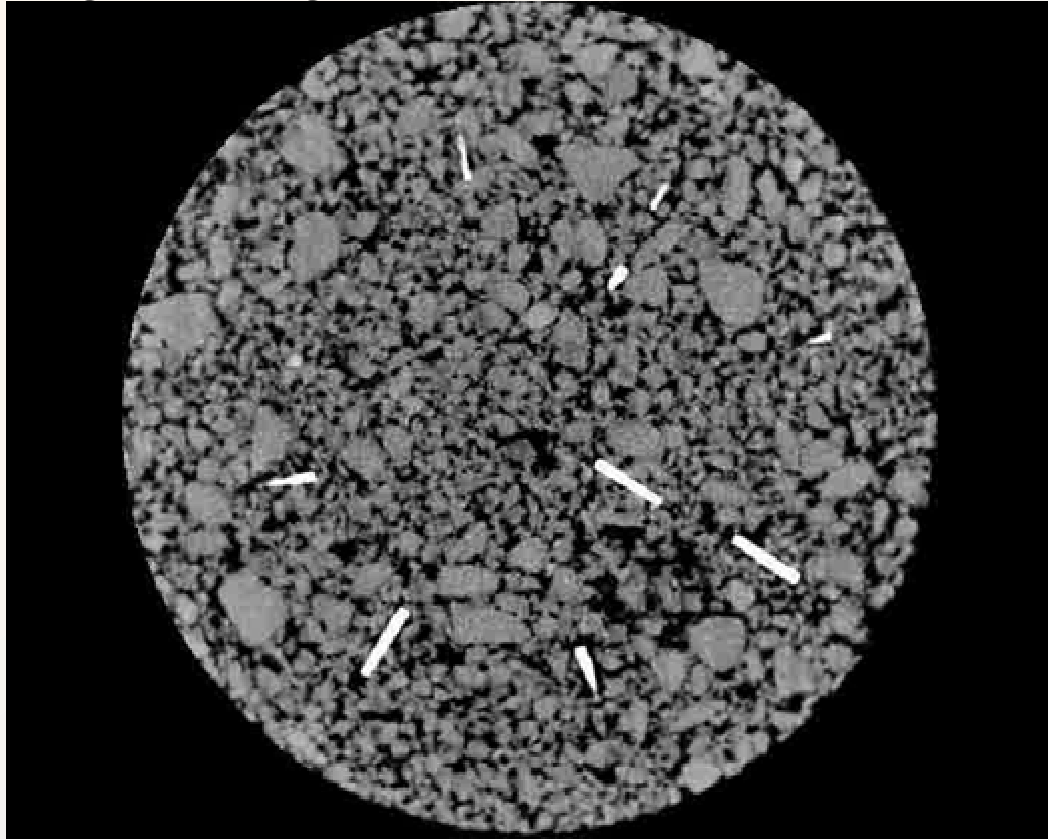


- Amount of pores is reducing during compaction.
- The large outlined aggregate suffered a major crack between 5 and 20 blows.

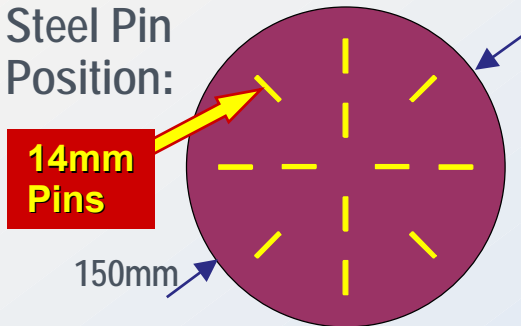


Gyratory Compaction: Pin Movement

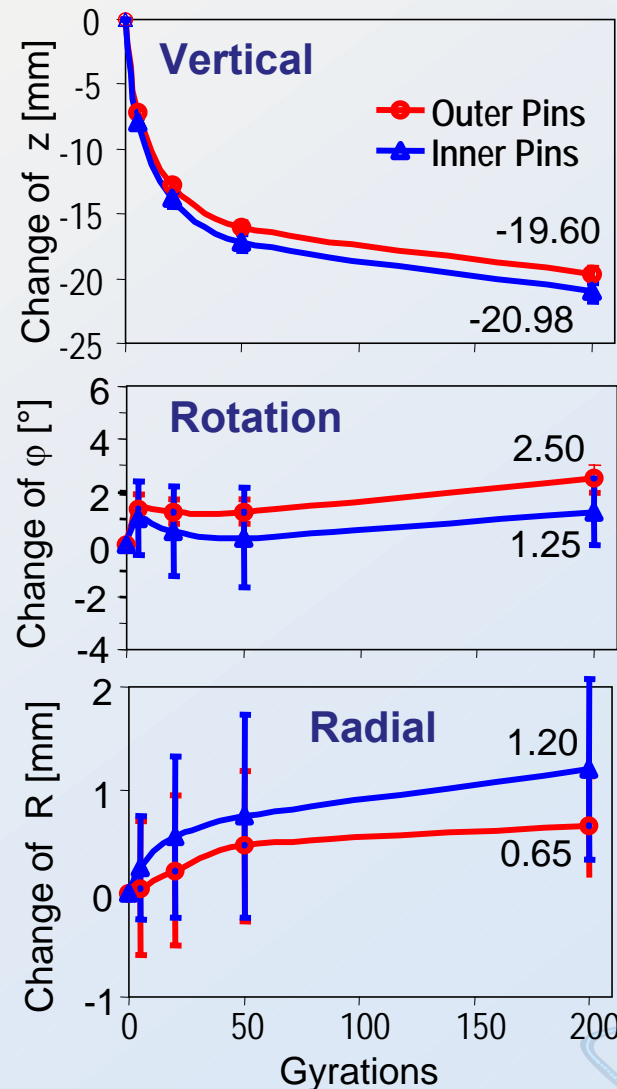
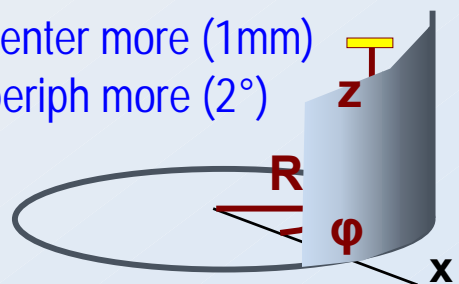
M. Jönsson, A. Flisch,
M.N. Partl



Steel Pin
Position:

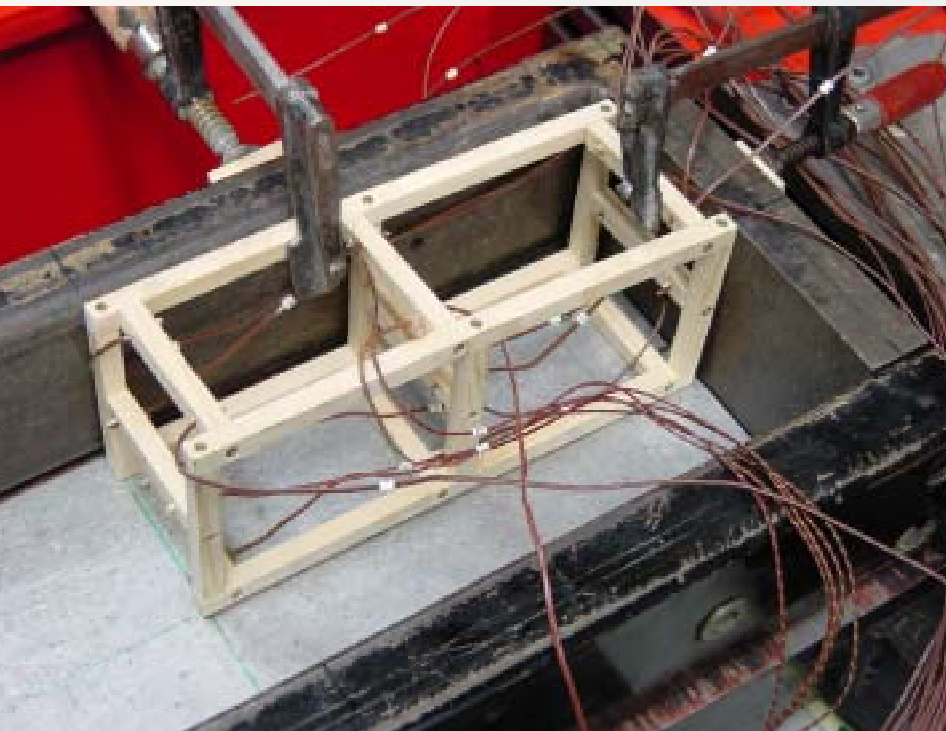
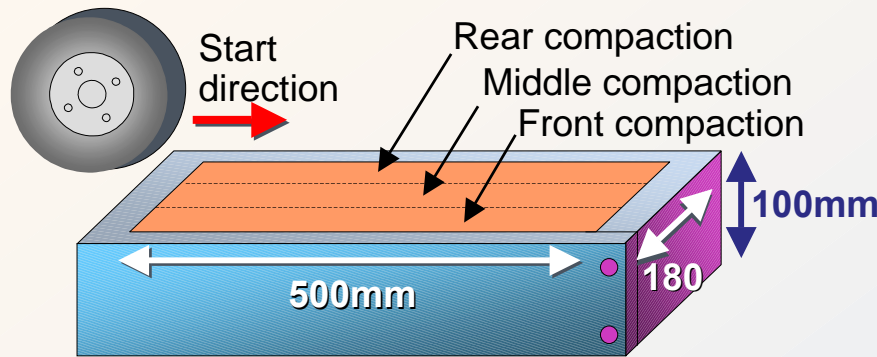


- z: center moves 1mm more
- R: center more (1mm)
- φ: periph more (2°)



Tire Roller-Compactor

K. Sokolov, P. Kumar



Measuring of Temperature Flow
During Compaction Process

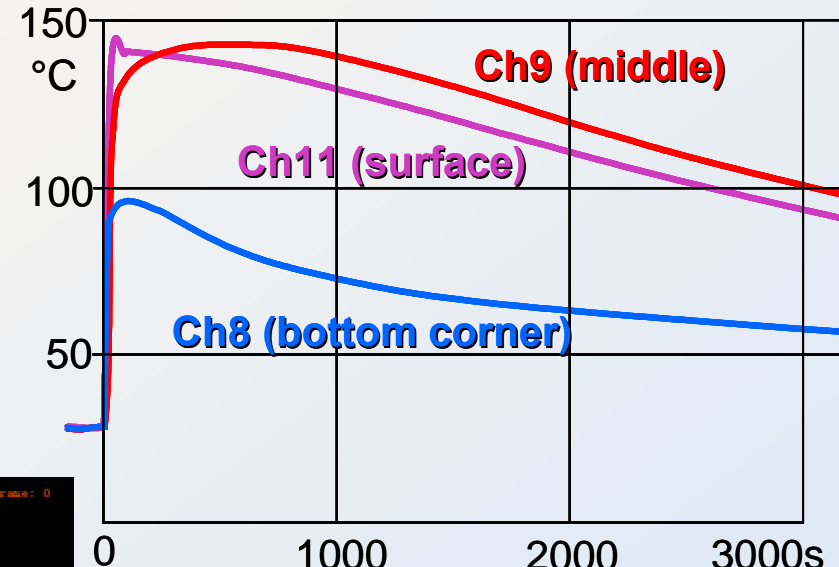
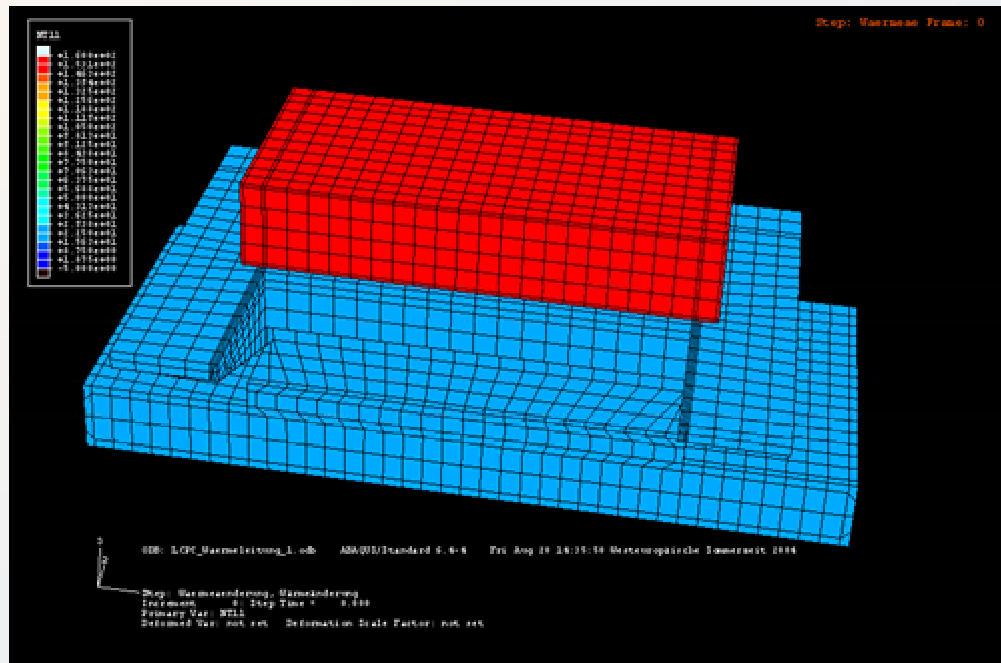
Tire Roller-Compactor

K. Sokolov, P. Kumar

Measurements (cold Mould) →

ABAQUS FE-Model of Heat Dissipation during Compaction

Thermal Conductivity Asphalt $\kappa=0.062$ W/m.K
Total time: 1000s

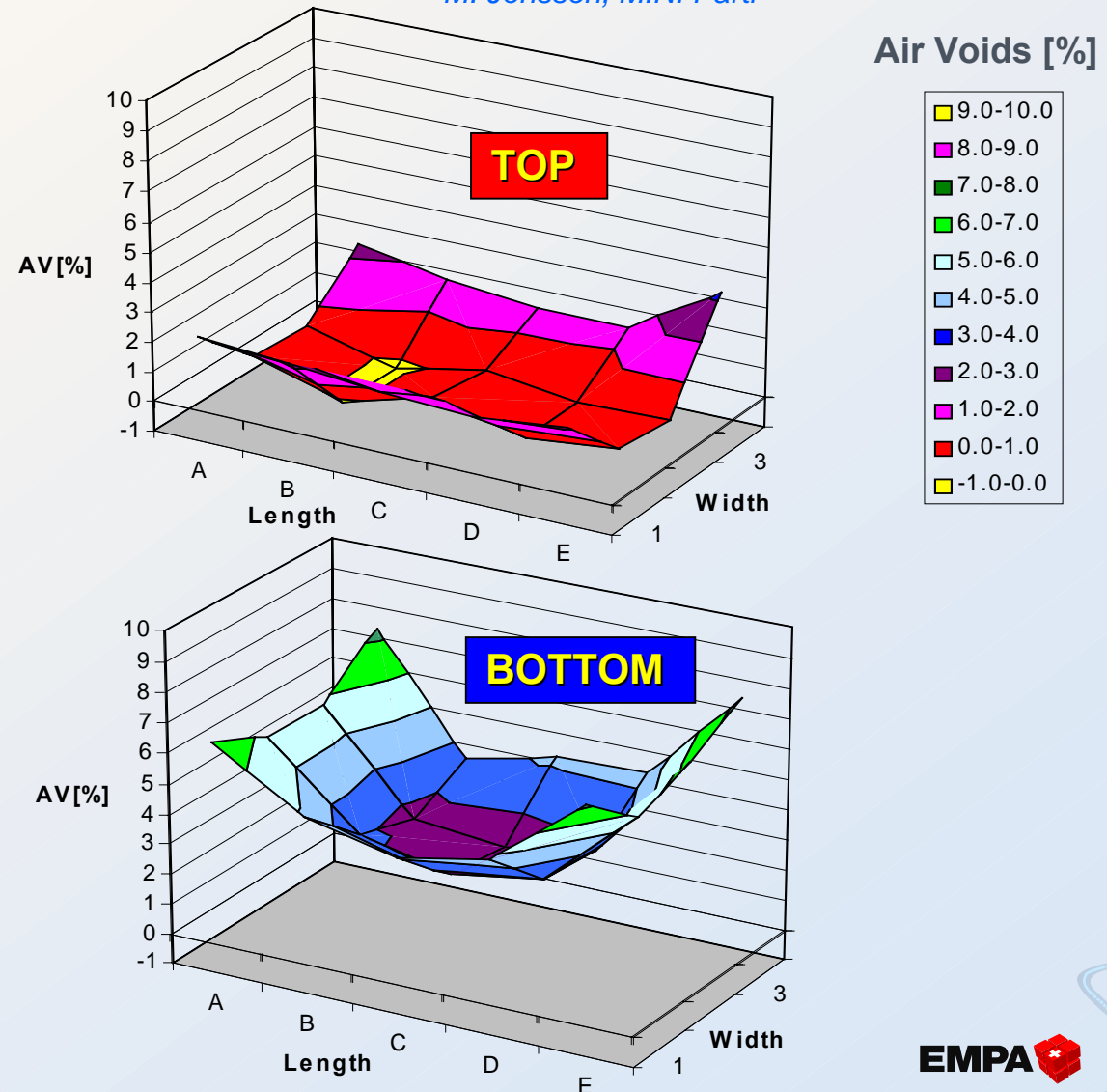
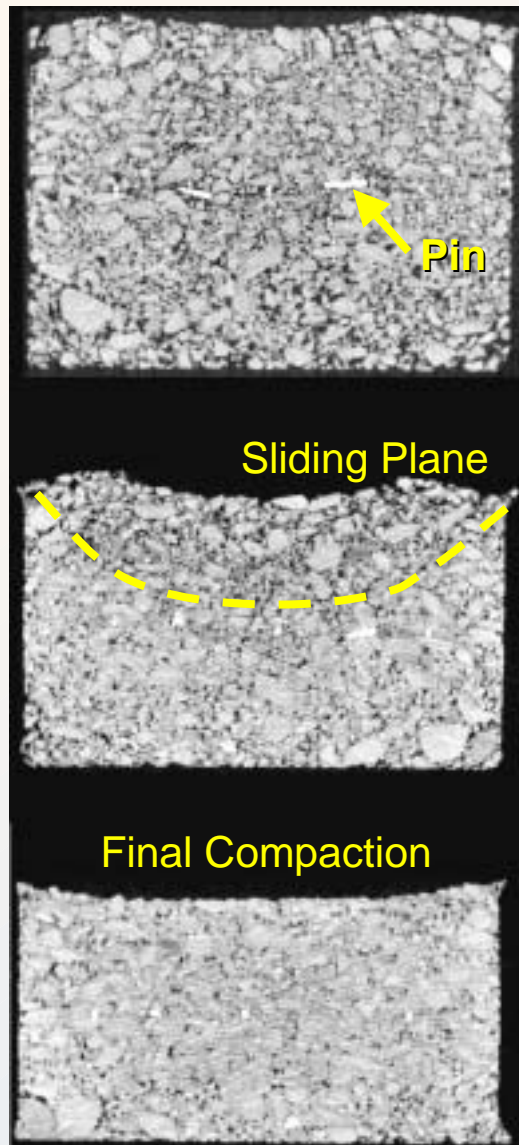


During Compaction:

- Specimen cools on surface (from side) $150 \rightarrow 125^\circ\text{C}$
- Mould cools down (bottom up) $150 \rightarrow 70^\circ\text{C}$
- Heat dissipates into base $25 \rightarrow 50^\circ\text{C}$

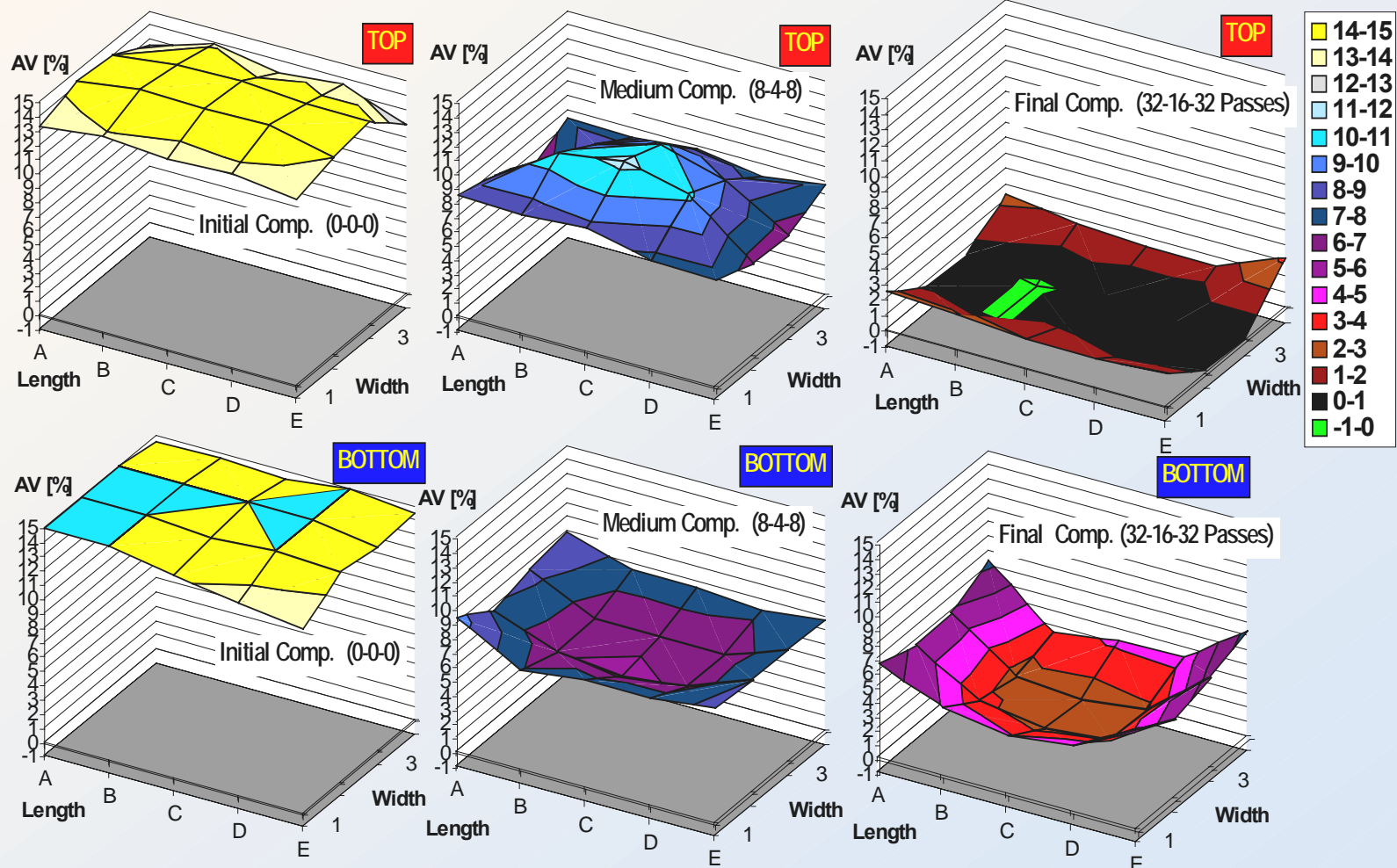
Tire Roller Compactor

M. Jönsson, M.N. Partl



Tire Roller Compactor

Air Voids

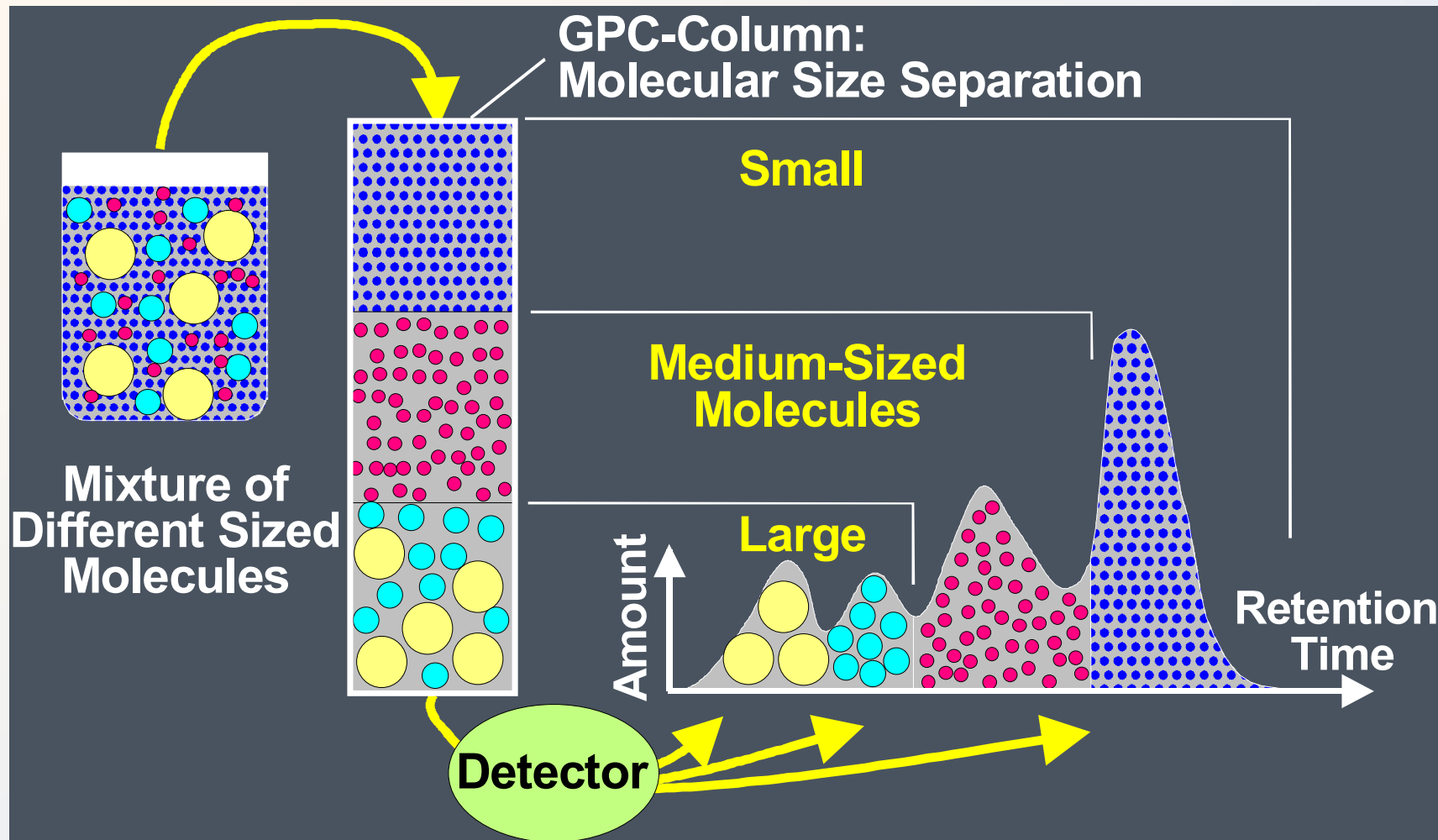


Aging and Durability

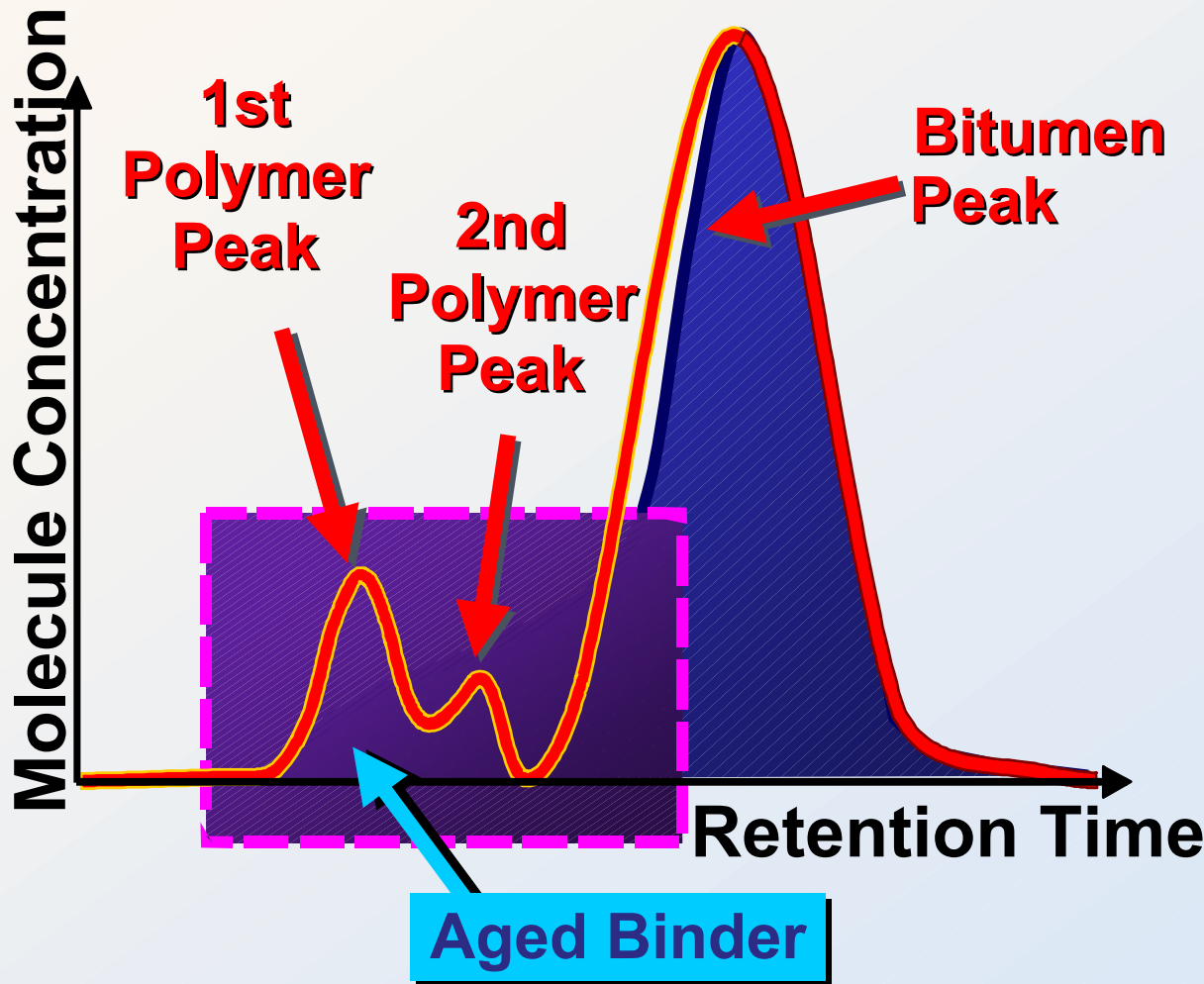
Gel Permeation Chromatography

Gelpermeation Chromatography

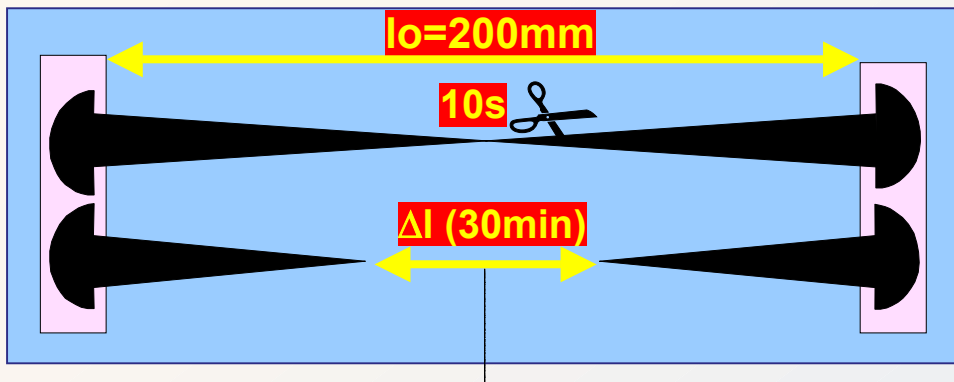
GPC: Principle



GPC Polymer Modified Binder



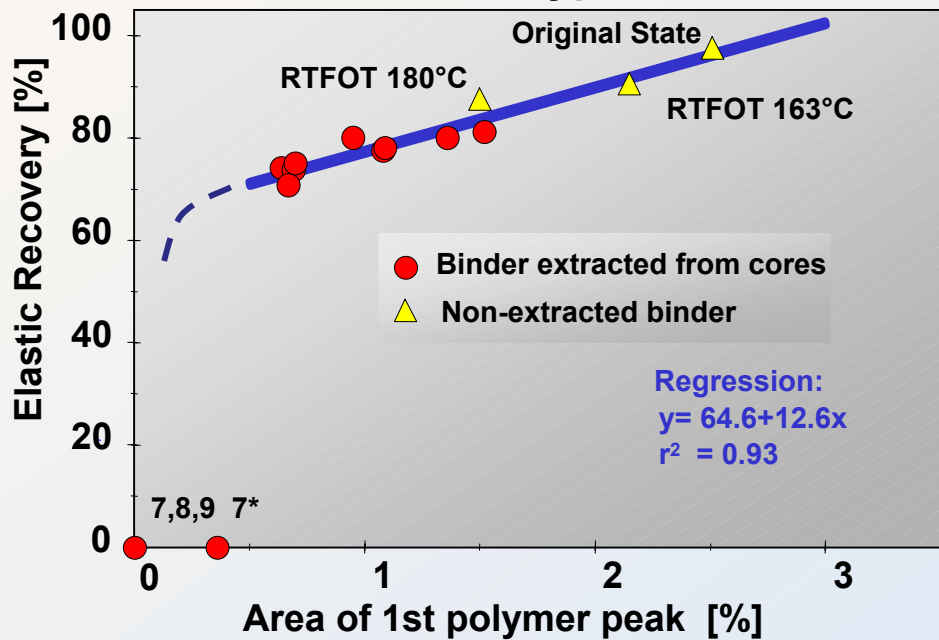
Elastic Recovery SBS fom PA (Results)



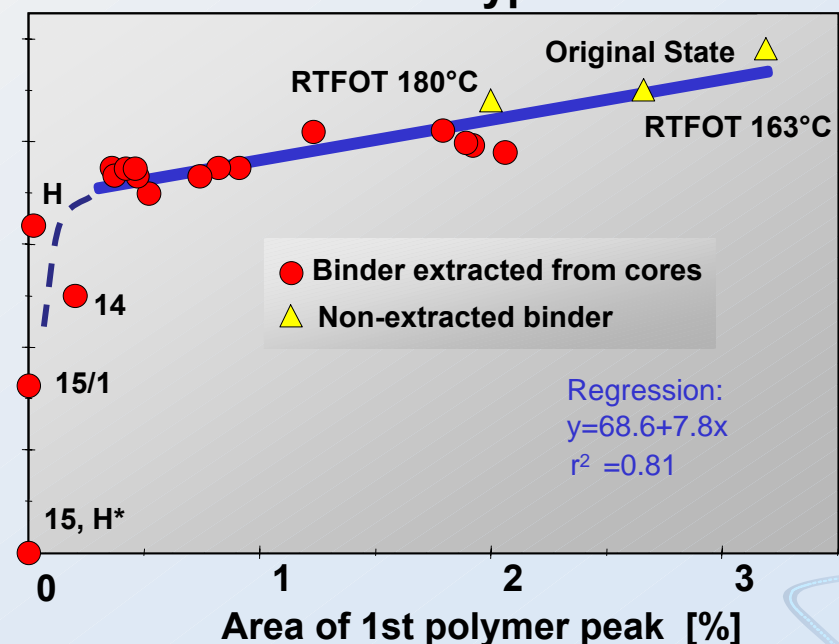
M. Hugener



Binder type I



Binder type II



High Frequency Measurements

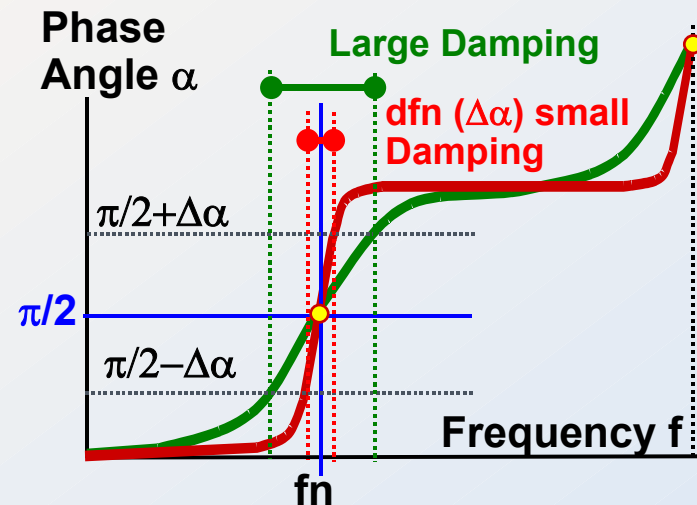
HFT(R) (High Freq. Tors. Rheom)

M. Sayir, A. Hochuli, K. Häusler, L.D. Poulikakos, M.N. Partl

Damping inversely prop. to $\alpha(f)$ -slope at resonance. It follows from frequ. difference $dfn(\Delta\alpha)$ at $\alpha = \pi/2 \pm \Delta\alpha$.

Measurement of:

- ★ Elastic Response related to resonance frequ. f_{air} , f_{bit} at $\varphi = 90^\circ$. Resonance Frequ. $\Delta f = f_{air} - f_{bit}$
- ★ Damping prop. to frequ. difference df for $\varphi = \pi/2 \pm \alpha$. Here: Damping $df_{22.5} = df_{22.5,air} - df_{22.5,bit}$



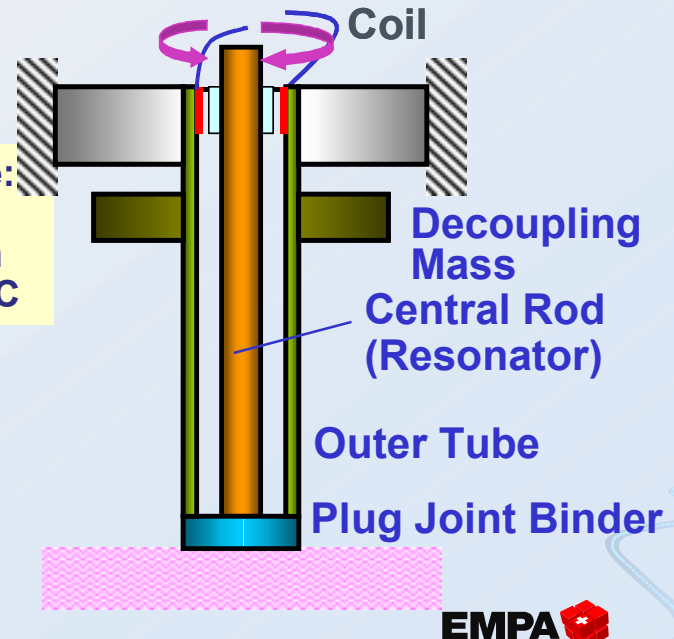
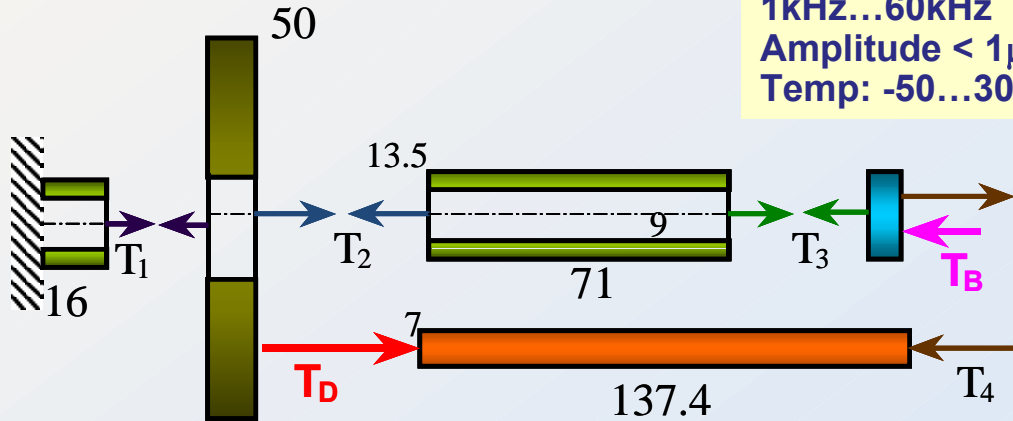
From simple Viscoelastic Spring Modeling:

- ★ Storage & Loss Moduli due to interaction with medium.

$$T_B = C^* \theta_B = (C' + i C'') \theta_B$$

with $cd = C' / C_0$, $ld = C'' / C_0$

Frequency range:
1kHz...60kHz
Amplitude < 1μm
Temp: -50...300°C



HTFR – DSR Comparison

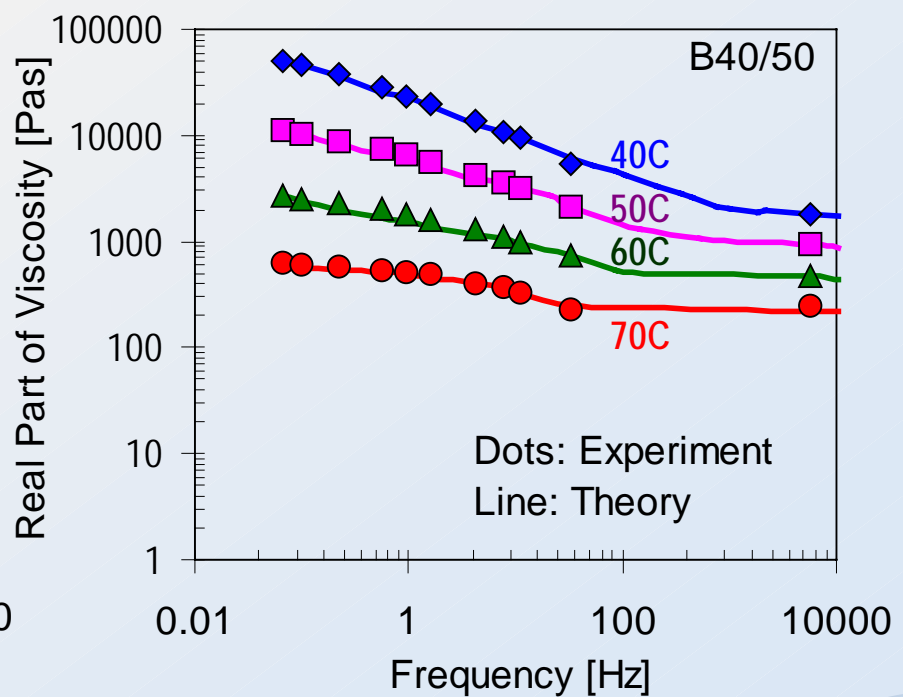
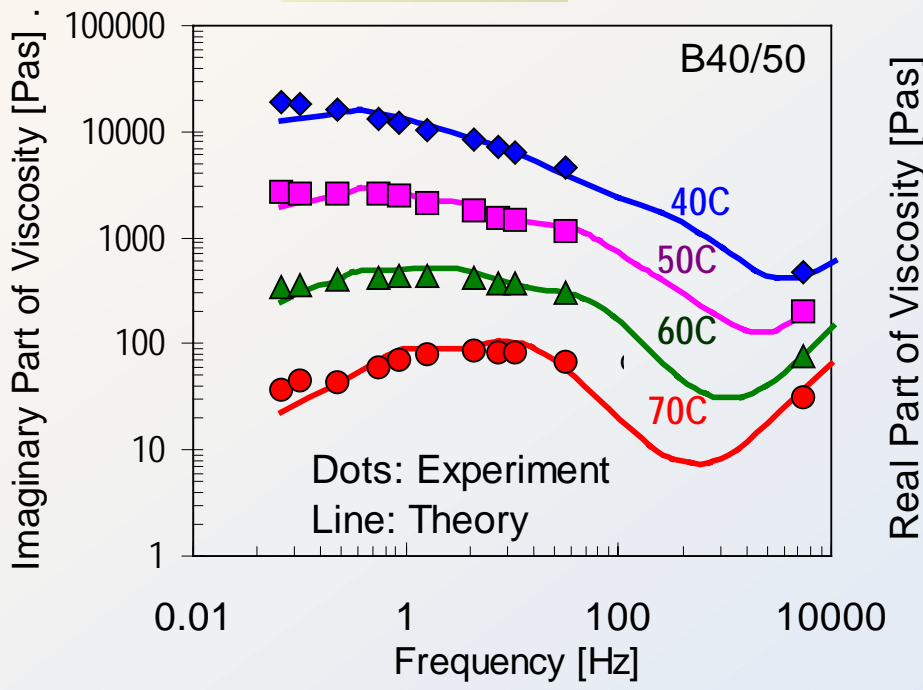
$$\eta^* = \eta_0 \cdot e^{i\omega t} = \eta' + i\eta'' = \frac{\tau^*}{\omega} = \frac{G''}{\omega} - i \frac{G'}{\omega}$$

for Maxwell Model $G(t) = G_0 \cdot e^{-t/T}$
 $(G_0$ elastic spring, T relaxation time)

hence

$$\eta' = \frac{TG_0}{1 + \omega^2 T^2}$$

$$\eta'' = \frac{\omega T^2 G_0}{1 + \omega^2 T^2}$$

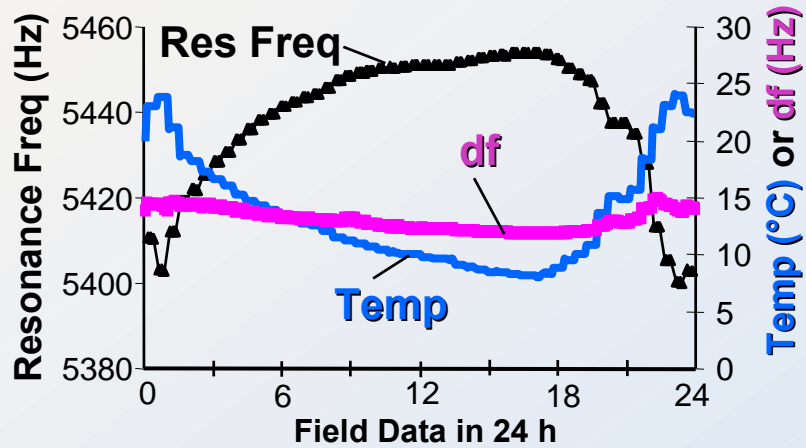
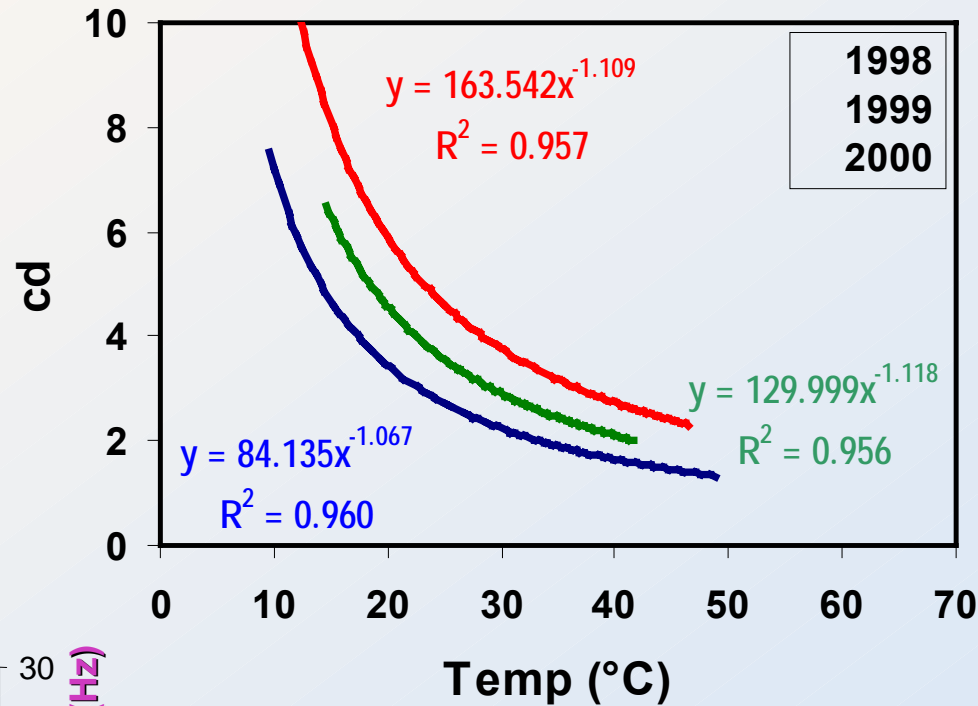


Example: HFTR for APJ Monitoring

(Aug. 1998 ... Sept. 2000)



M. Sayir, A. Hochuli, L.D. Poulikakos, M.N. Partl



$$T_B = C^* \theta_B = (C' + i C'') \theta_B$$

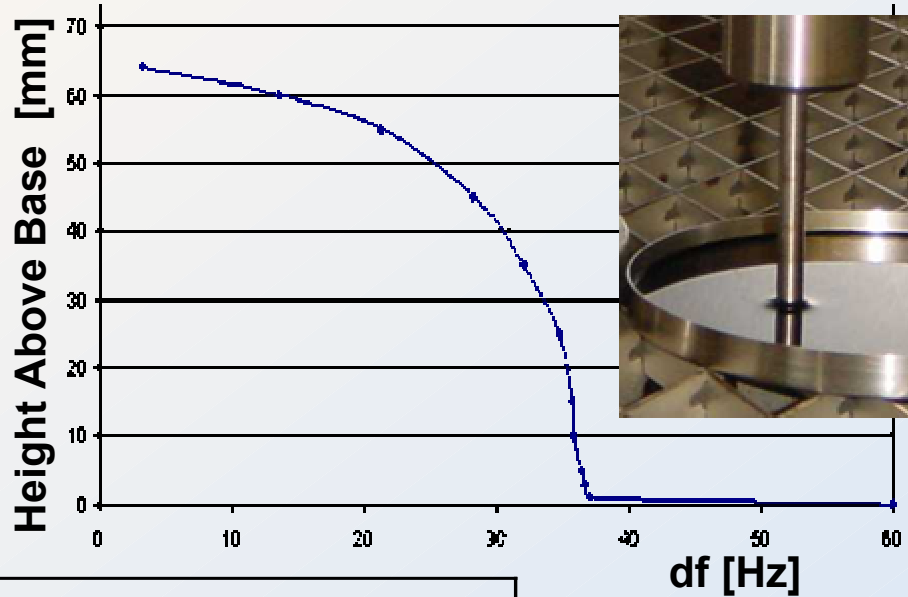
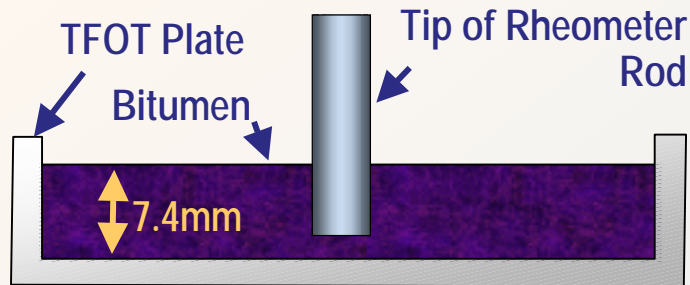
$$cd = C' / C_0$$

$$ld = C'' / C_0$$

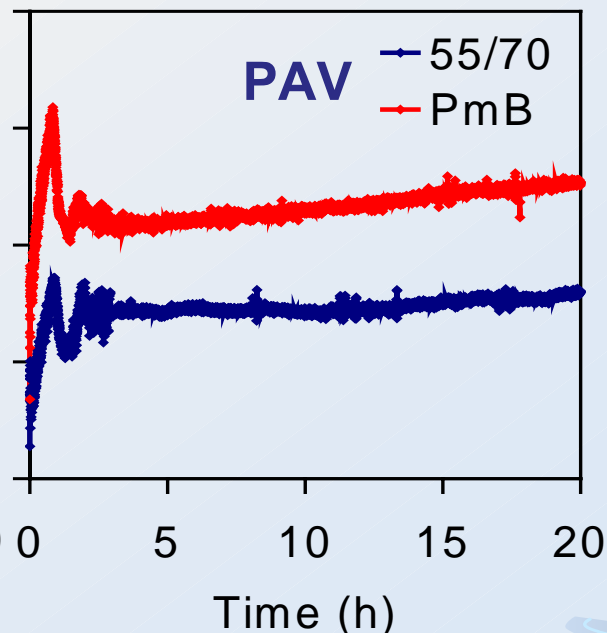
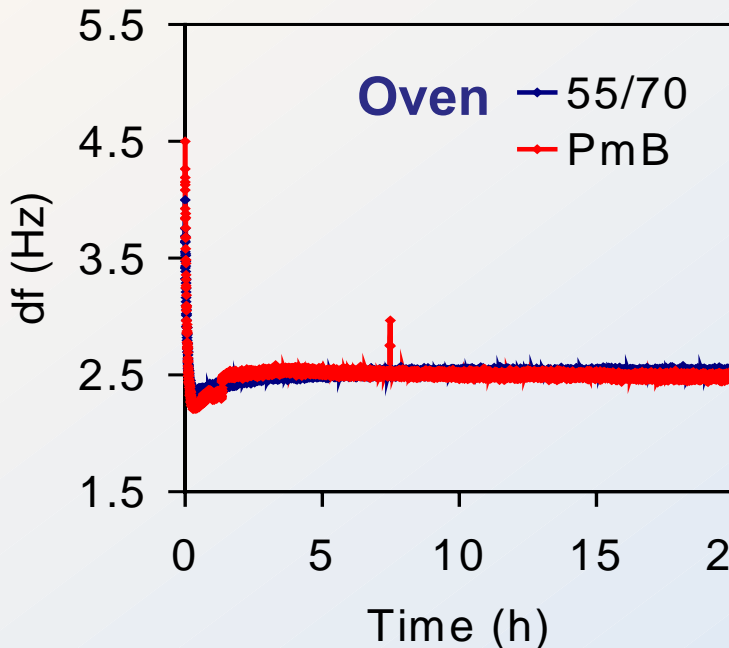
HFTR Lab Measurements

C. Toovey, E. Connery, L.D. Poulakos

Dipping Test



Oven/PAV 110°C Aging



Water Susceptibility evaluation of Mixes

Contact

Remy Gubler

remy.gubler@empa.ch



General Remarks (1)

- Testing/modeling of moisture effects is still in an early empirical stage.
- New promising research deals with
 - **Permeability k** , based on Kozeny-Carman equation (*e.g. Al-Omari et al, AAPT 2002*)

$$k = f(n) \cdot C \cdot D_s^2 = \frac{n^2}{(1-n)^2} \frac{\gamma}{\eta} C D_s^2$$

n: effective %air voids; γ : unit weight water; η : viscosity, **C**: shape factor of particles (for spheres $C=1/180$); **D_s** average particle diameter

- **Surface free energy Γ** of the binder-aggregate system to predict moisture damage potential (*Cheng et al, AAPT2002*)

$$\Gamma = \Gamma^{LW} + \Gamma^{AB}$$

Γ : surface free energy of binder or aggregate; Γ^{LW} : apolar Lifshitz–van der Waals component of surface free energy; Γ^{AB} : acid-base component of surface free energy.

General Remark (2)

- One main problem is the characterization of the moisture of a specimen. Traditionally this can be done in three ways:
 - Saturation \mathbf{S} :** volume of water in the pores (by volume)

$$S = \frac{V_{\text{water}}}{V_{\text{pores}}}$$

- Effective Saturation \mathbf{S}_{eff} :** Volume of water in a specimen (by volume)

$$S_{\text{eff}} = \frac{V_{\text{water}}}{V_{\text{specimen}}}$$

- Moisture content \mathbf{MC} :** the amount of water in a specimen (by weight)

$$MC = \frac{m_{\text{water}}}{m_{\text{specimen}}}$$

- Often materials are simply characterized/compared as **dry** and **wet**, (e.g. strength ITSR, or modulus CAST)
- The following concentrates on dry-wet **testing** aspects of mixtures

CAST

Coaxial Shear Test

(dry)

CAST: Co-Axial Shear Test

J. Junker, R. Gubler, K. Younger, K. Sokolov, M.N. Partl

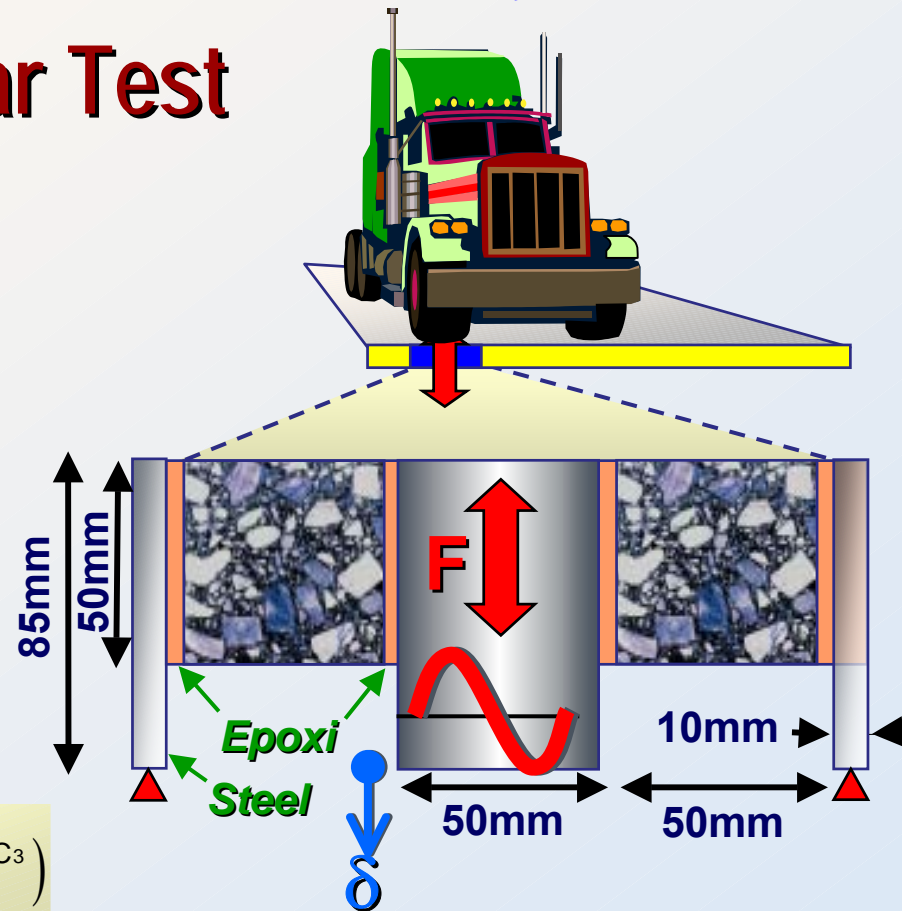
Concept

- Triaxial, e.g. laterally confined
- Laboratory & field cores
- Multilayer testing possible
- Loading in traffic direction
- Testing of in situ surface
- Conventional test equipment
- Displacement (δ) & temp. controlled

Basic Equation:

$$G^* = G^*_{r,r} = \frac{F_a}{\delta_a} \cdot C_{FE}(G^*_{s,s}) = \frac{F_a}{\delta_a} (C_1 + C_2 \cdot G^*_{s,s}^{C_3})$$

- G^* : Complex modulus (recursive by iteration)
 $G^*_{r,r}, G^*_{s,s}$: Resulting and starting value during iteration
 F_a : Force amplitude in central cylinder
 δ_a : Displacement amplitude of central cylinder
 C_{FE} : Coefficient function derived from FEA
 C_1, C_2, C_3 : Constants depending on geometry only

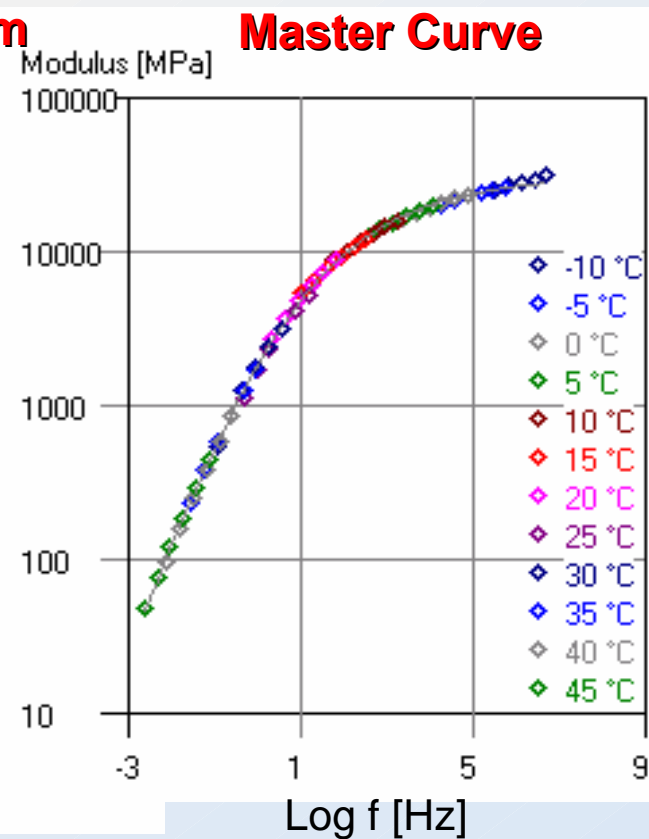
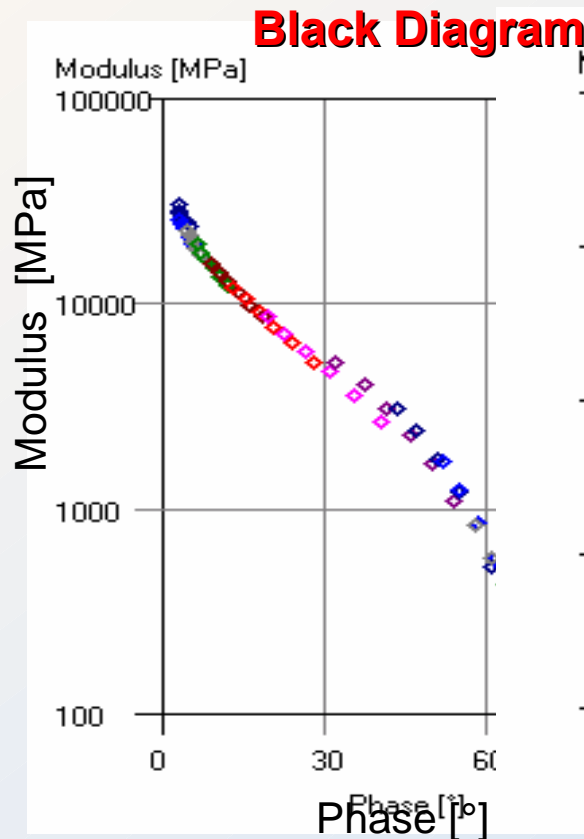
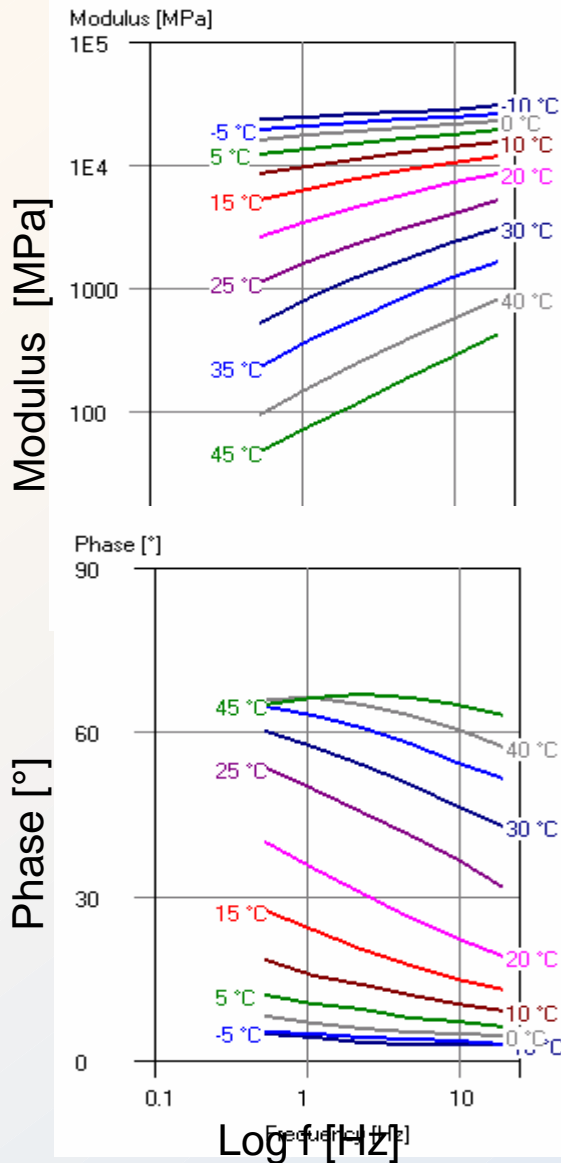


Technical Data

$T = -20..70^\circ\text{C}$; $f = 0.01..16\text{Hz}$
 $\delta = \pm 5\text{mm}$; $F = \pm 10\text{kN}$

Results (Examples)

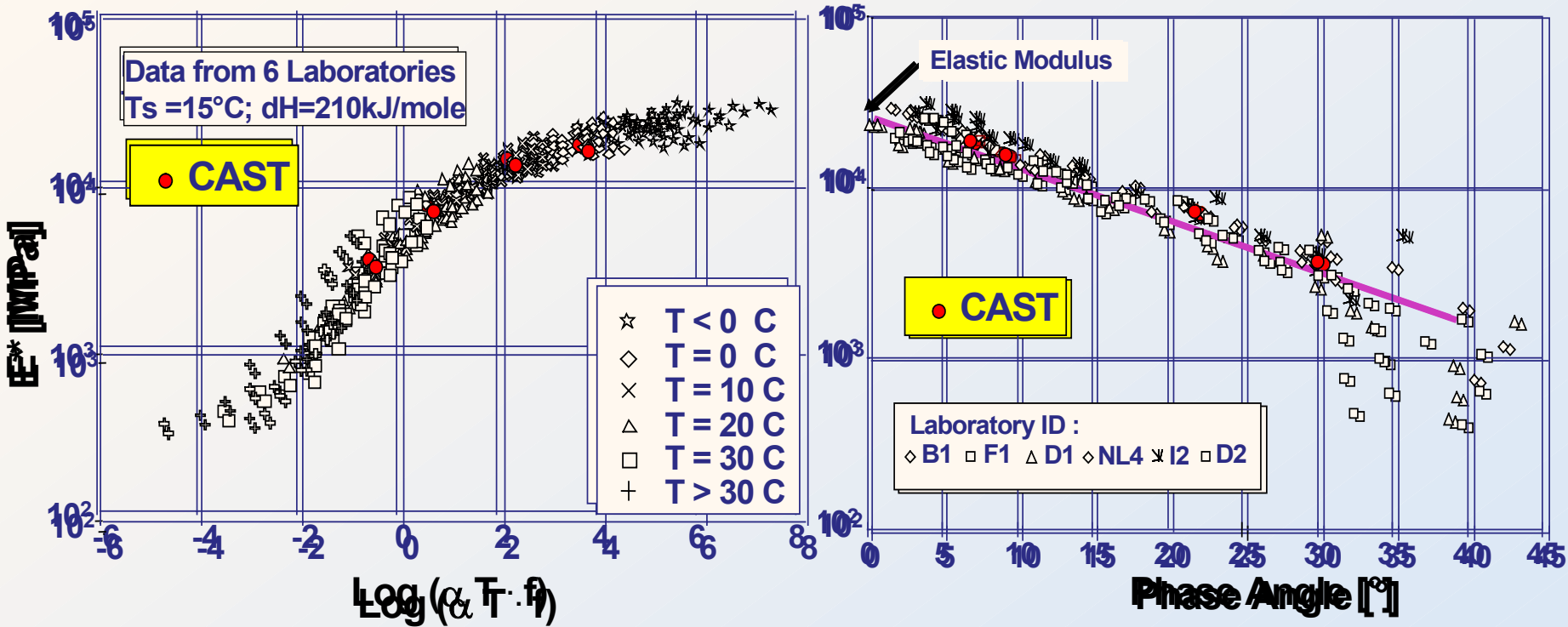
R. Gubler



CAST Modulus (RILEM Inter-Lab. Test)

Comparison with Data from RILEM Report Nr 17 (1998)

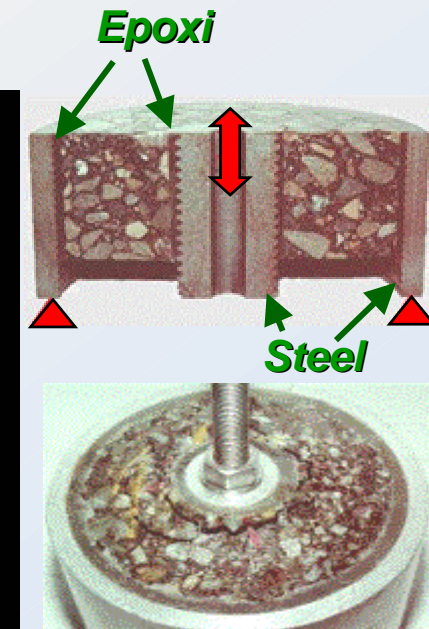
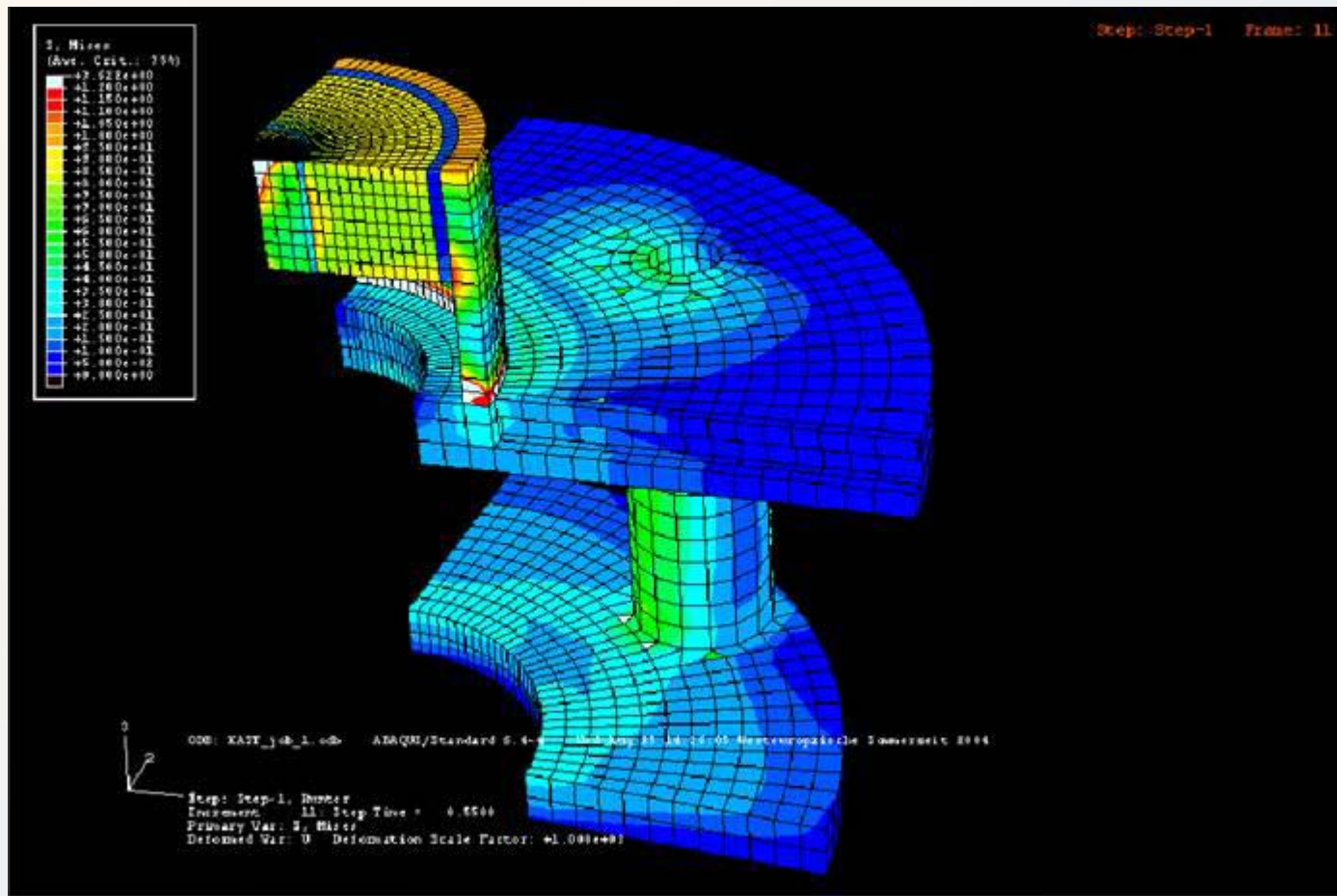
R. Gubler, K. Younger, M.N. Partl



CAST von Mises Stress

K. Sokolov

Modeling of CAST including test support and epoxi glue



CAST

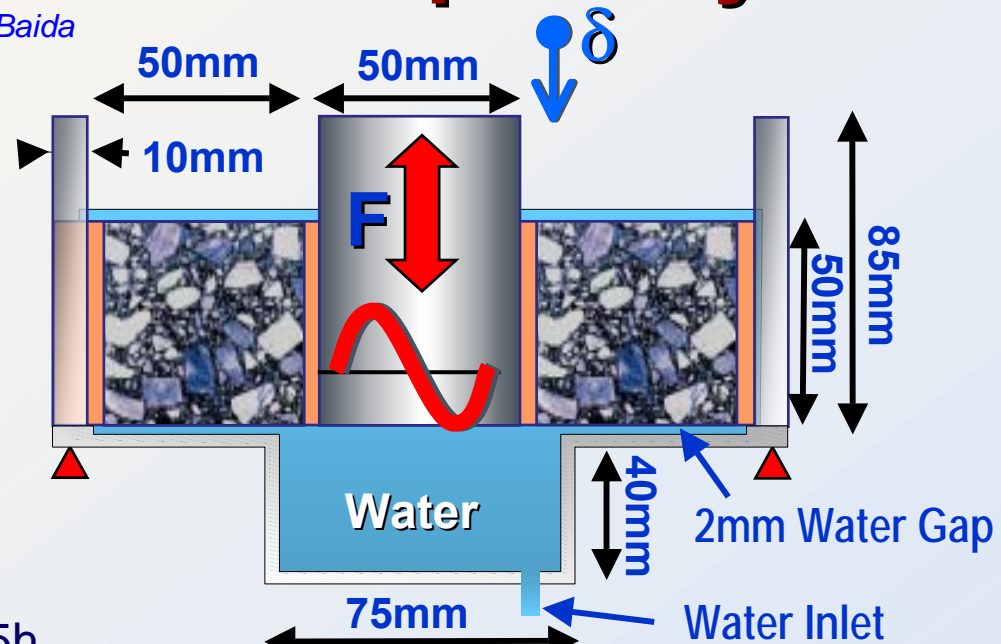
Coaxial Shear Test (moisture tests)

CAST for Water Susceptibility

R. Gubler, M.N. Partl, L. Baida

Concept

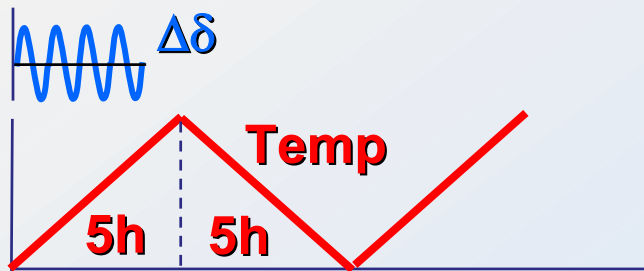
- Like CAST
- Testing submerged in water
- Cyclic load, displacement & temp. constantly recorded
- Displacem. & temp. controlled



Technical Data

$T = 30..40^\circ\text{C}$ ($27..32^\circ\text{C}$) ramps in 5h
(5 up/down cycles)

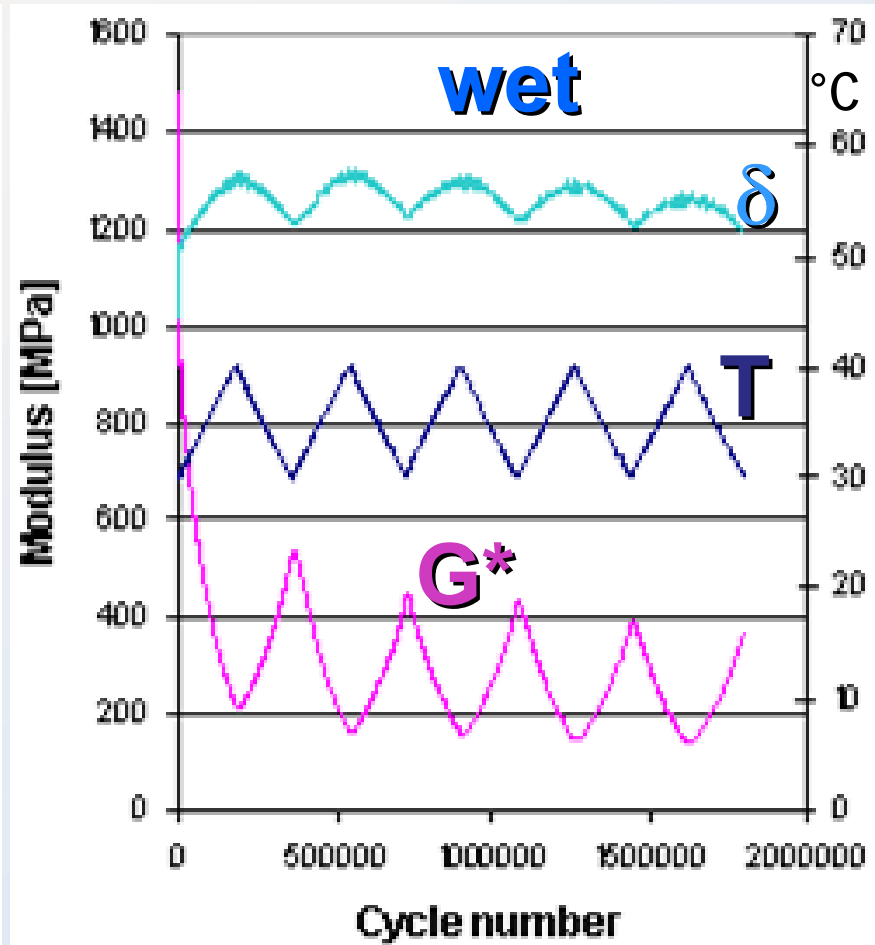
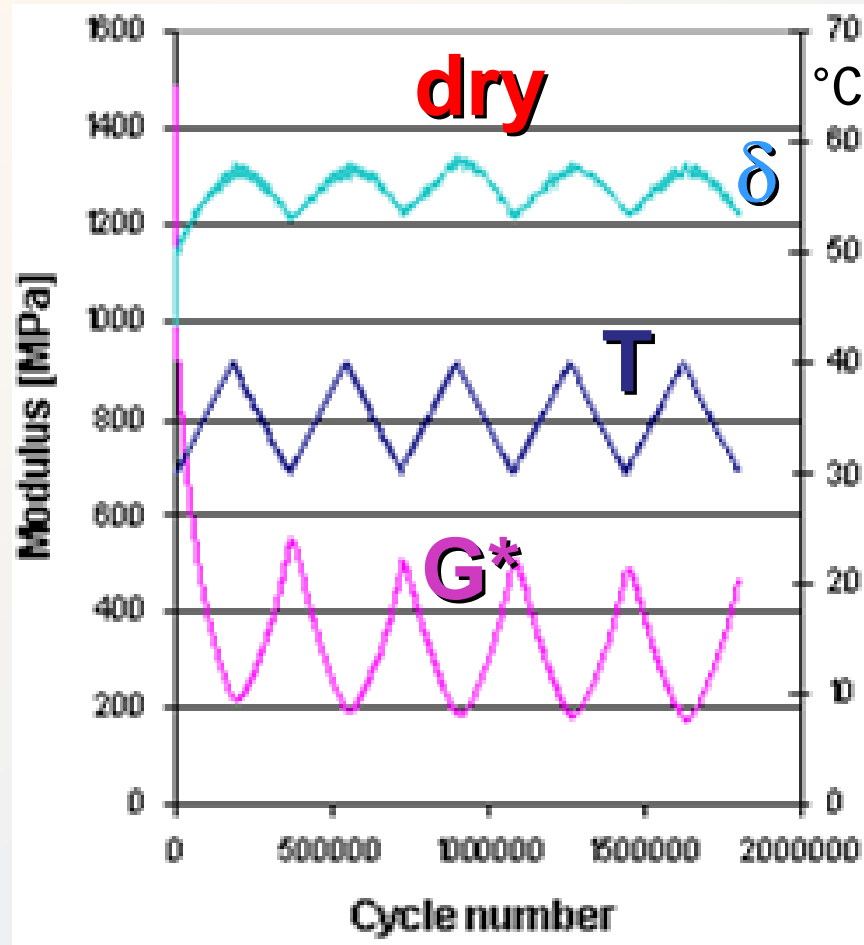
Amplit. $\Delta\delta = 0.02\text{mm}$; $f = 10\text{Hz}$



CAST Typical Curve

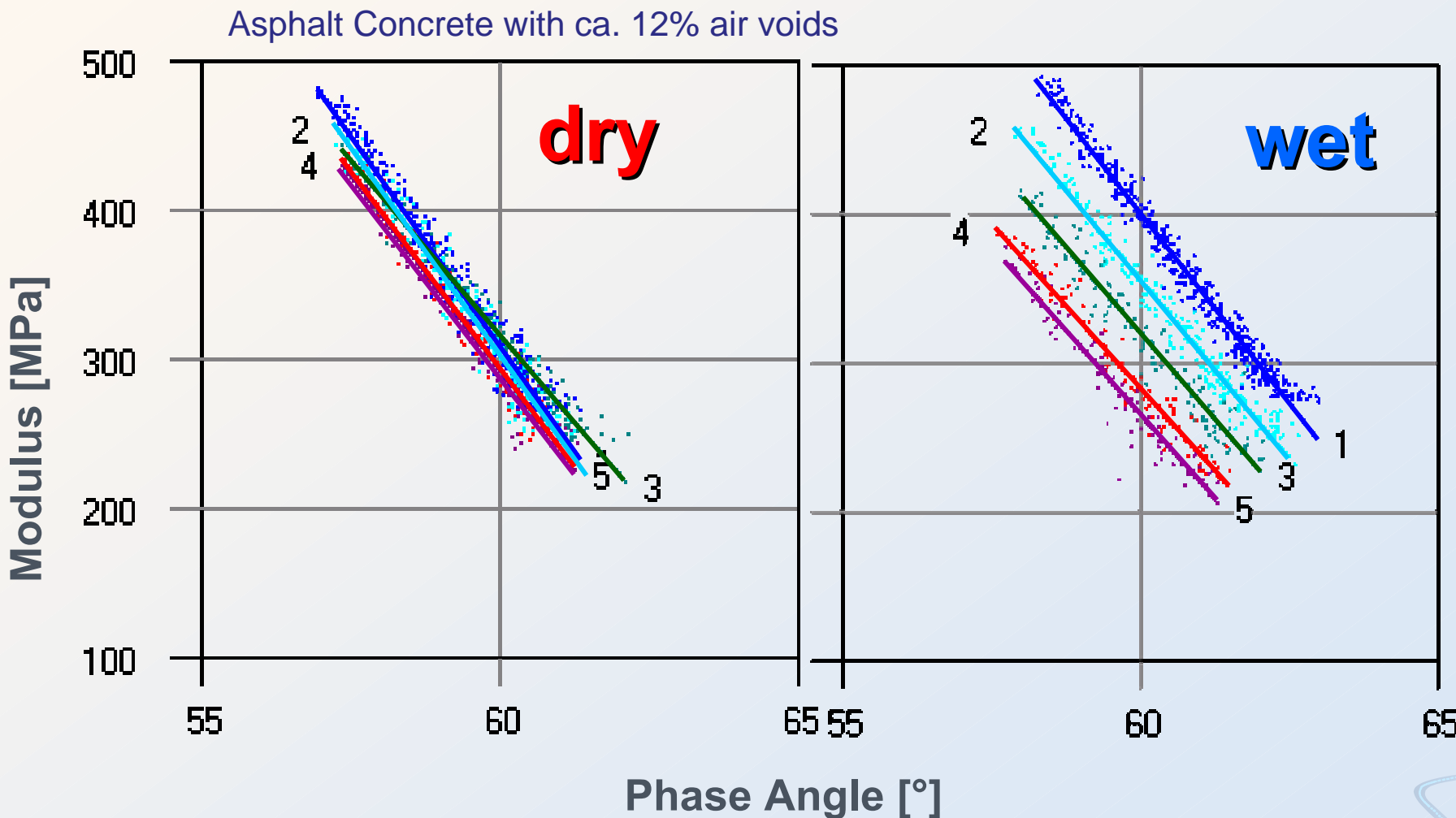
R. Gubler, L.G. Baida, M.N. Partl

Asphalt Concrete with ca. 12% air voids

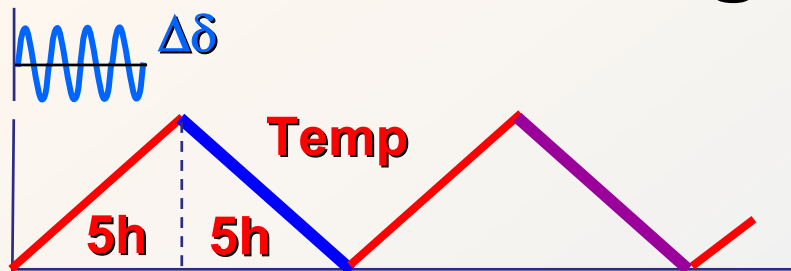


Example: High Water Susceptibility

R. Gubler, L.G. Baida, M.N. Partl

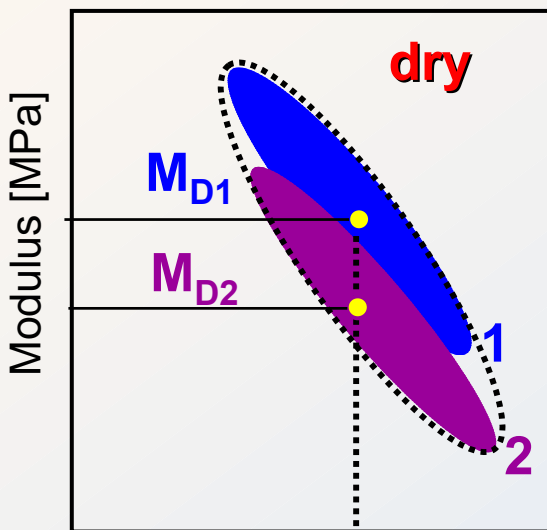


Water Damage Index WDI

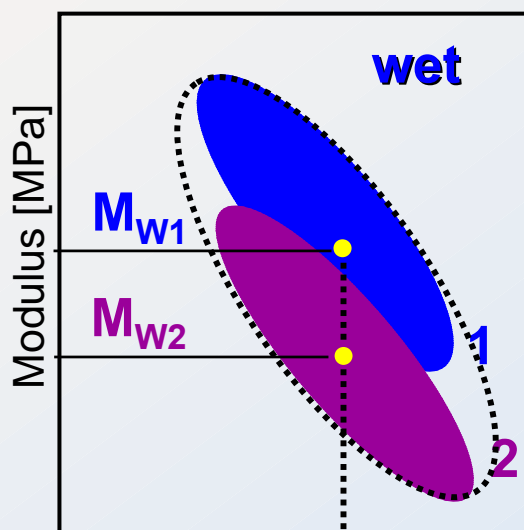


$$WDI = \frac{M_{D1} - M_{W1} + M_{D2} - M_{W2}}{2}$$

Downward Ramp



Phase Angle, Temp.



where:

WDI : Water damage index;

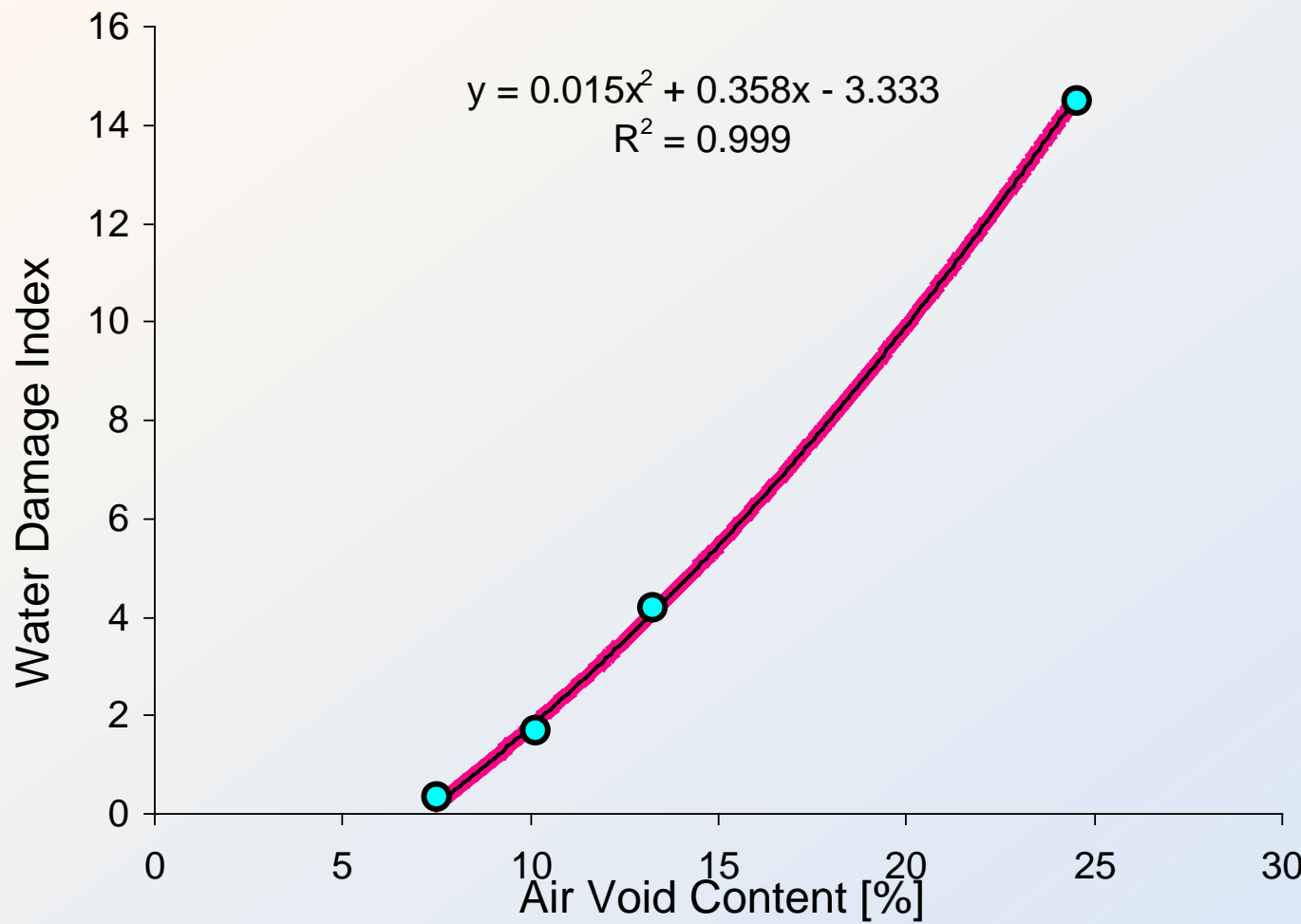
M_{W1} : Modulus @ average phase angle for 1st wet downward ramp;

M_{W2} : Modulus @ average phase angle for 2nd wet downward ramp;

M_{D1} : Modulus @ average phase angle for 1st wet downward ramp;

M_{D2} : Modulus @ average phase angle for 2nd wet downward ramp;

Water Damage Index WDI

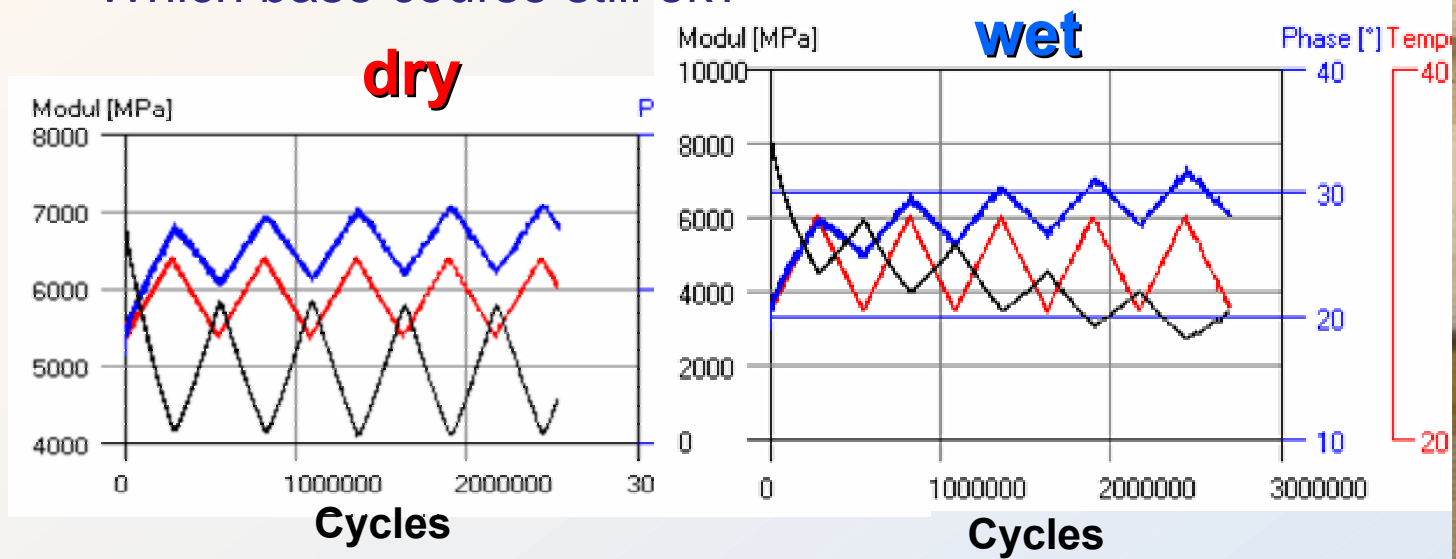


Water Damage in a Road

Observations

- Bad adhesion
- Water from below
- Which base course still ok?

R. Gubler



Course	Damage	G^* [MPa]		ΔG^* per Temp Cycle (%)		
		dry	wet	dry	wet	Difference
Upper Base C.	Water from below	7091	8565	0.4	12.2	11.8
Lower Base C	Interlayer Shear Movement	2350	2056	2.4	3.1	0.7

Inlayer and Interlayer Bond

Contact

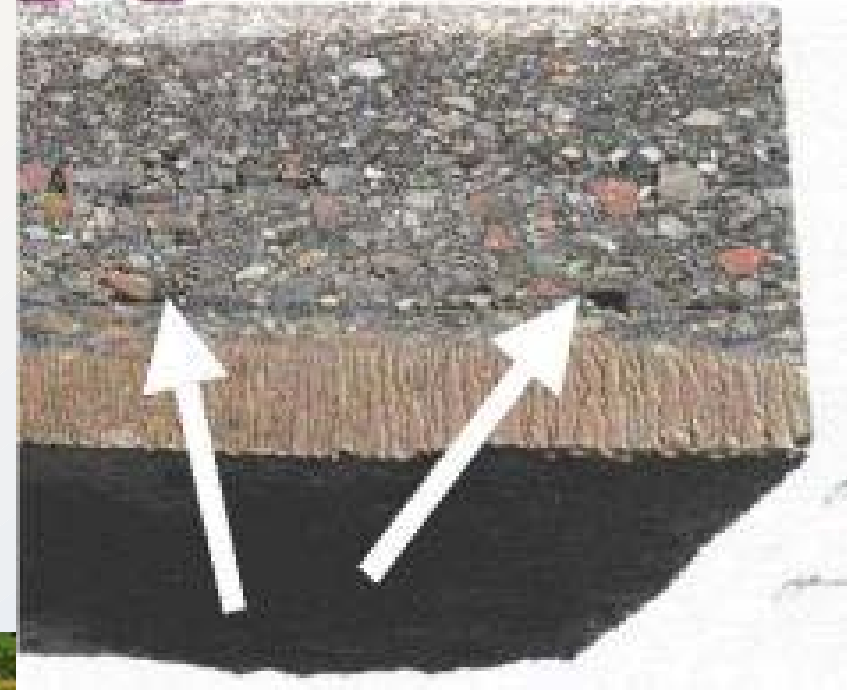
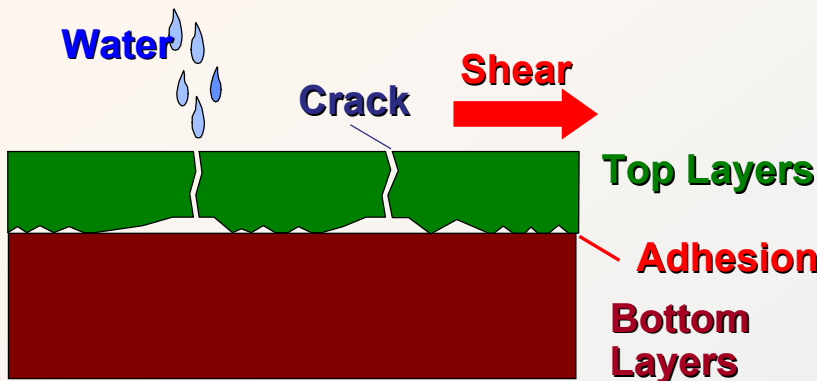
Christiane Raab

christiane.raab@empa.ch

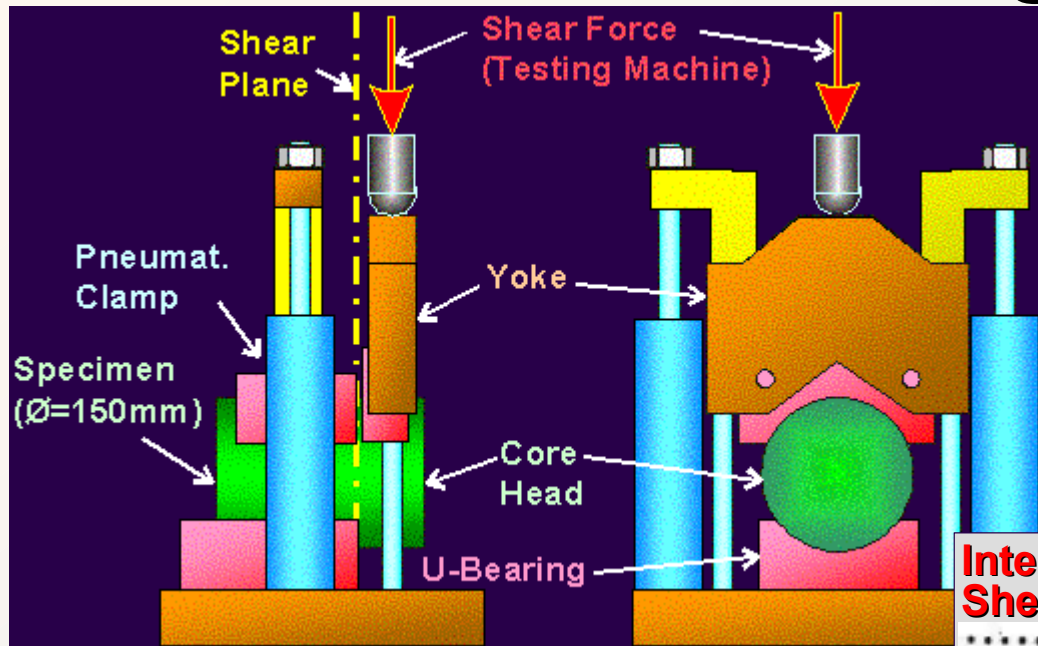


Interlayer Adhesion Problems

C. Raab, M. N. Partl



LPDS Investigation

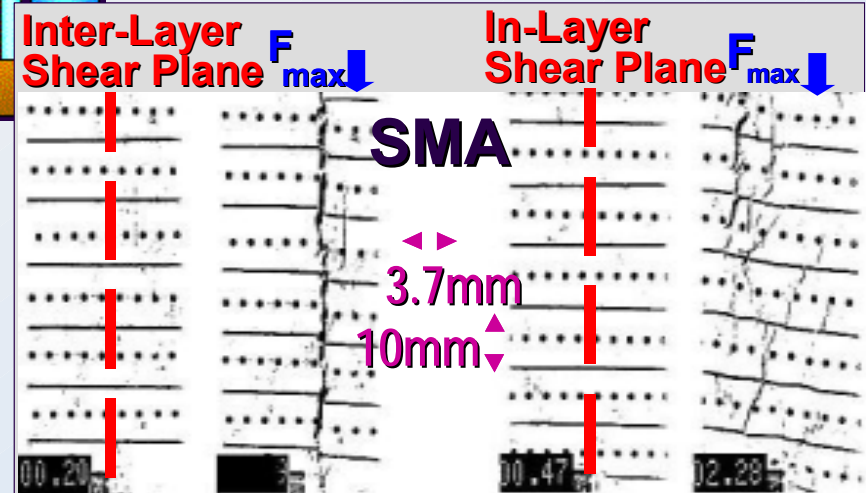
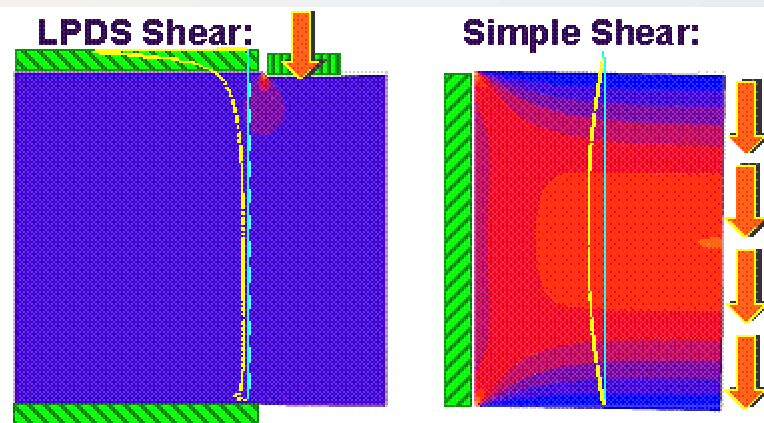


Linear
Parallel Direct
Shear (LPDS)

Optical measurements

Inter-Layer Shear Plane F_{max}

In-Layer Shear Plane F_{max}



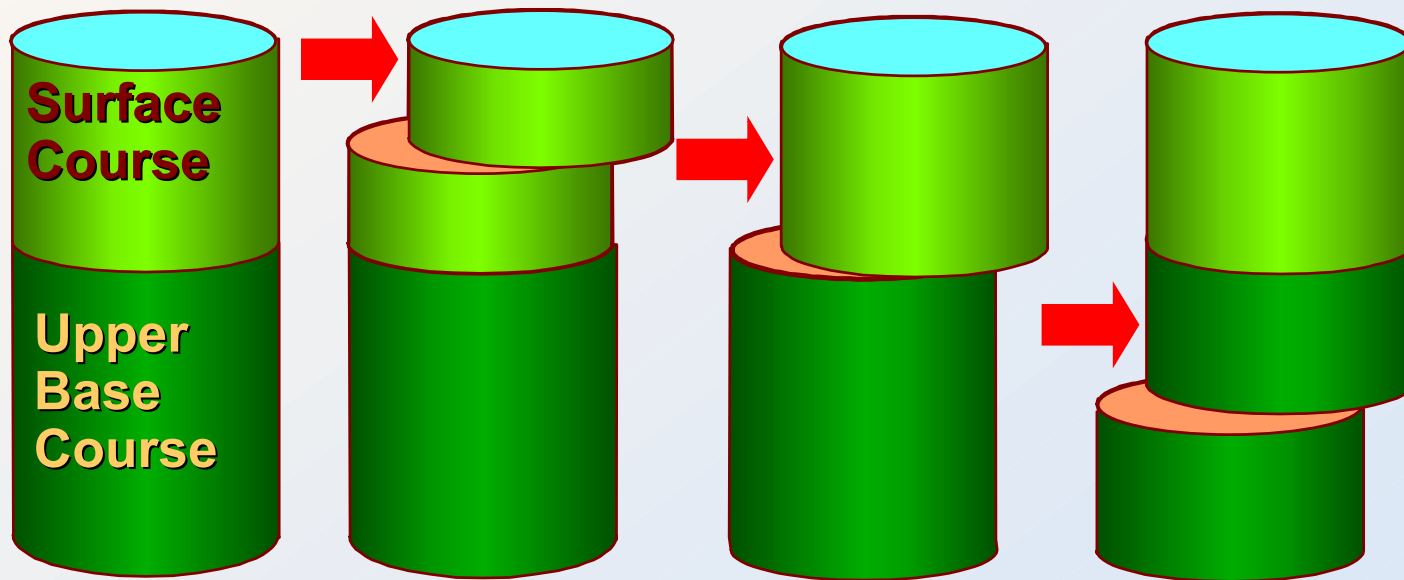
Shear Planes in Cores

Core

In-Layer
Shear Force
Surface C.

Inter-Layer
Shear Force
SC/UBC

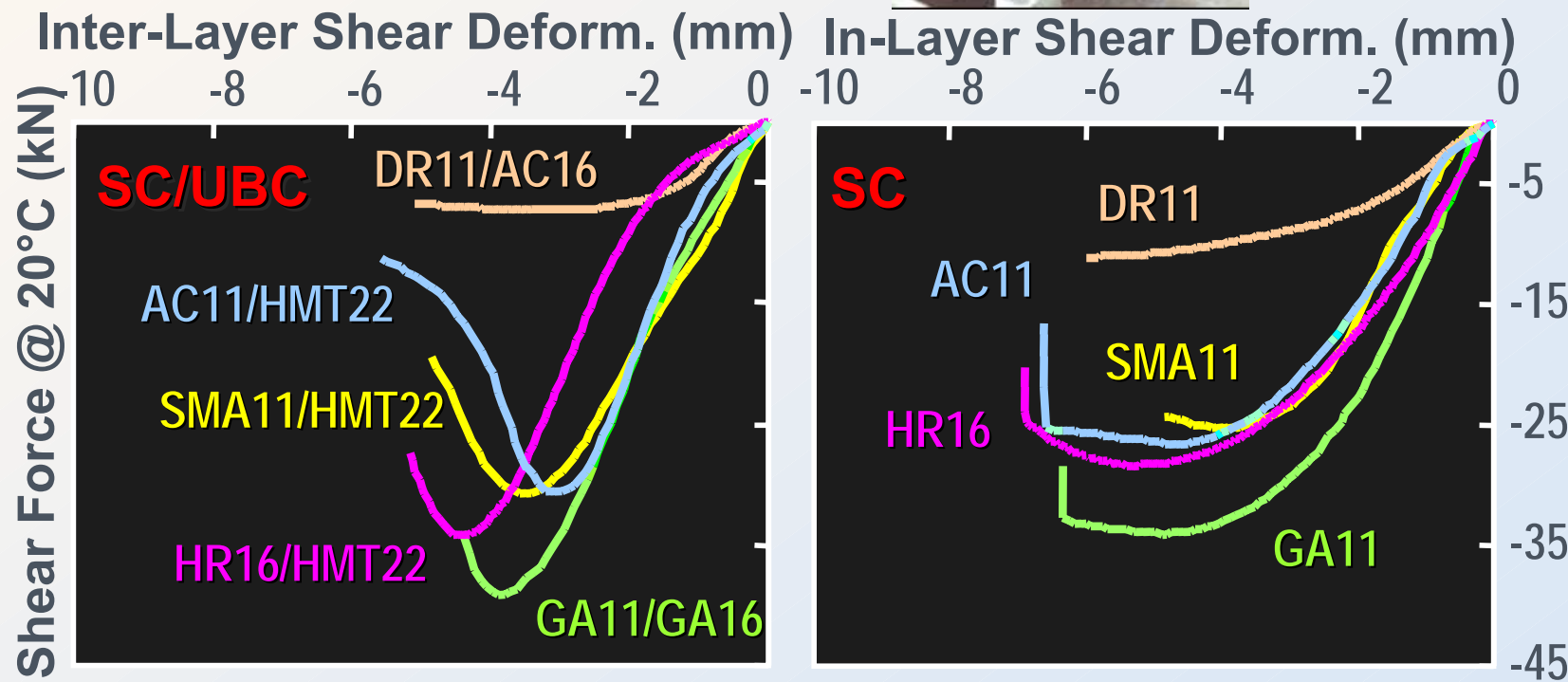
In-Layer
Shear Force
Upper Base C.



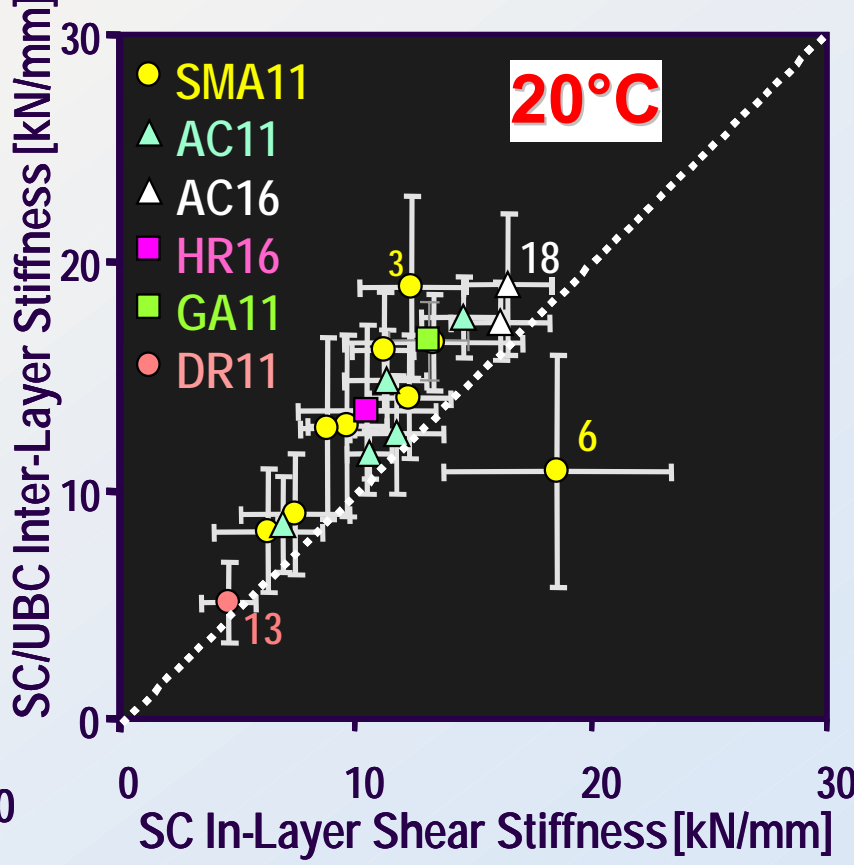
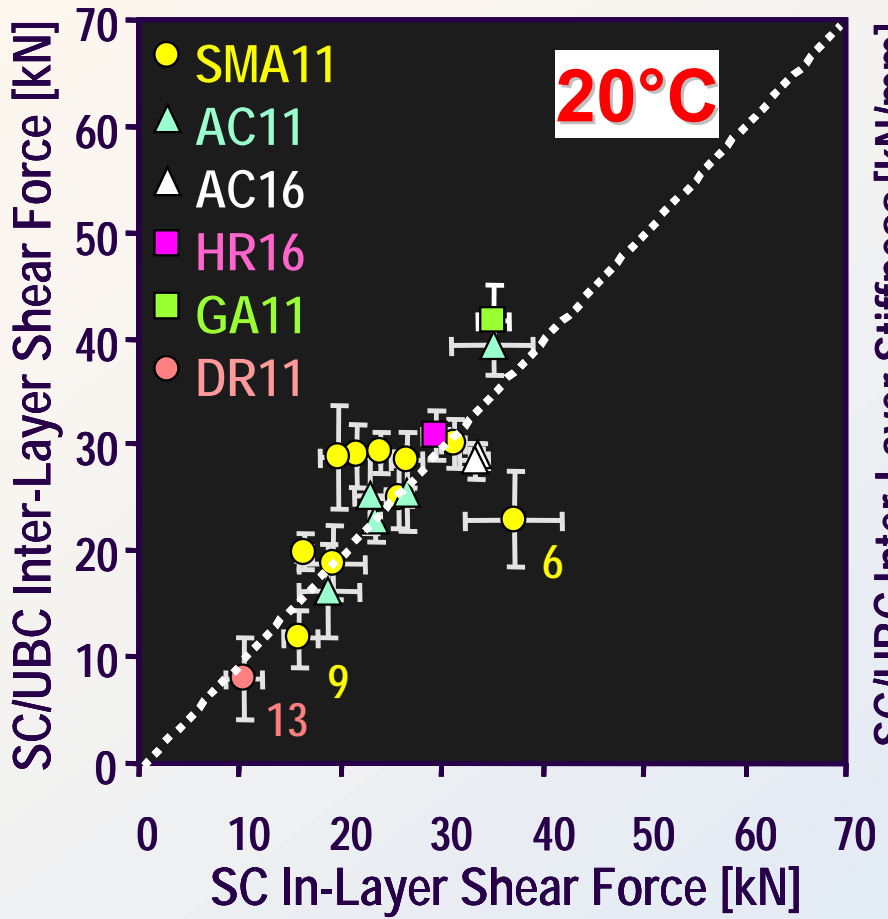
LPDS Inter- & In-Layer Shear @20°C



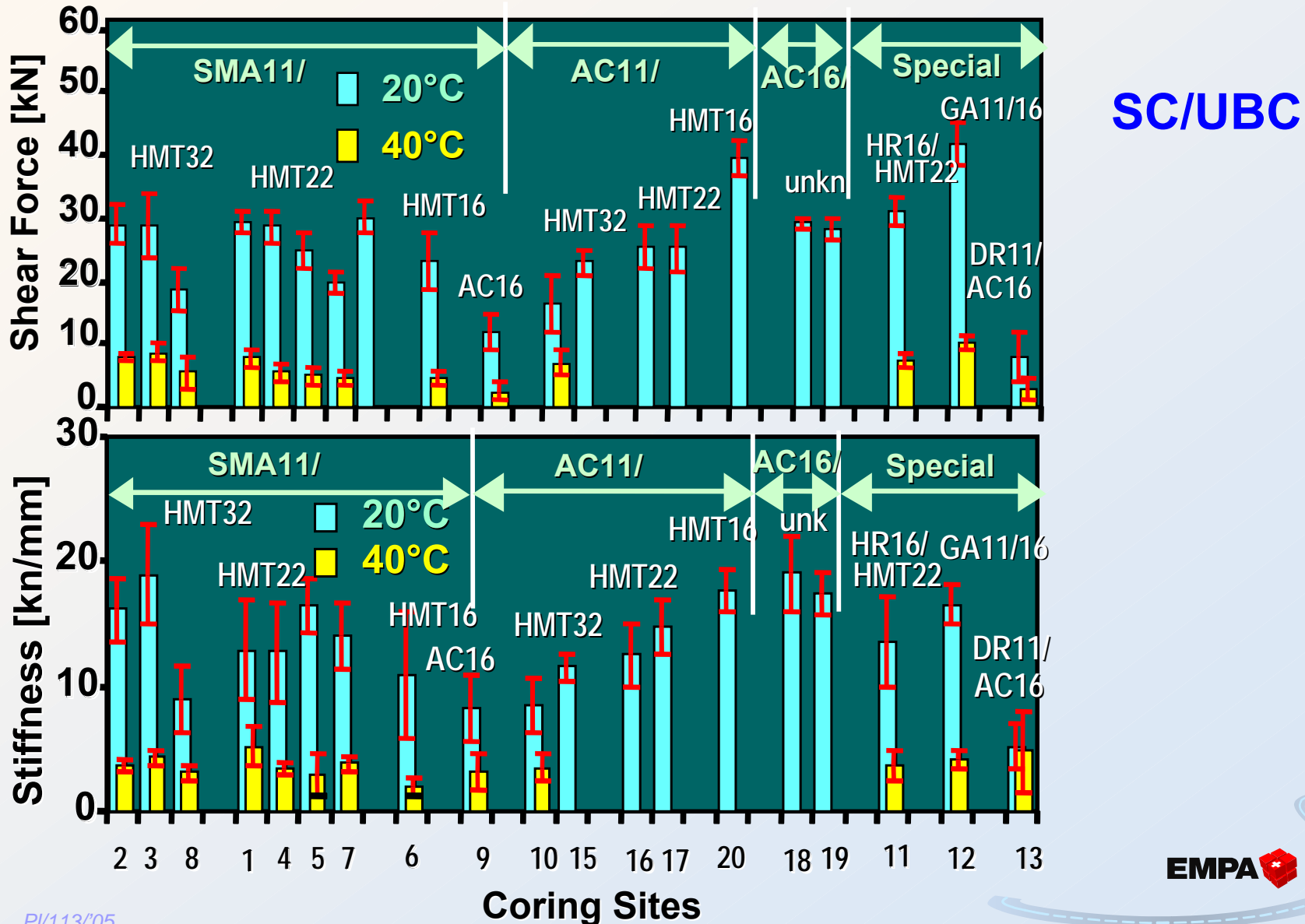
Linear Parallel
Direct Shear
(LPDS)



LPDS Results

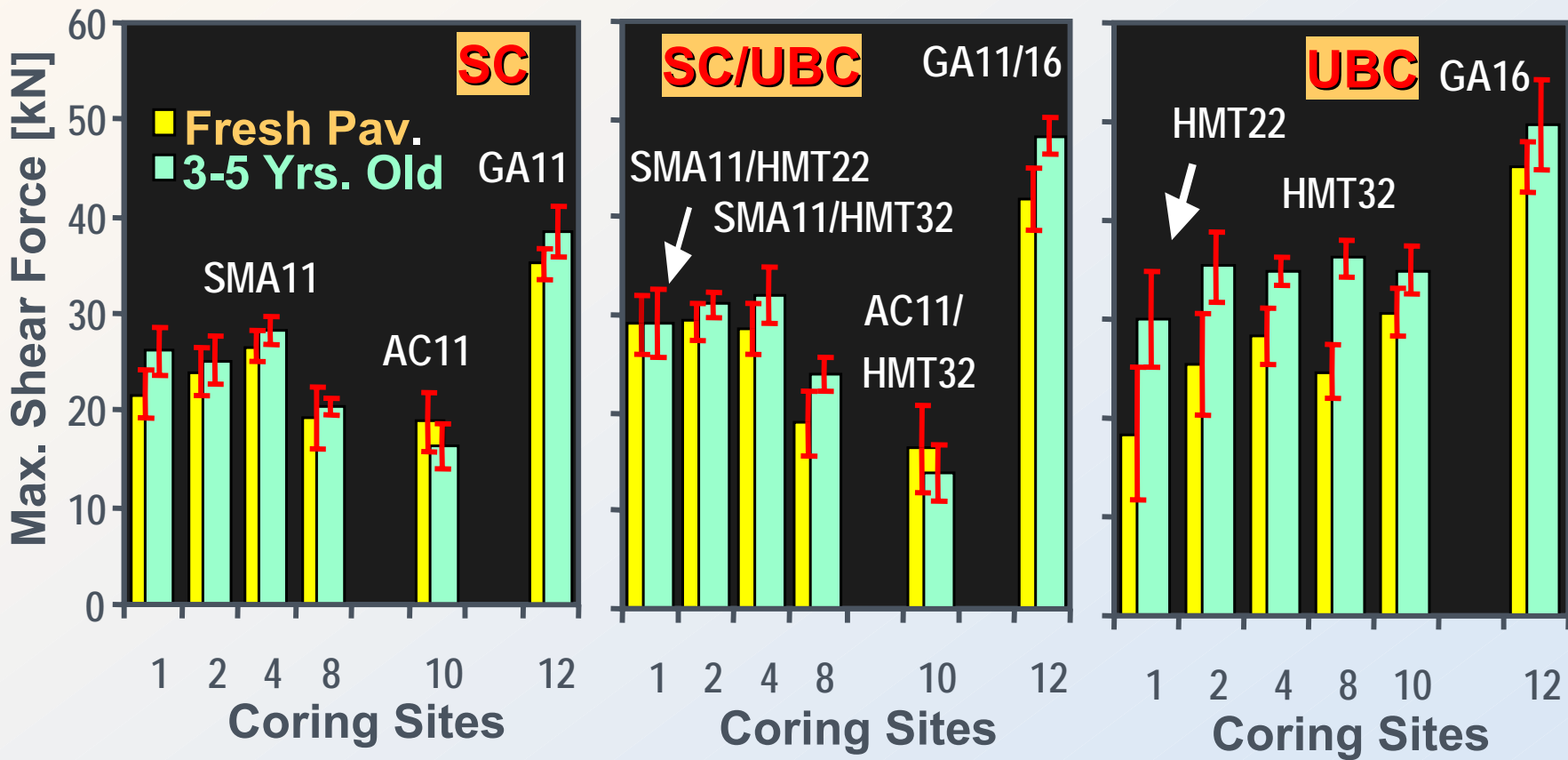


Interlayer Adhesion Temp. Influence



LPDS Traffic & Age:

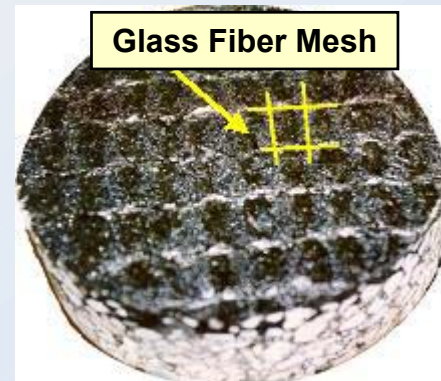
Shear Force @20°C



Interlayer Shear Figures

Asphalt/Asphalt	Standard	Possible
Surface C	>0.9MPa	1.3 MPa
Base C	>0.7MPa	

Asphalt/Concrete	Mean Measured
Glass Fiber Mesh	0.4MPa
Steal Mesh	0.2MPa
Tack Coat	0.9MPa



Accelerated Pavement Testing APT

Contact

Kirill Sokolov

kirill.sokolov@empa.ch

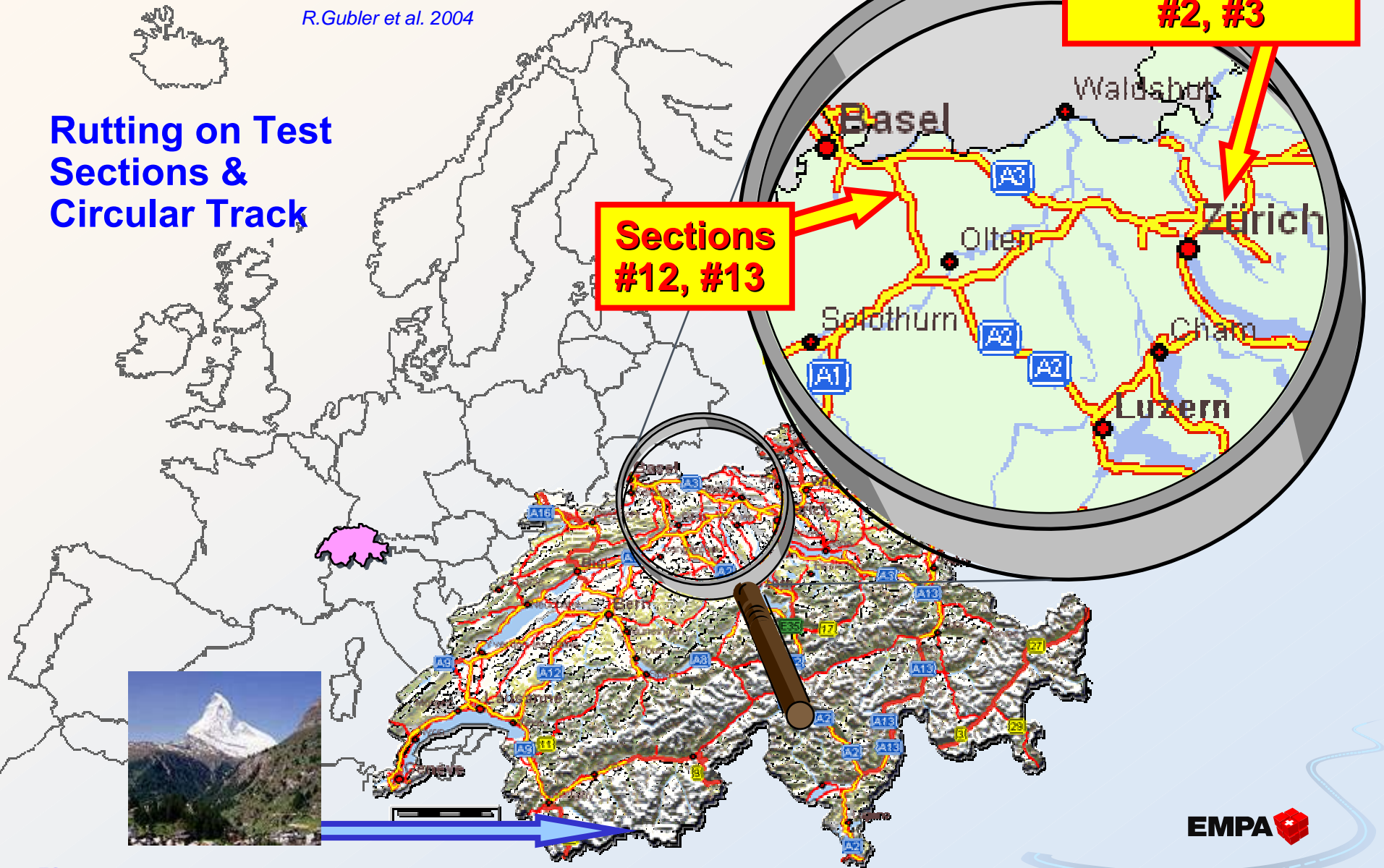
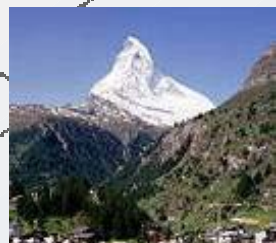


APT Testing in situ

Maintenance U2000

R.Gubler et al. 2004

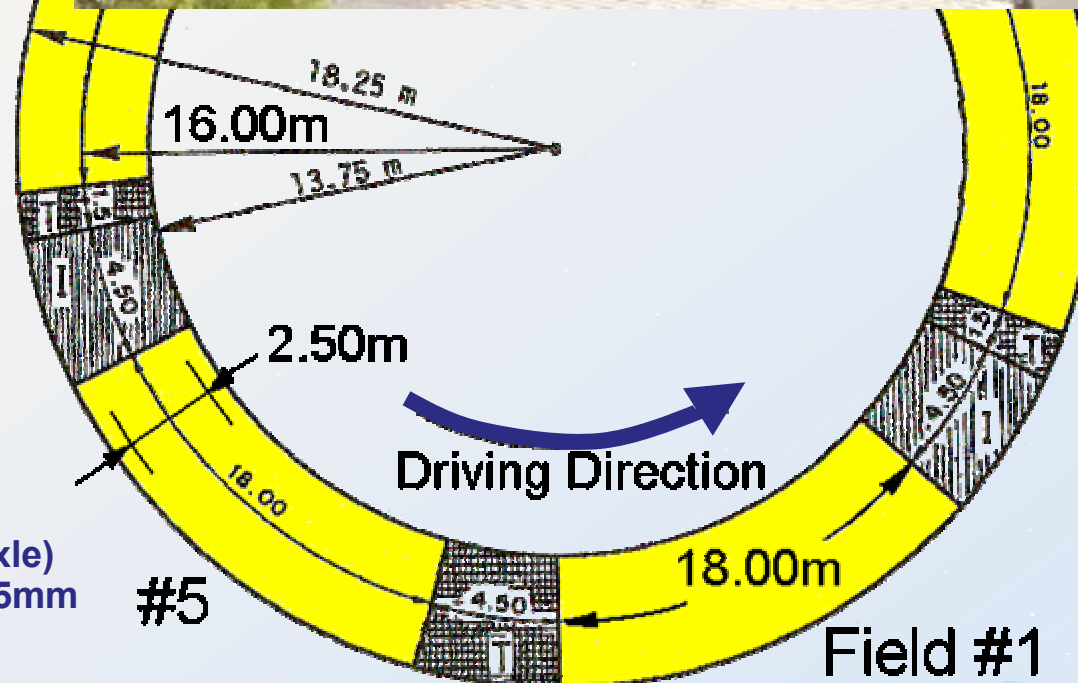
Rutting on Test
Sections &
Circular Track



Circular Track ETHZ@ EMPA



#4



Materials, Design U2000

A2 Motorway

#12

30mm	MR8, B50/70
80mm	HMT22, B50/70 Gasperini
uncertain	Existing old HMT

Gravel-Sand
100% crushed

#13

MR8, B50/70
HMT22, B70/100 Gasp. & Sp. Filler
Existing old HMT

Gravel-Sand
100% crushed

	Motorway	Circular test track
Base Material	Compacted Gravel-Sand	Compacted Gravel-Sand
Lower bearing course	Remaining old bearing course	70 mm HMT 22S
Upper bearing course	80 mm HMT 22S	70 mm HMT 22S
Wearing course	30 mm MR 8	40 mm AB 11S

Circular Test Track

#2

40mm	AC11S, B50/70
70mm	HMT22, B50/70 Gasperini
70mm	

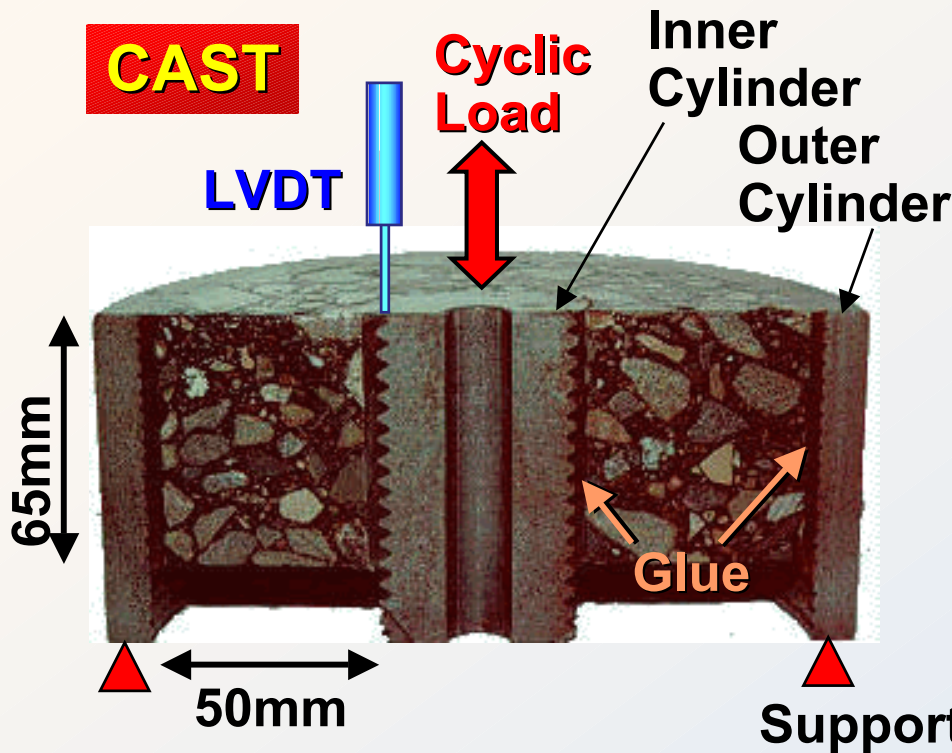
Gravel-Sand
100% crushed

#3

AC11S, B50/70
HMT22, B70/100 Gasperini & Special Filler

Gravel-Sand
100% crushed

Mixture Tests



Data

$d_o=150\text{mm}$
 $d_i=50\text{mm}$
 $T=5\ldots40^\circ\text{C}$
 $f=0.01\ldots10\text{Hz}$
 $h<100\text{mm}$

LCPC-WT

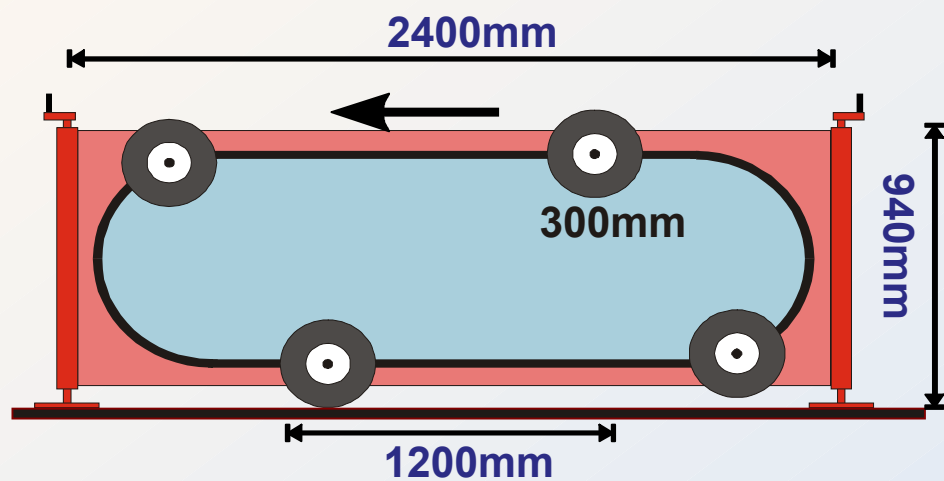


Data

$T=1\ldots10\text{min}$

$L \times W \times H = 500 \times 180 \times 100\text{mm}$
 $v=2\text{ Passes/s} = 2\text{Hz}$
 $N=7200\text{ Passes/h}$
 $N_{\max}=30'000\text{ Passes}$

MMLS3- Principle



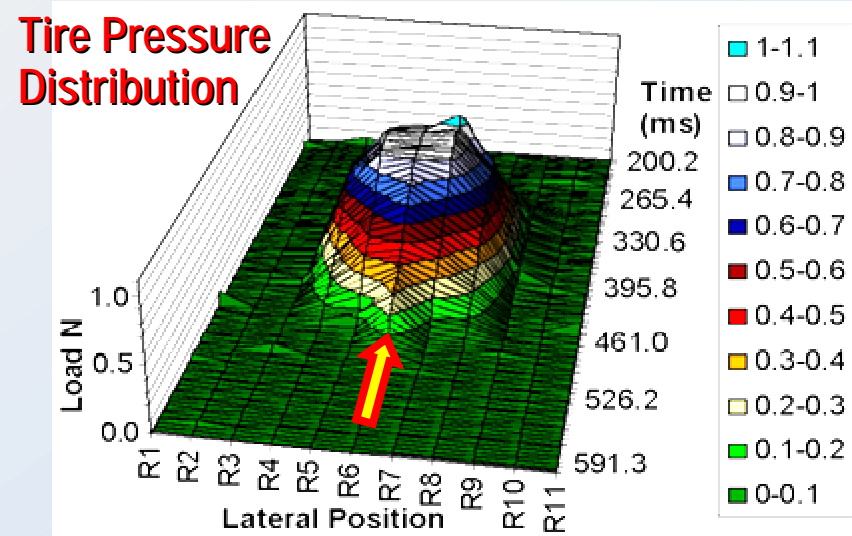
Data

$I=2400\text{mm}$

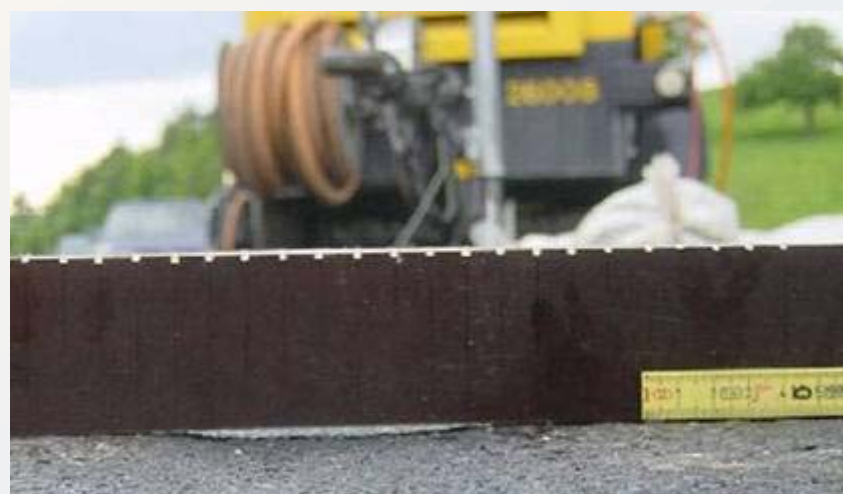
$D=300\text{mm}$

$p=60\text{kg/mm}^2$

$v=3\text{m/s} = 9\text{km/h}$
 $N=7200 \text{ Passes/h}$
 $N_{\max}=72'000 \text{ Passes}$
 Lateral wandering: No

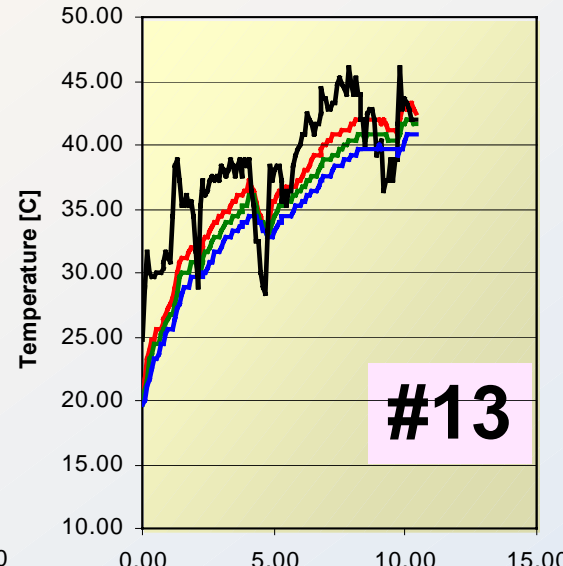
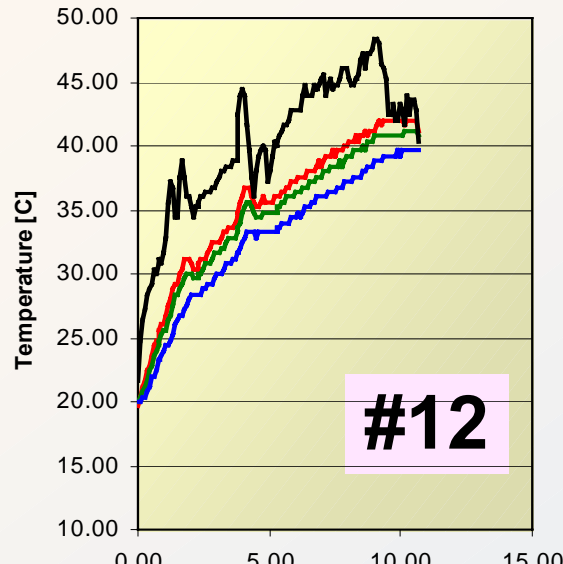
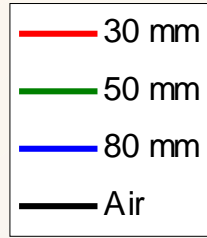


MMLS on A2 (Basel) & Circular Track @ EMPA



MMLS3 Pavement Temp.

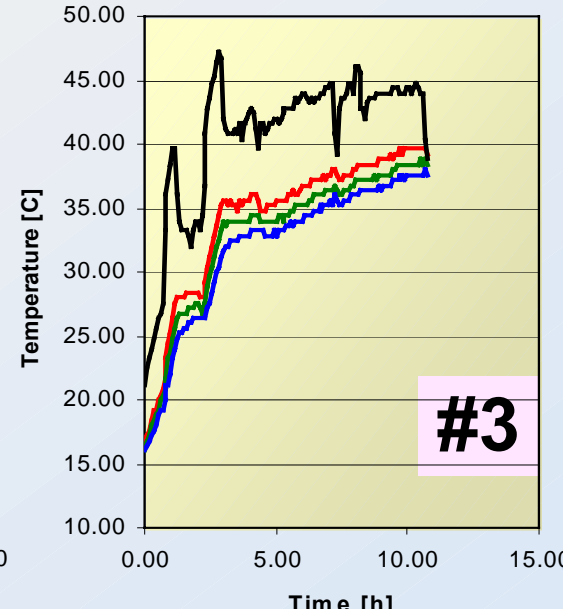
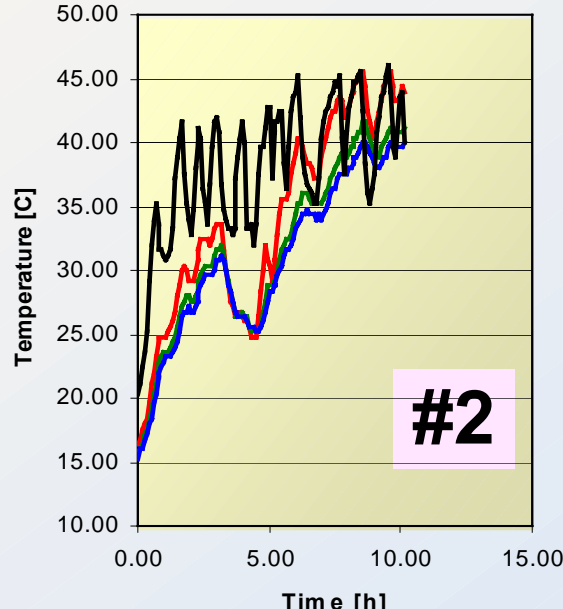
A2
Motor-way



Temp.
Range in
3cm Depth:

#12
(20...42°C),
#13
(18..43°C),

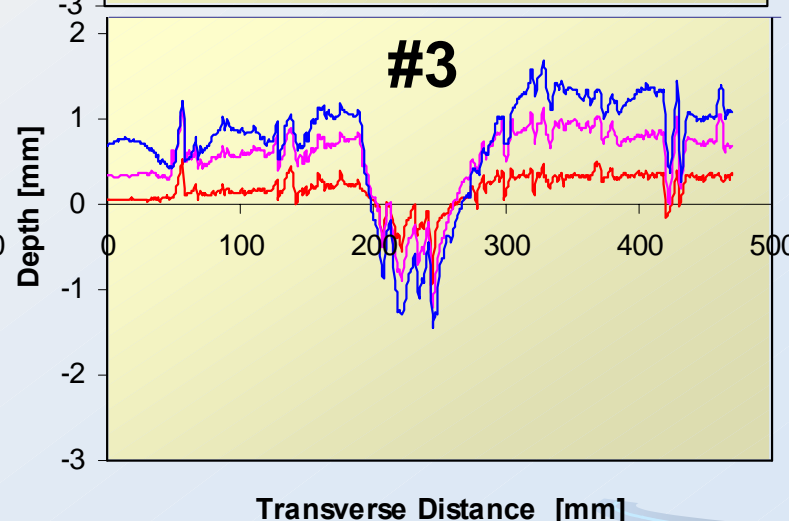
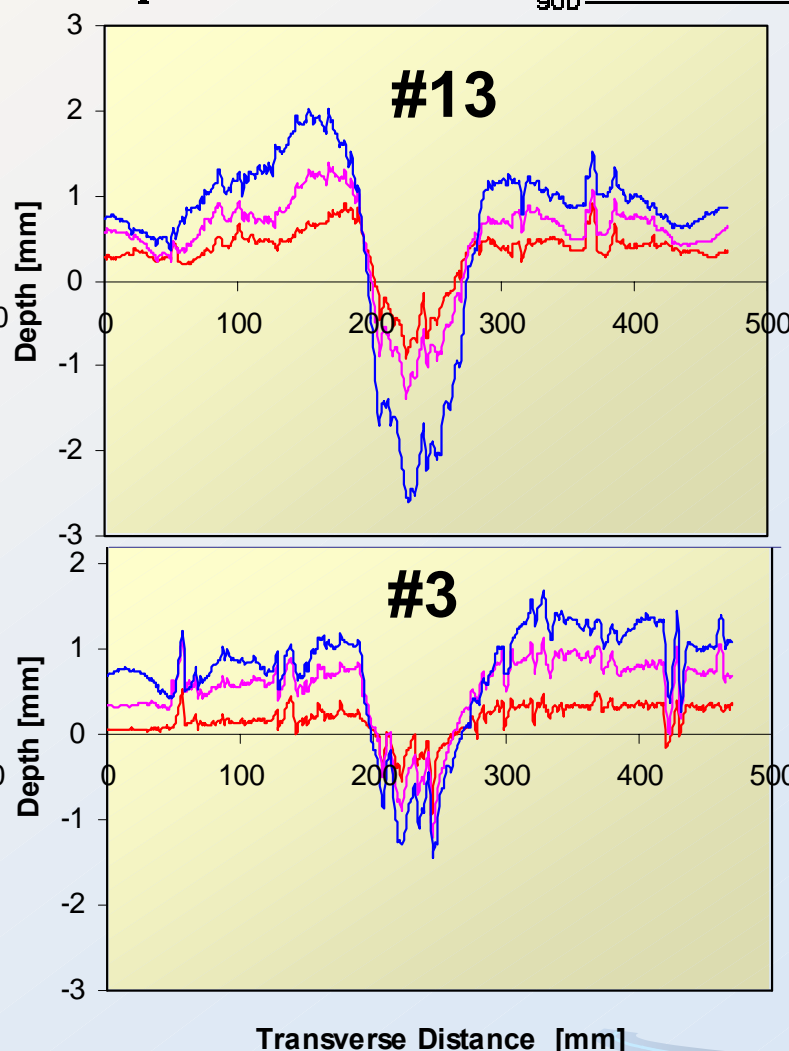
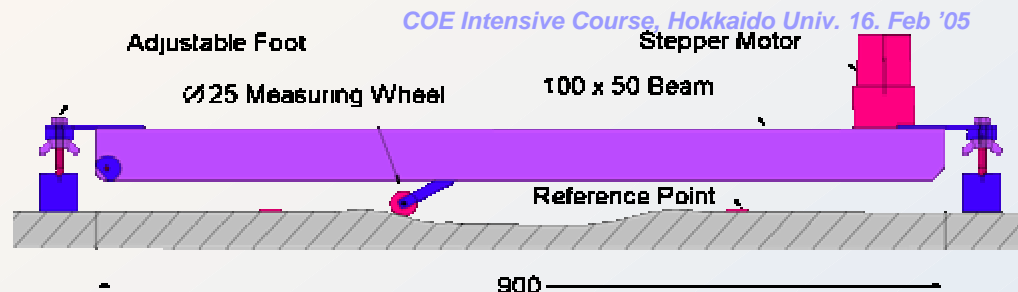
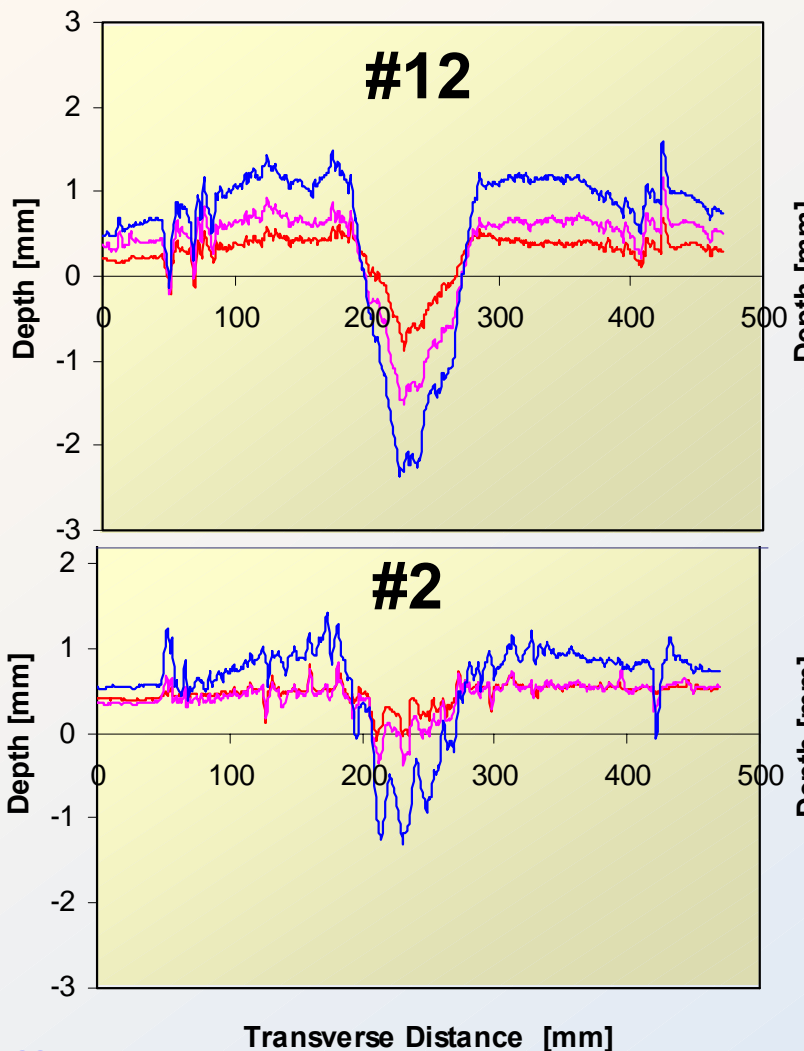
Circular
Test
Track



#2
(13.6...45°C),
#3
(15.2...39°C)

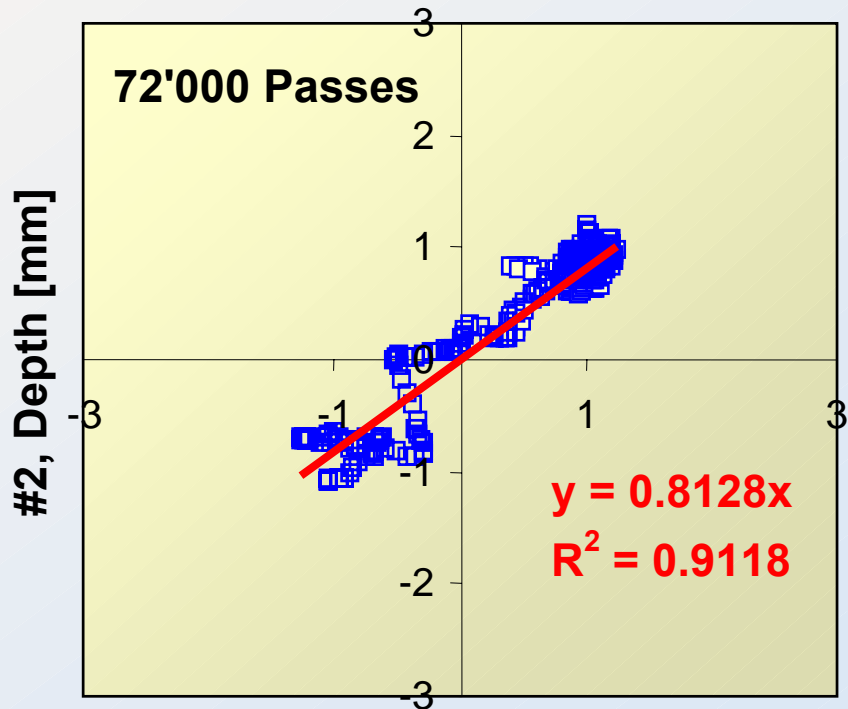
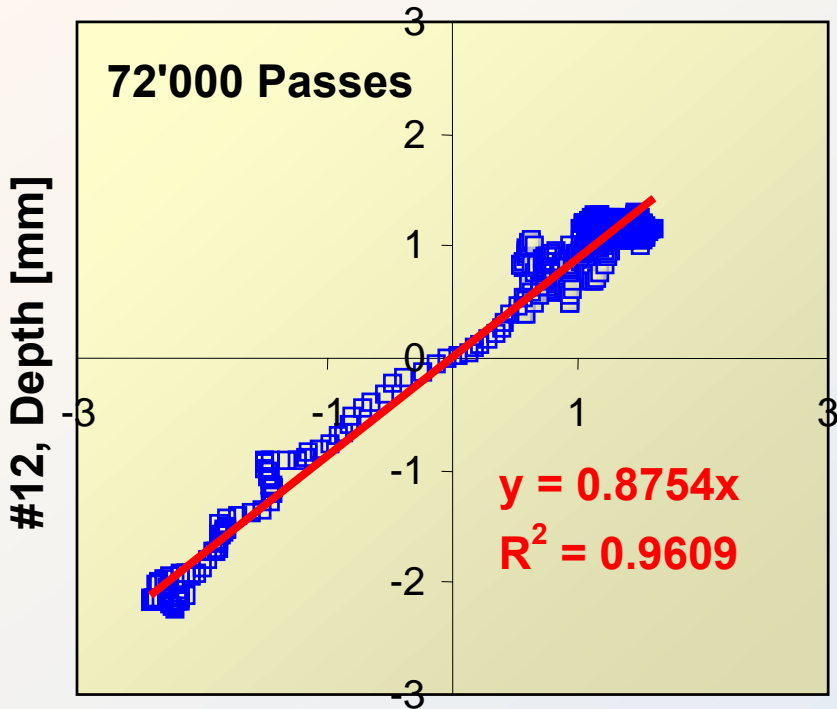
Results MMLS

#12, #13 Motorway A3
#2, #3 Circular Test Track



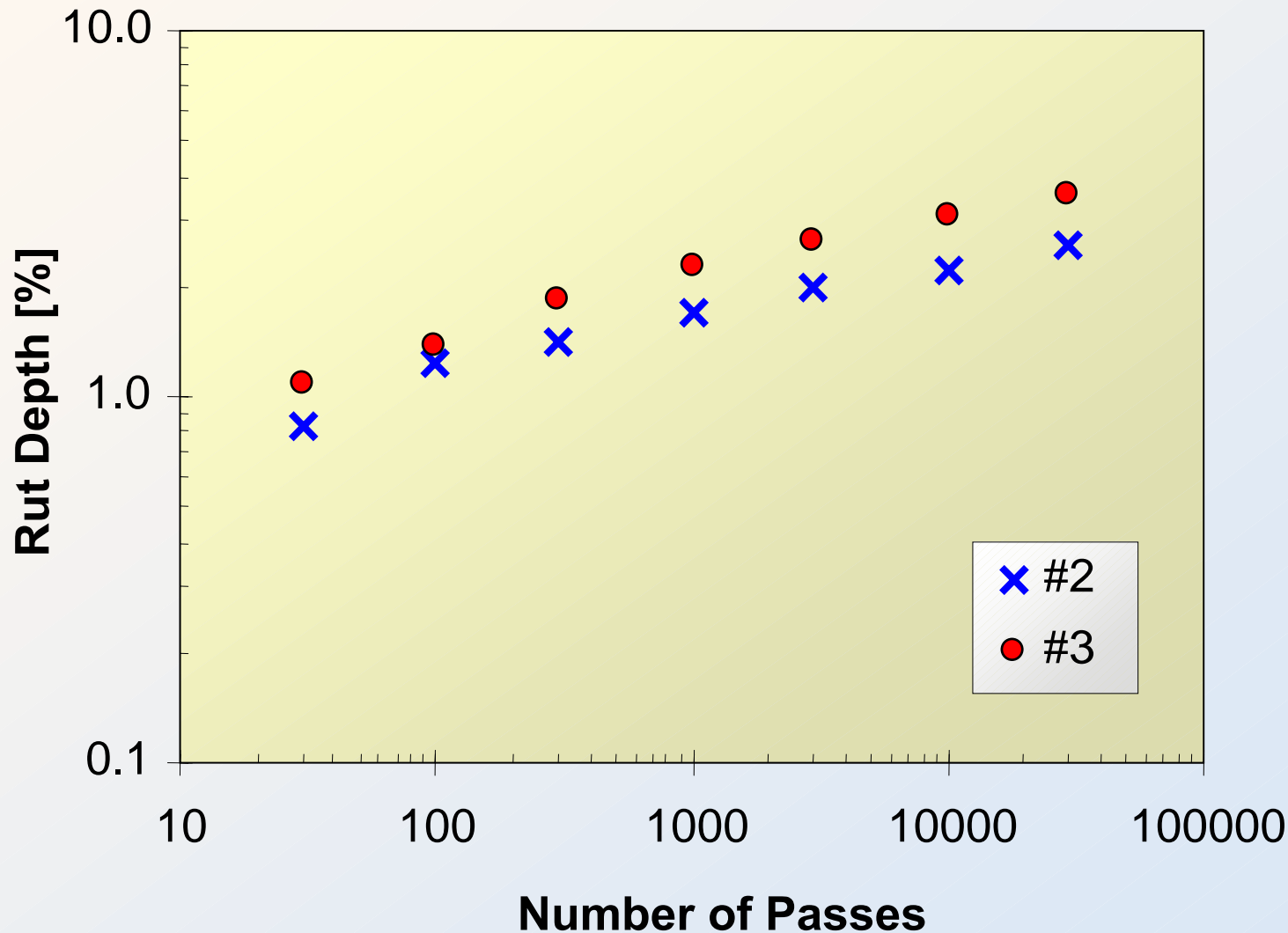
MMLS Rutting Circular Track /Section

#12, #13 Section; #2, #3 Circular Track



- Sections generally more deformation than circular track
- #12,#2 less rutting than #13,#3 mixture in both cases

LCPC Rut Test of Compacted Mix



Comparison Field & Lab Testing

Section	Cross Section Rut of MMLS ca.15..43C	Rut Depth LCPC Rut Test 60°C, 30'000 Passes	DSR 40°C, 2 Hz	CAST 40 °C, 2 Hz
	[mm ²]	[mm]	[MPa]	[MPa]
#12 (road)	154	-	0.0967	239
#13 (road)	171	-	0.0703	188
#2 circular track	75	2.56	0.0967	-
#3 circular track	84	3.55	0.0703	-

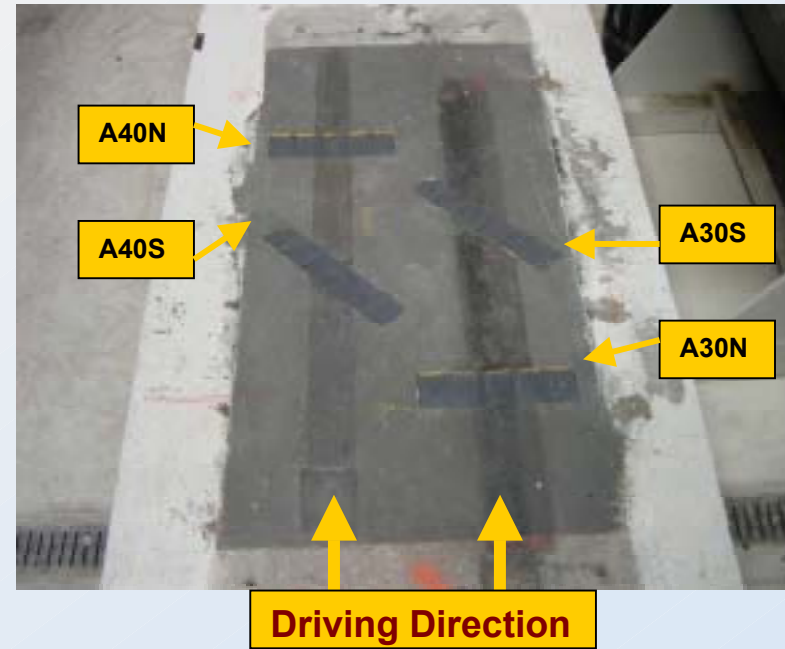
Ratios of „Soft“ : „Stiff“ Mix

MMLS rut area [mm ²] ca 15..43°C, Ratio (#13/#12)	1.11
MMLS rut area [mm ²] ca 15..43°C, Ratio (#3/#2)	1.12
LCPC rut depth 60°C [mm], Ratio (#3/#2)	1.39
DSR 40°C, 2Hz G* [MPa], Ratio (#3/#2) ⁻¹	1.38
CAST 40°C, 2Hz G* [MPa], Ratio (#3/#2) ⁻¹	1.27

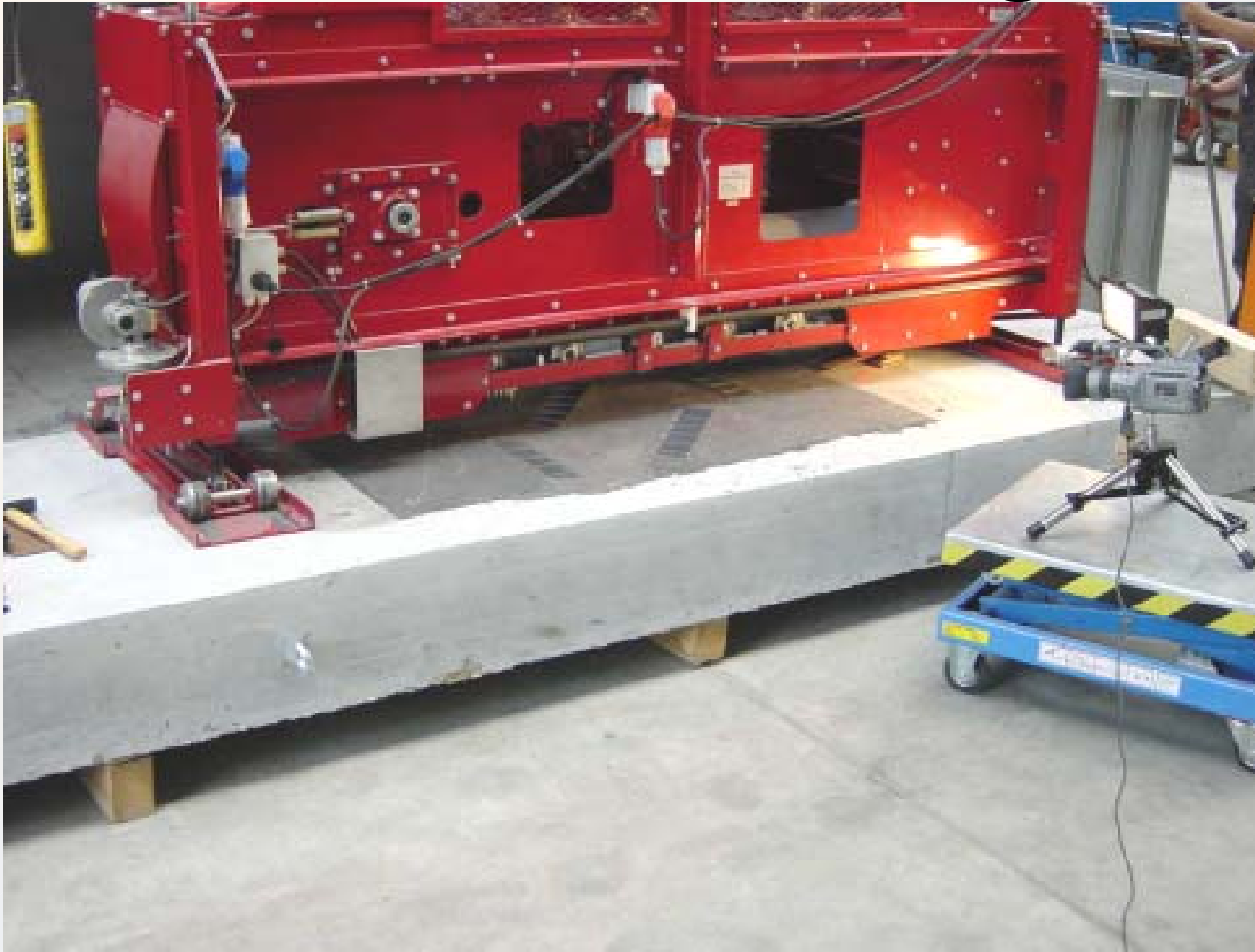
Reflector Testing

Test Program

- MMLS Tests 200'000 cycles at 30°C and 40°C
- Series A: Reflectors applied on old asphalt slab
- Series B: Reflectors applied on new asphalt slab
- Reflectors tested diagonal and rectangular



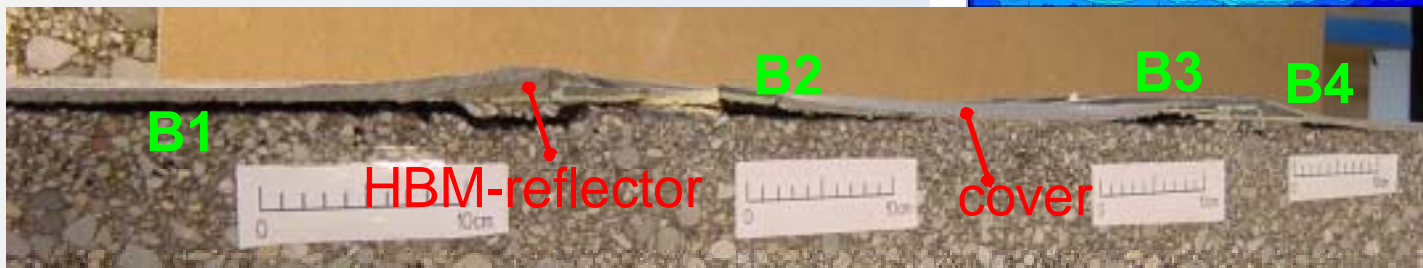
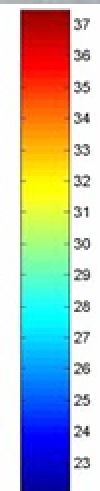
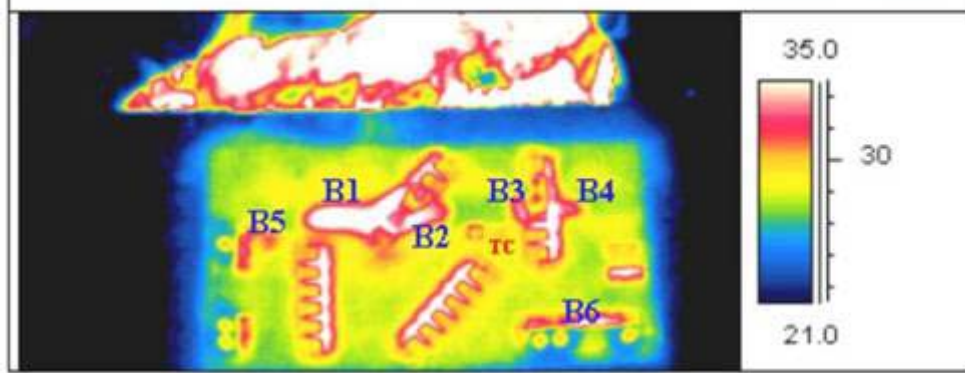
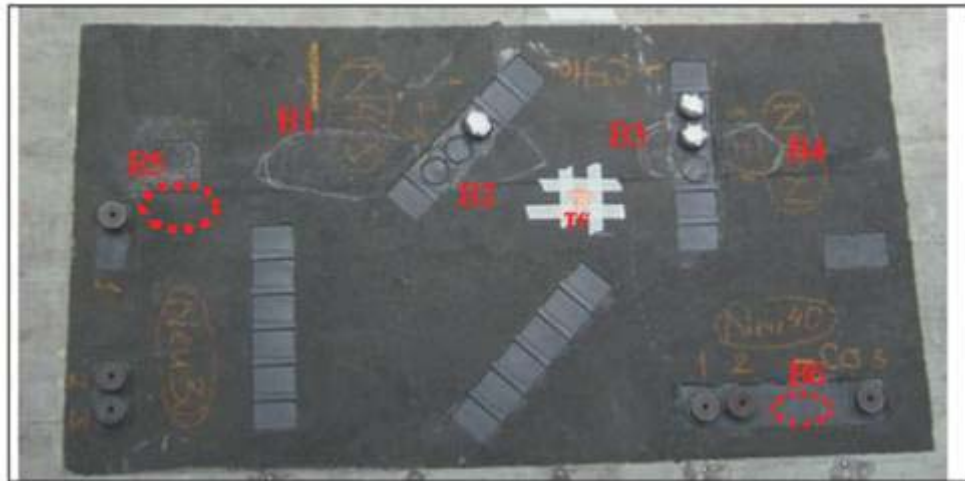
Reflector Testing



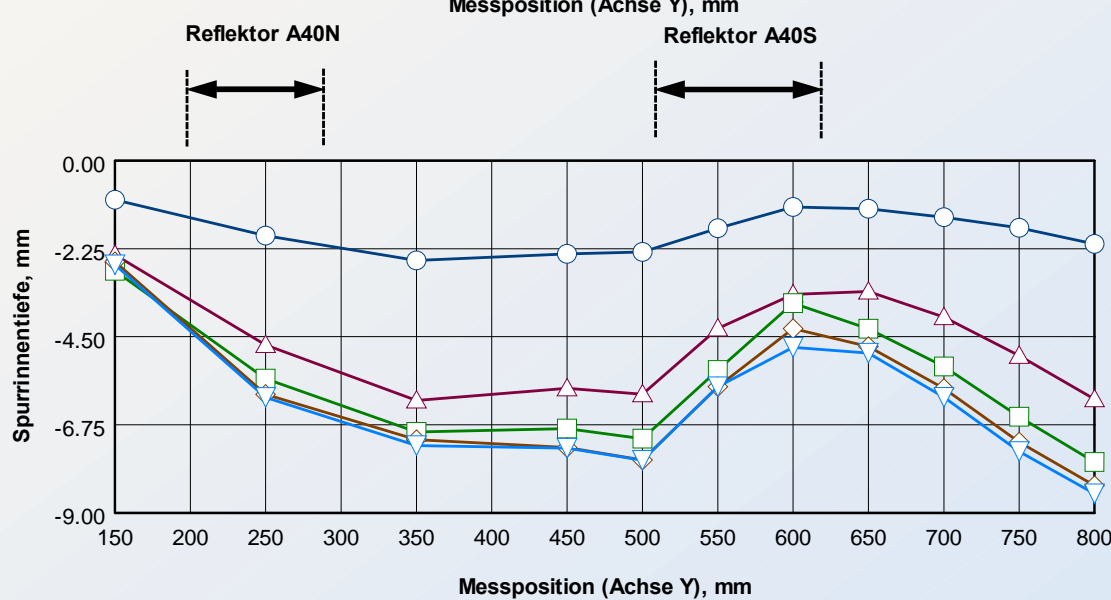
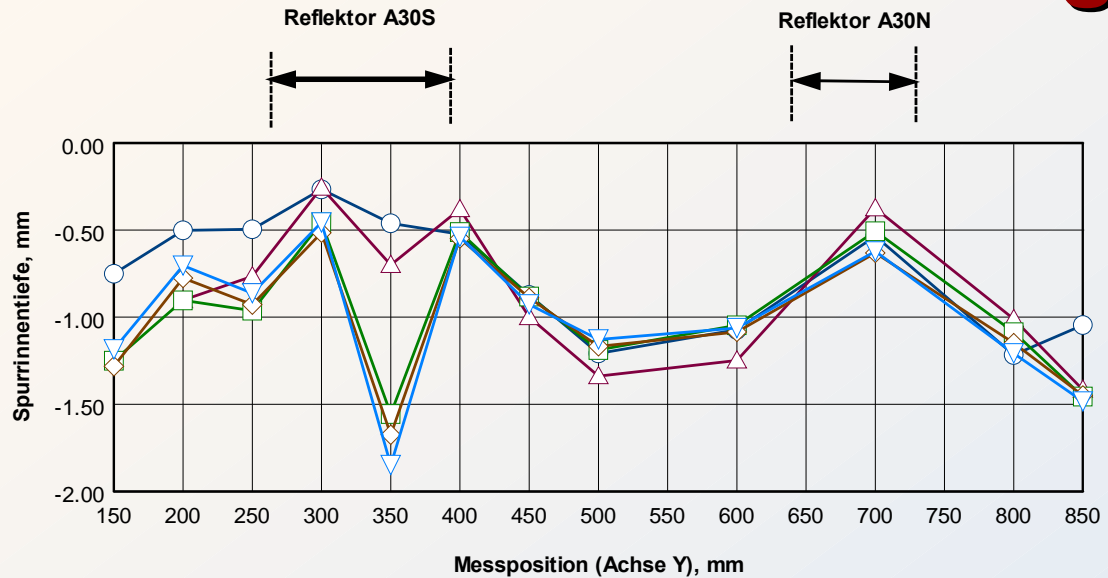
Reflector Damage MMLS3

COE Intensive Course, Hokkaido Univ. 16. Feb '05

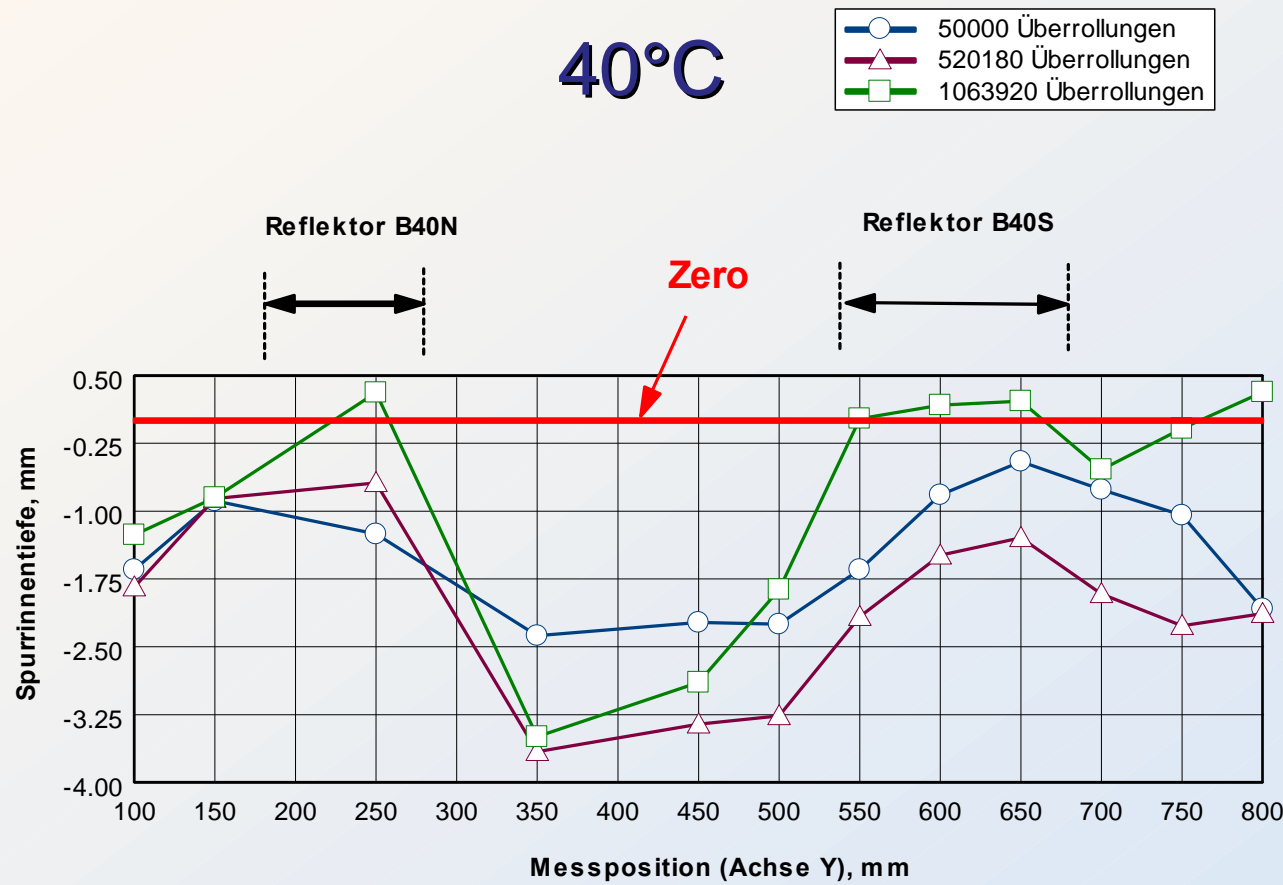
K.Sokolov



Results Series A Length Profile



Results Series B Length Profile



Summary of Results

- MMLS was a very helpful tool for accelerated testing of reflectors.
- Series A (old pavement) behaved successfully after 200000 cycles at 30°C and 40°C
- Series B (new pavement) showed at 40°C delamination of the polymer cover after 50'000 cycles (B3) and 500'000 cycles(B1)
- Surface preparation and primer application before glueing the reflectors is very important

Joints

Contact

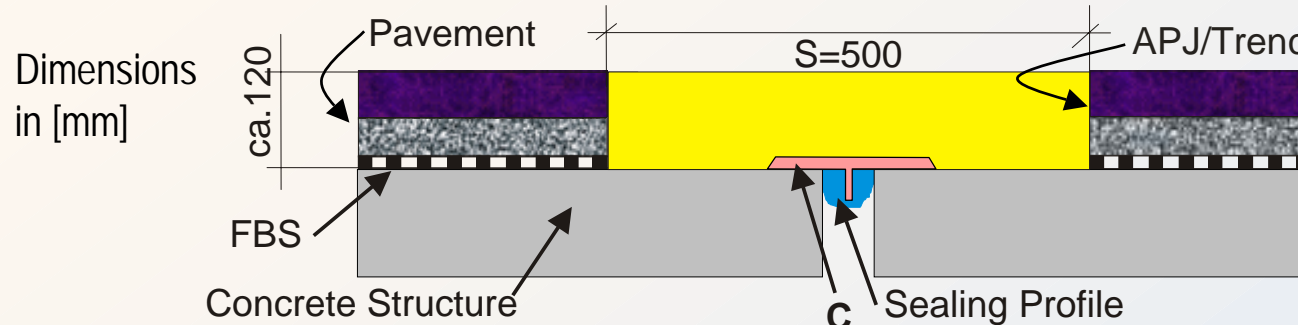
Sivotha Hean

sivotha.hean@empa.ch



Asphaltic Plug Joints for Large Movements

Asphaltic Plug Joint (APJ) Systems

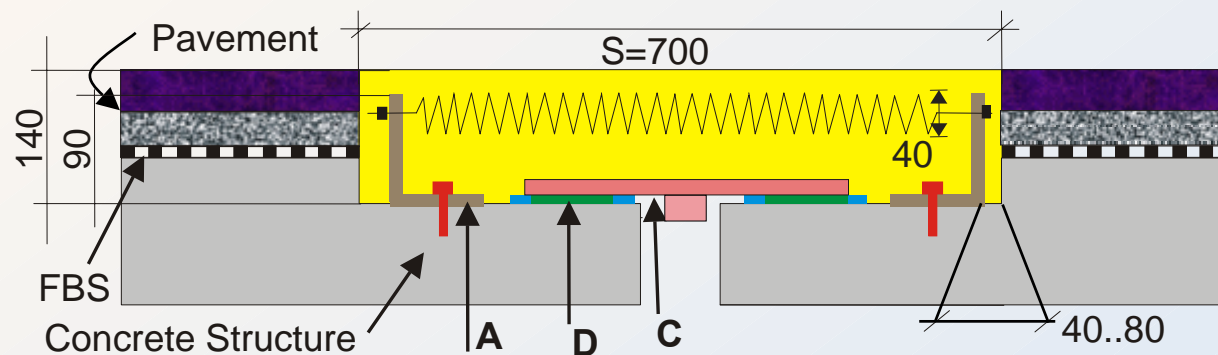


System TJ

S=500 mm

$\Delta W_{max,yr}=37.5\text{mm}$

C: Steel Plate (floating),
FBS: Flex. Bit. Sheet.

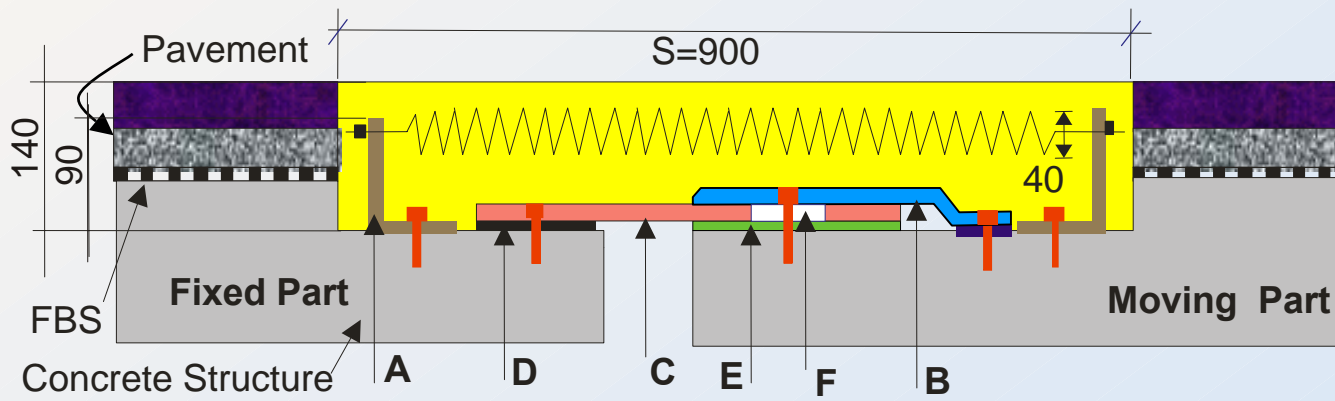


System SJ700

S=700 mm

$\Delta W_{max,yr}=70\text{mm}$

A: Spring Anchor
D: Slider-Bearing



System SJ900

S=900 mm

$\Delta W_{max,yr}=100\text{mm}$

B: Upper Steel Plate,
C: Bottom Steel Plate,
E: Deformation Layer,
F: Slide-Hole

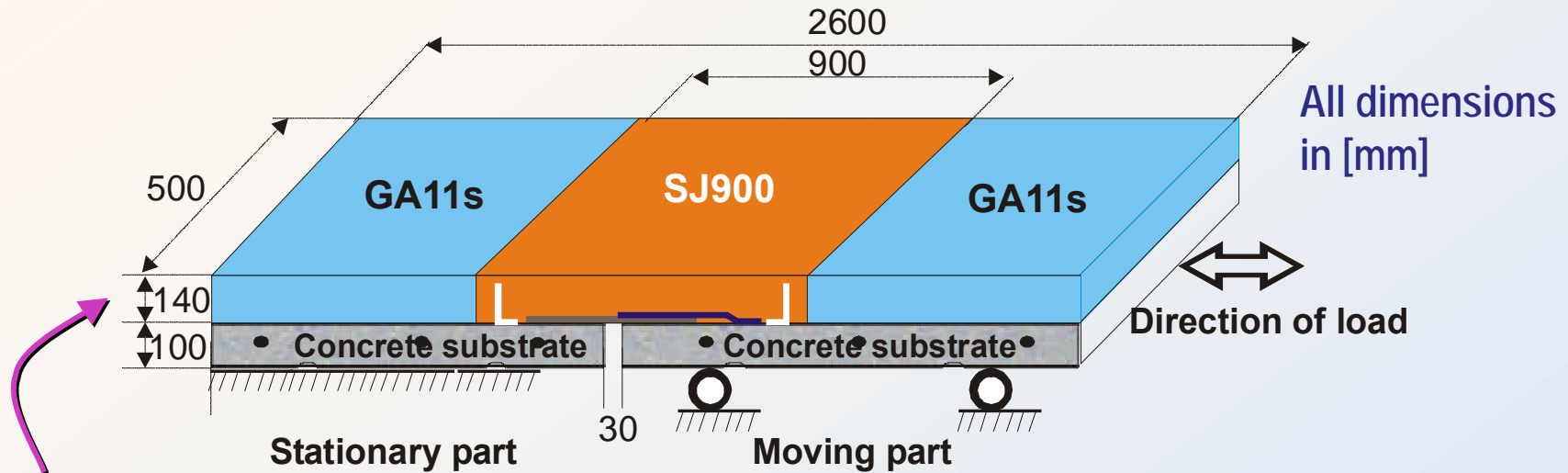
SJ Construction

Example: Montbijou Bridge in front of Swiss Parliament in Bern

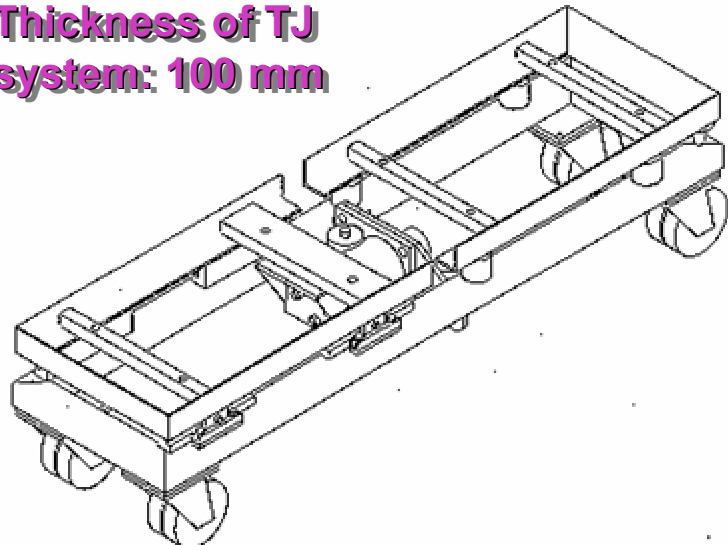




Joint Movement Simulator JMS



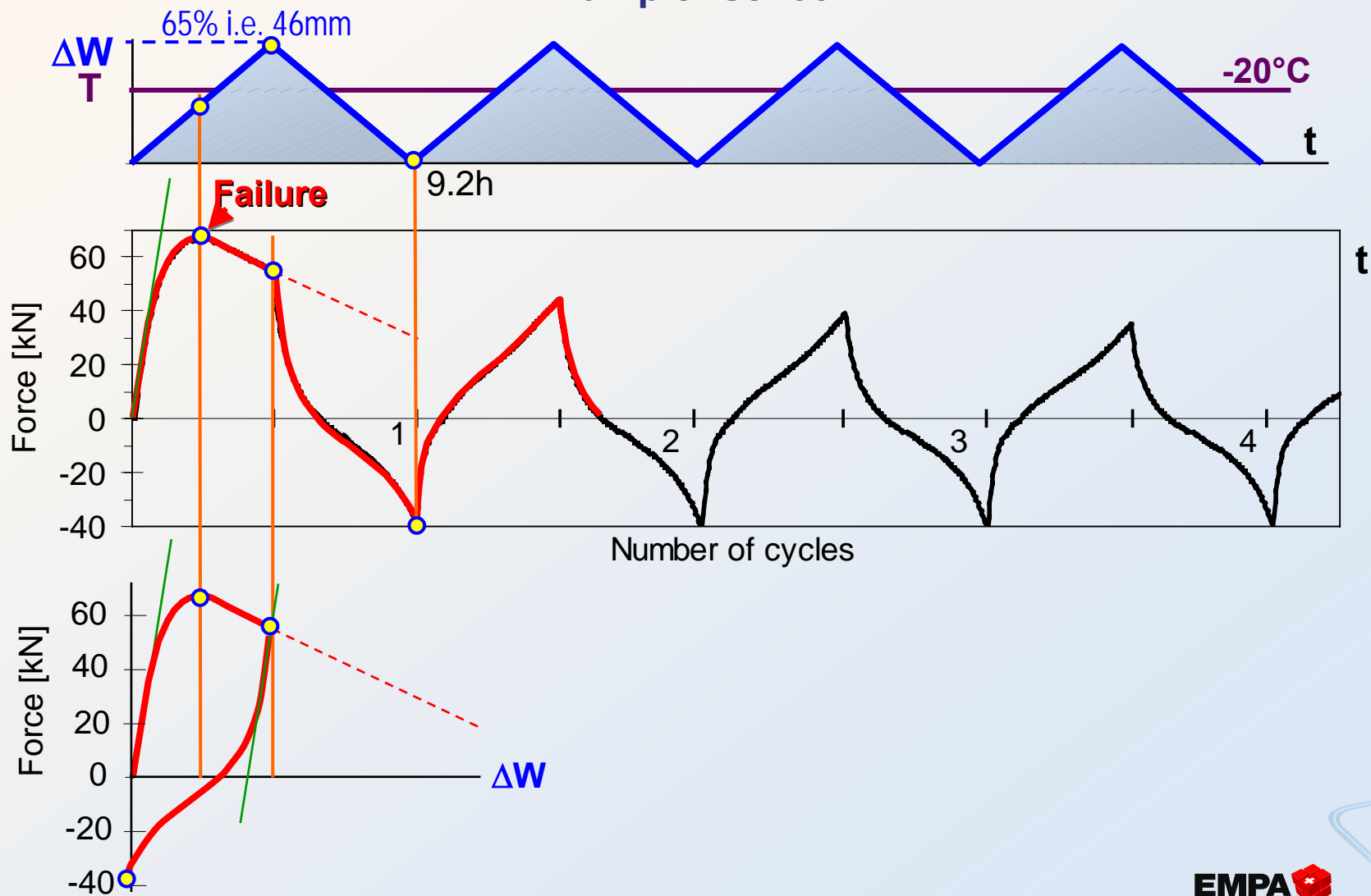
Thickness of TJ system: 100 mm





Typical Force-Time Curve @-20°C

Example: SJ700





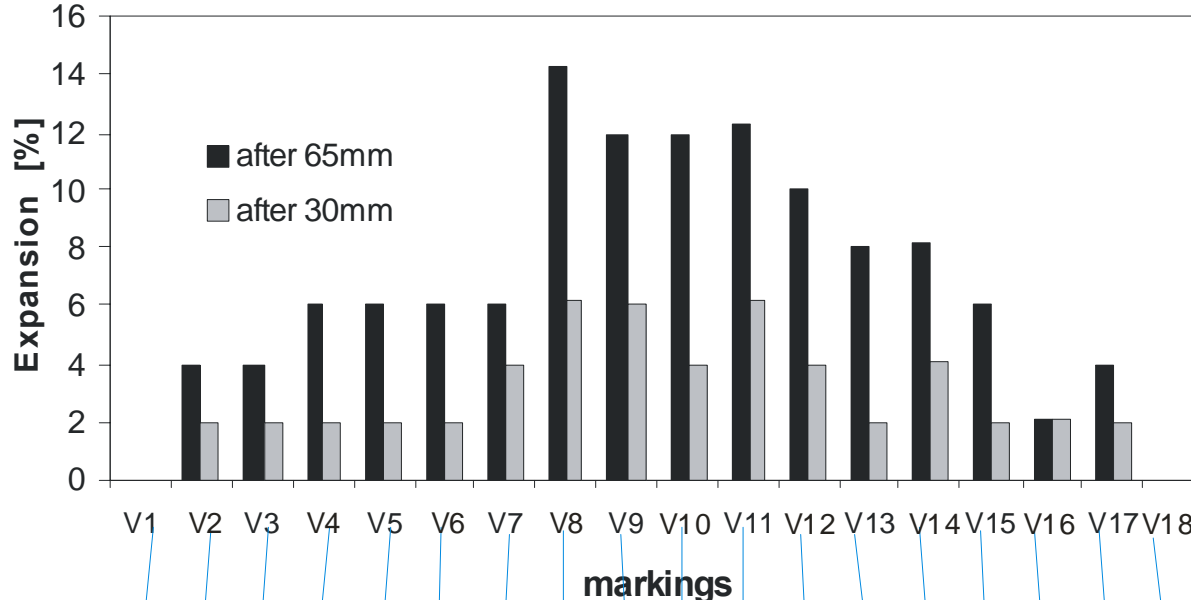
Results of the Quasi-Static Fatigue Test on SJ at Low Temperatures

Number of Specimens	Conditions	Result
SJ900		
2	-20°C , $\Delta W = 65 \text{ mm}$	OK
1	-10°C , $\Delta W = 65 \text{ mm}$	OK
1	-5°C , $\Delta W = 65 \text{ mm}$	OK
SJ700		
1	-20°C , $\Delta W = 46 \text{ mm}$	Cracks after 18 cycles
2	-20°C , $\Delta W = 46 \text{ mm}$	OK

OK = after 20 cycles neither cracking nor de-bonding



SJ900 Horizontal Expansion



L-shaped steel for anchoring the springs

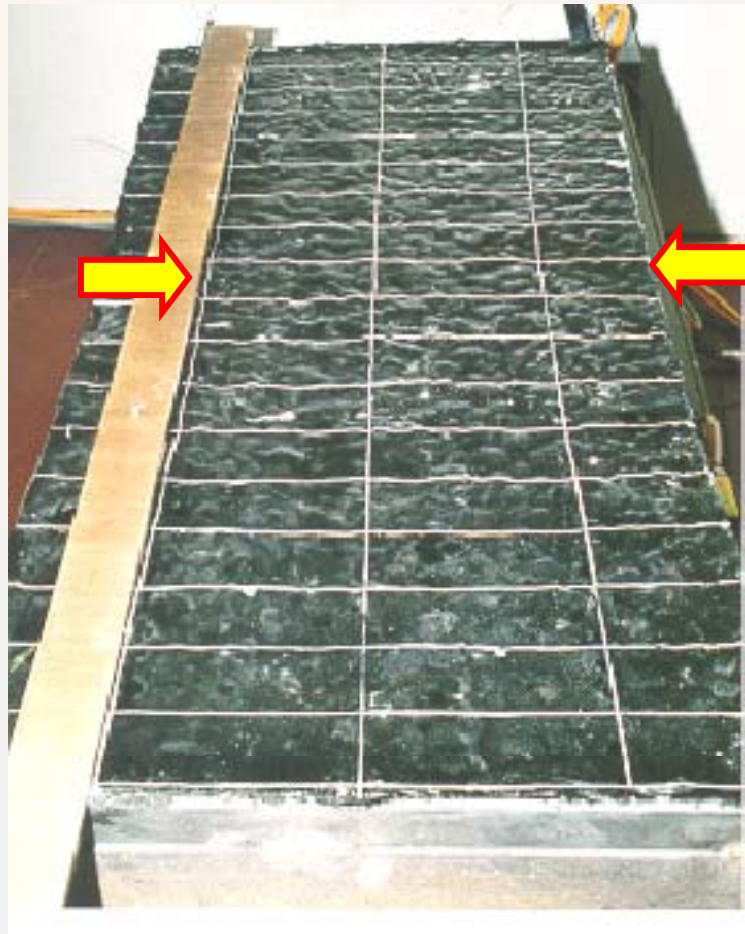
L-shaped steel as substitutes for the adjoining pavement

Horizontal expansion in the APJ at joint openings of 30 mm and 65 mm in the case of an SJ900 test specimen at -20°C

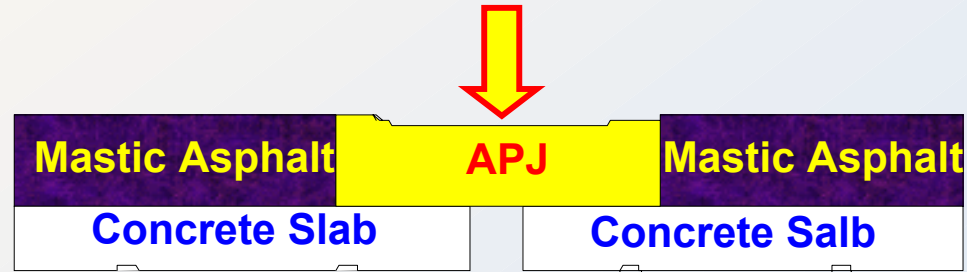


Lateral Contraction during Expansion

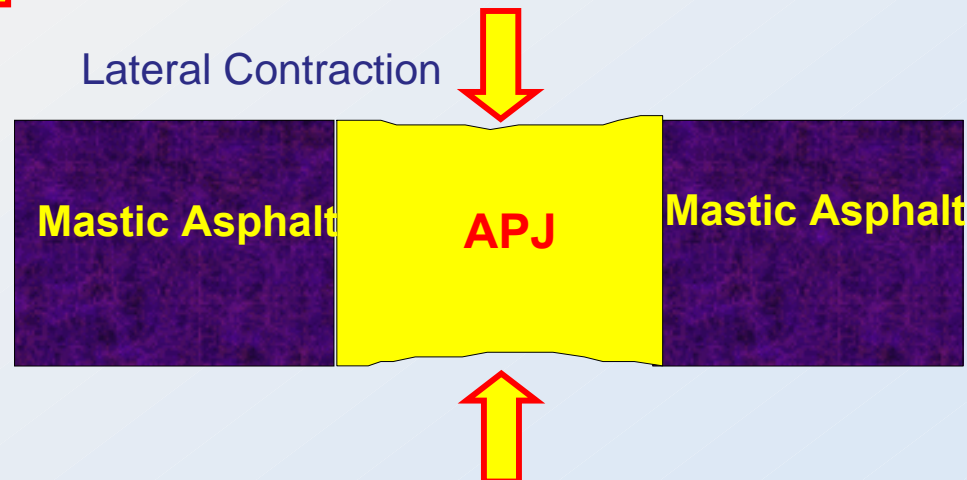
Lateral Contraction during joint opening.



Reduction of Thickness

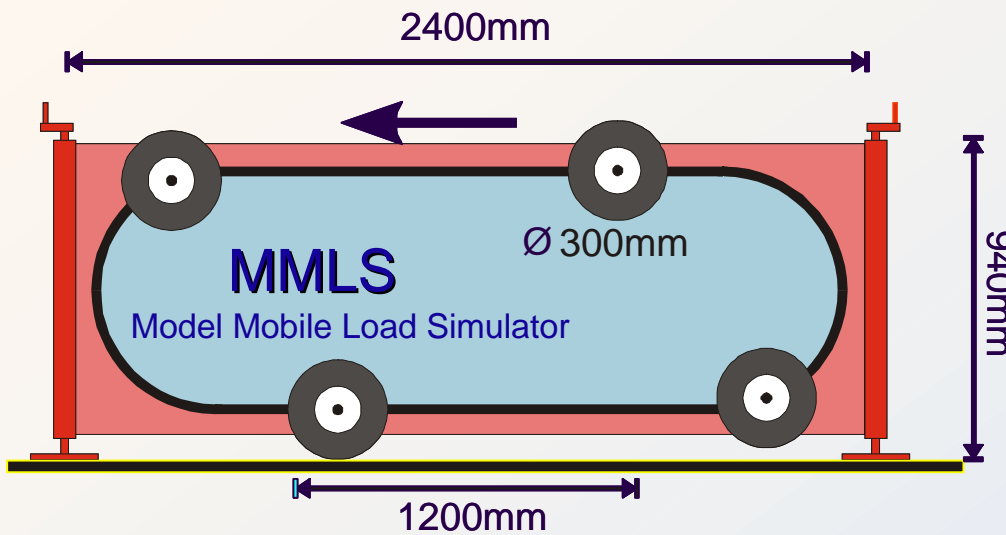


Lateral Contraction





Model Mobile Load Simulator



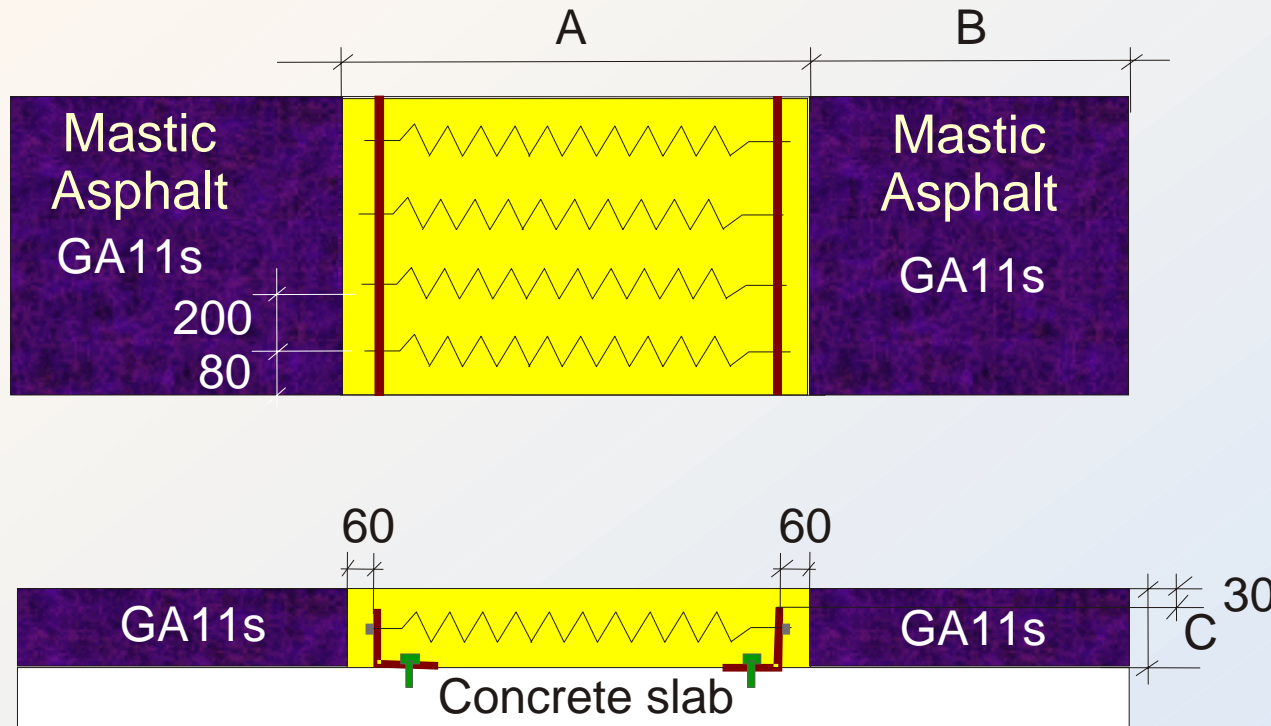
MMLS dimension: 2,400 x 940 mm
Length of the test section: 1.200 mm
Wheel diameter: 300 mm
Tire pressure: 600 kPa
Axe load: 2.1kN
Tire width: 160mm
Passing speed: 78m/s
Number of passings: 15'000
Temp: 23 & 35 °C
Lateral wandering: no (in this study)





Dimensions of the Test Specimen

Dimensions of the test specimens in [mm]



SJ:

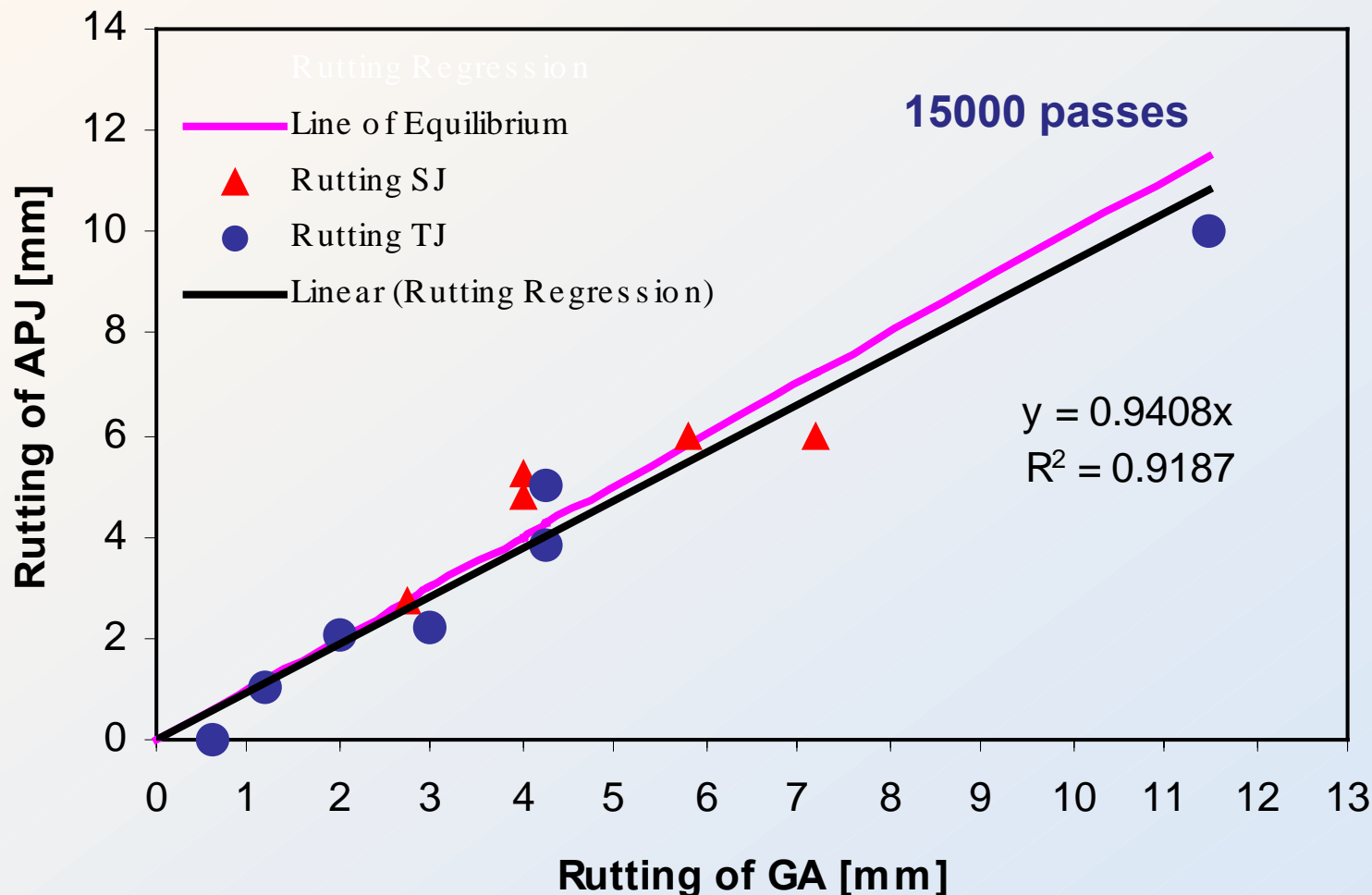
A = 1,000mm
B = 850mm
C = 120mm

TJ:

A = 500mm
B = 1,050mm
C = 100mm



Rutting of GA11s APJ @35°C



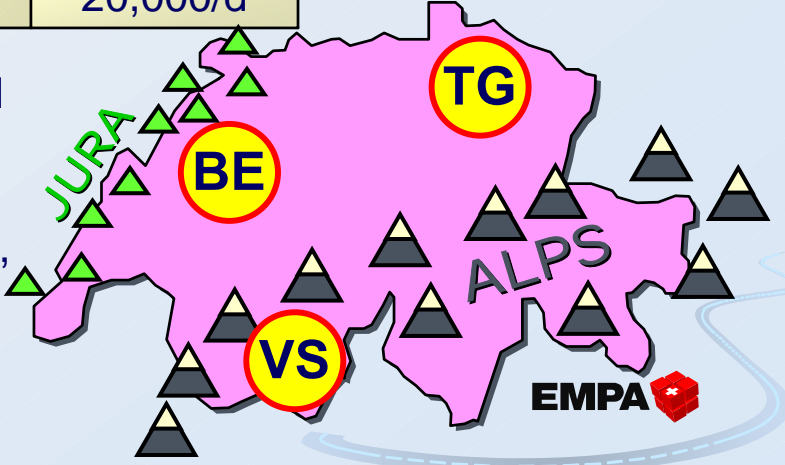


SJ Inspection Sites in Switzerland

Canton	Bridge	Num. of APJ's	Place-ment [yr]	Annual joint movement [mm]	SJ	Traffic
BE	#1	2	1995	65	900	7,000/d
	#2	1	1998		700	Moderate
	#3	1	97/98	60		Average
	#4	2	2000	100	900	22,000/d
VS	#5	4	2001	70	700	*)
	#6	1				
	#6	1		80	900	
TG	#7	4		100		20,000/d

- #1: "Bönzigen"-Ramp,
- #2: St. Johannsen,
- #3: Biel/Alfermée,
- #4: "Monbijou"-Bridge,
- #5: "Hang"-Bridge,
- #6: "Stuckisegg"-Bridge,
- #7: "Thur"-Bridge,

*) 250-800 lorries/d
BE: canton Bern,
VS: canton Wallis,
TG: canton Thurgau,





Visual Assessments of Sites (March/April 2002)

Canton	Bridge	Years under traffic	Water-tight	CR, SS, BL, MD	ES	Partially repaired	Assessment of state
BE	#1	6	Yes	None	None	Yes	Sufficient
BE	#2	4	Yes	None	None	No	Good
BE	#3	5	Yes	None	None	No	Good
BE	#4	2	Yes	None	None	No	Good
VS	#5	1	Yes	None	Moder.	No	Good
VS	#6	1	Yes	None	None	No	Good
VS	#6	1	Yes	None	None	No	Good
TG	#7	1	Yes	None	Moder.	No	Good

CR: Cracking,

SS: Side de-bonding (between pavement and SJ),

BL: Blistering,

MD: Material displacement,

ES: Edge de-bonding between SJ and concrete or metal plate at the bridge cordon or at the centre line of the motorway;

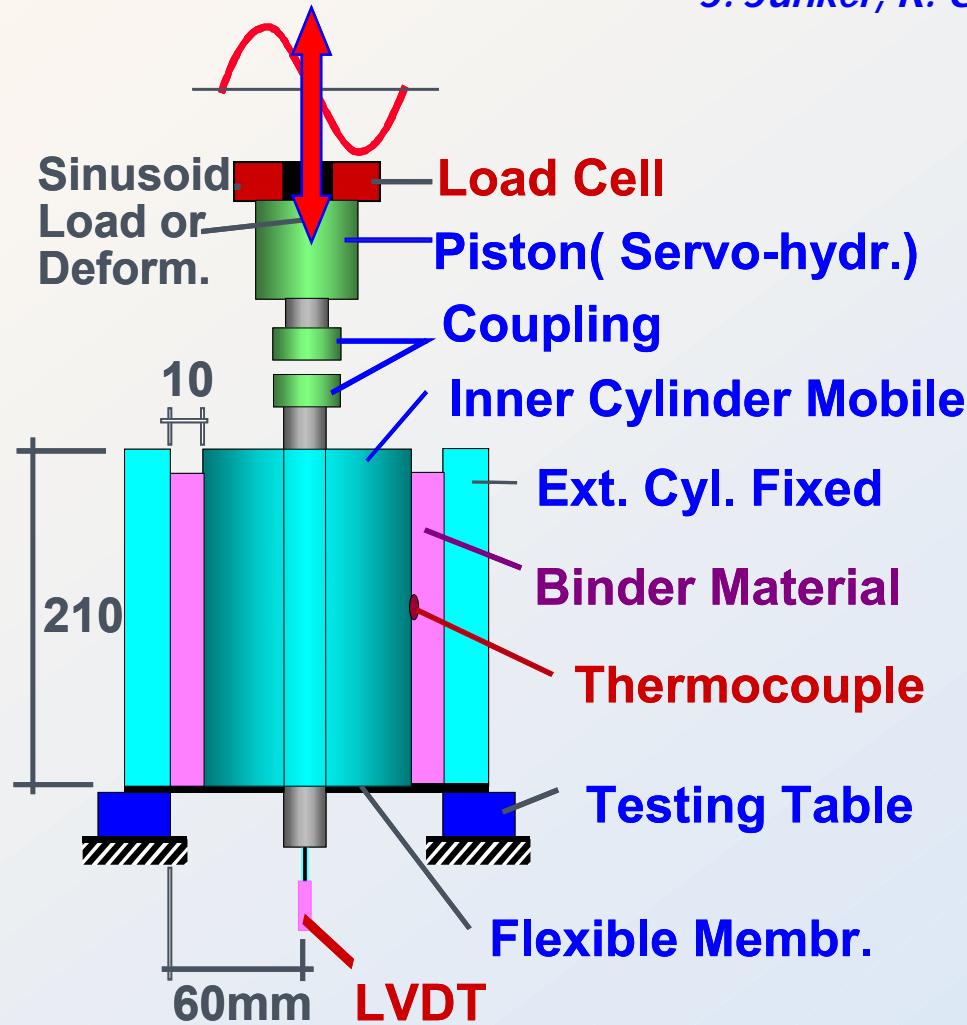
Findings

- The **APJ systems** SJ proved promising regarding certain properties in the lab and performance on site .
- The new SJ systems can be expected to absorb the relevant necessary horizontal joint movements at **low temperature**.
- Positive **rutting** performance is expected from MMLS tests at 35°C with mastic asphalt GA11s, where roughly similar behavior was found for SJ than for the conventional TJ system.
- The SJ sites **inspected** after approx. 1 ... 6 years were intact and evidently fulfilled their function as a joint sealing.
- Experience shows, that **non-substantial defects** from binder accumulation with detached chippings from the surface edging can be avoided by ensuring optimum placement.
- Two relatively new sites suffered **edge stripping** at the bridge cordon and the centre strip. This problem was confirmed by low temperature movement tests where lateral contraction occurred.
- Finally, the site observation confirmed suitability of the relatively elaborate **system tests** conducted at EMPA.

Joint Sealings

CoAxial Shear Test Binder

J. Junker, R. Gubler



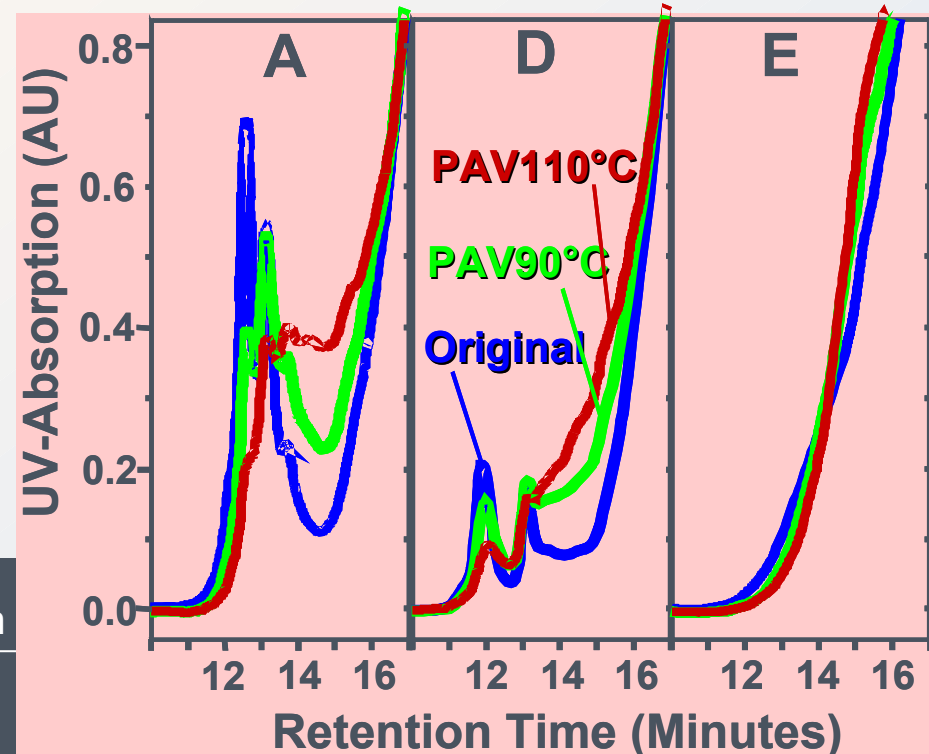
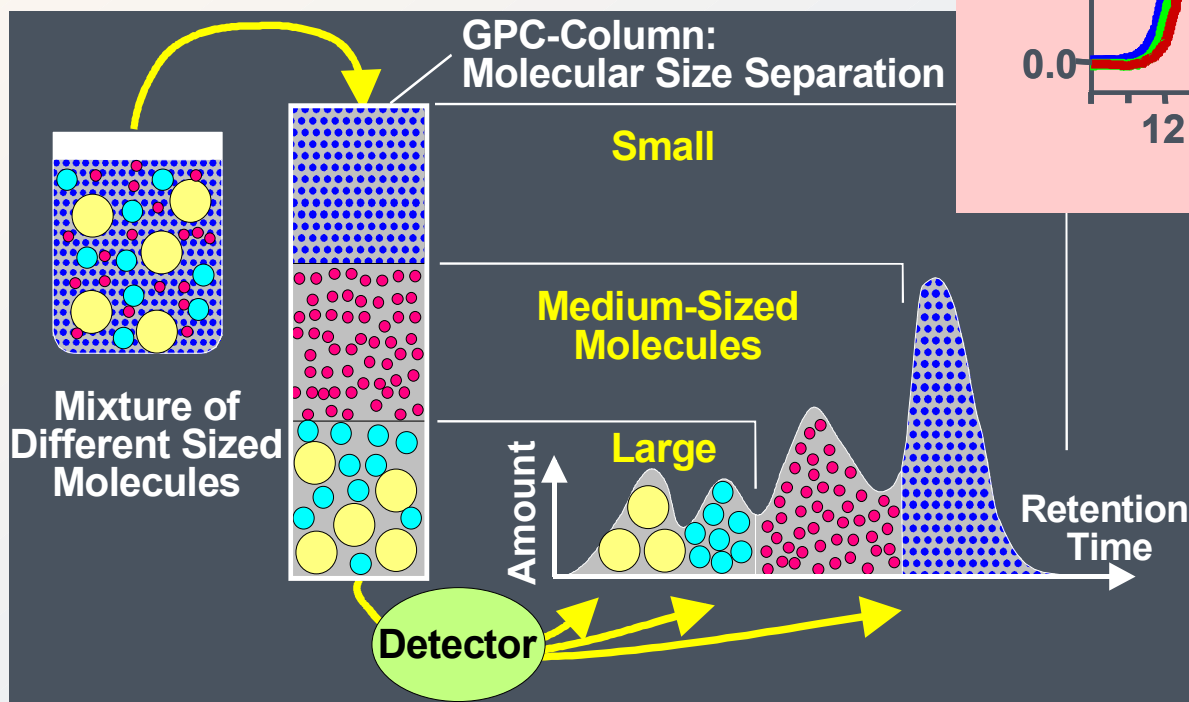
Temperatures:
-20, -15,...,40°C

Frequencies:
0.125, 0.25, 0.5,
1, 2, 2, 4, 8Hz

$$\begin{aligned}G' &= G^* \cos \Phi \\G'' &= G^* \sin \Phi \\\Phi &= \arctan(G''/G')\end{aligned}$$

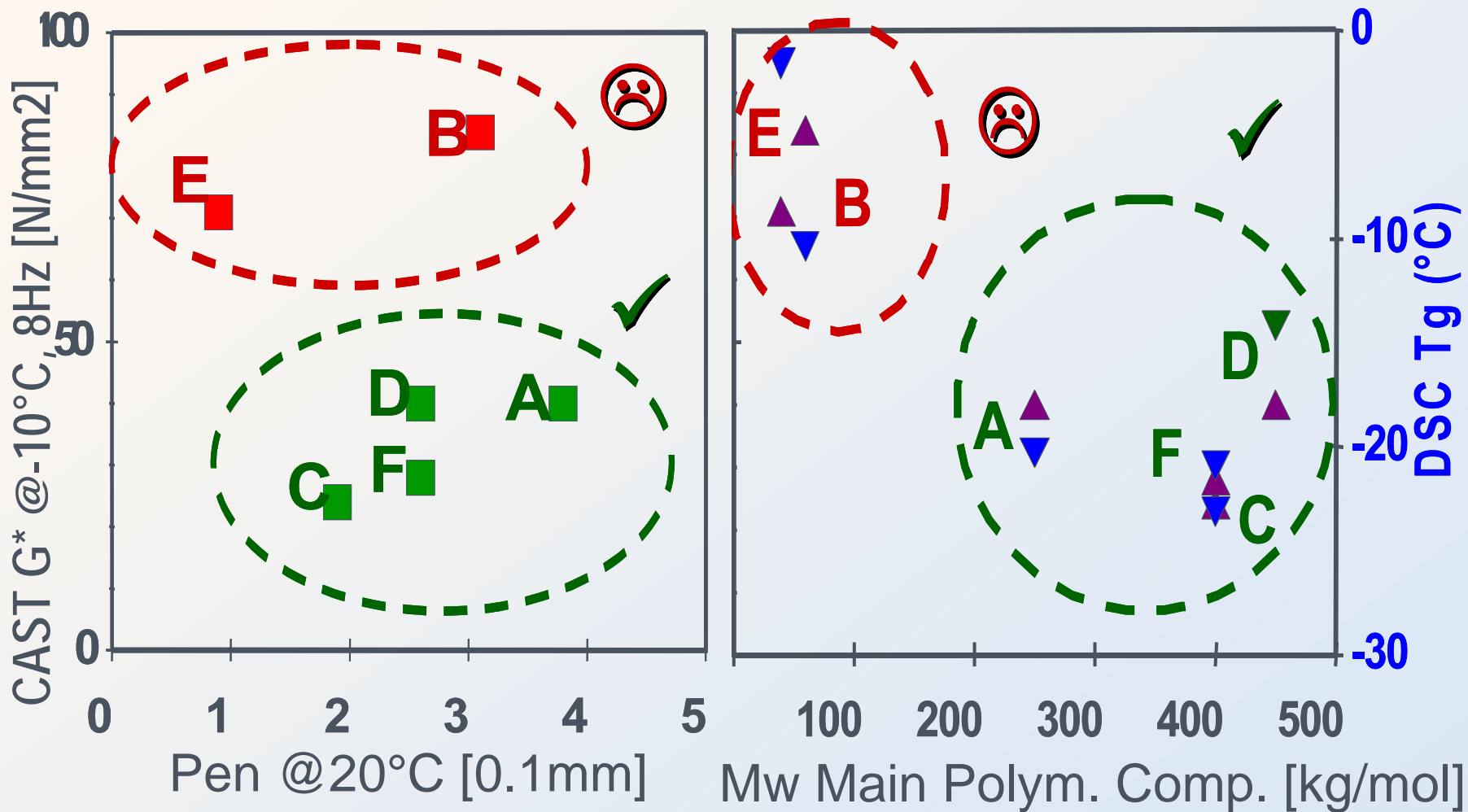
GPC Results

S. Hean



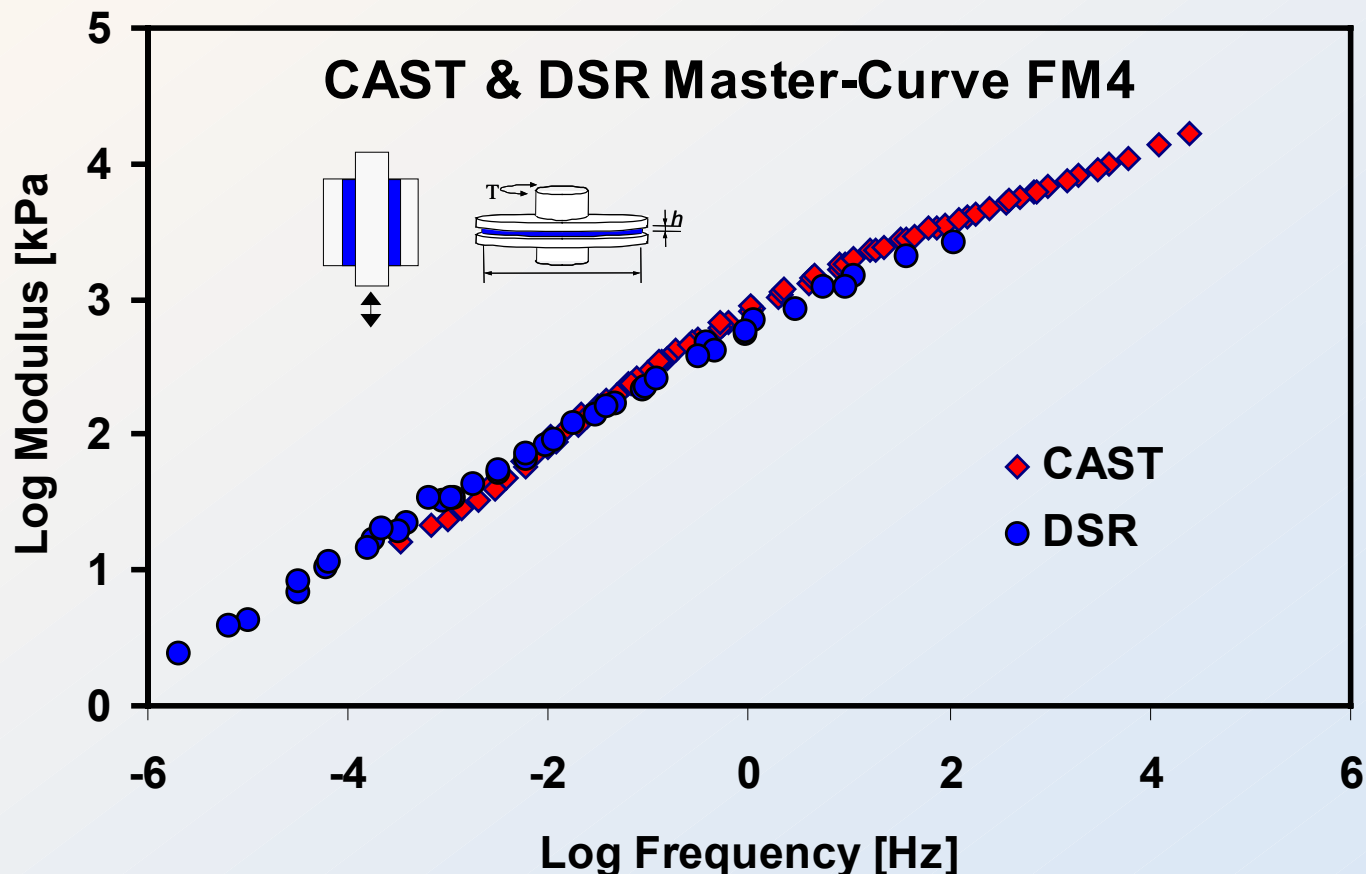
CAST/DSC/GPC/Pen(-20°C)

S. Hean



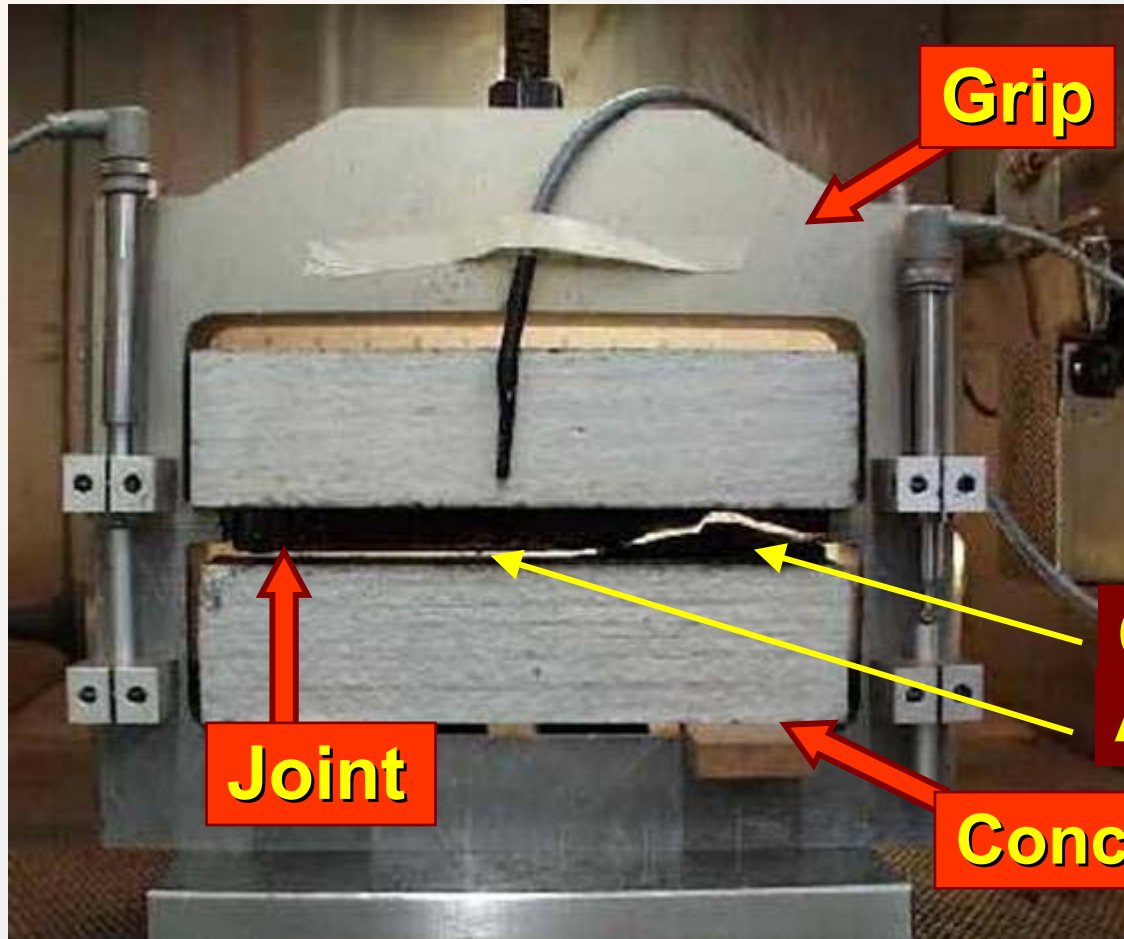
Joint Sealants CAST-DSR

S. Hean



Joint Sealants „LTPP“

- ★ SBS JS1...7; after 0,1,2.5yrs alpine exposure,Expansion Test (Concrete Joints)

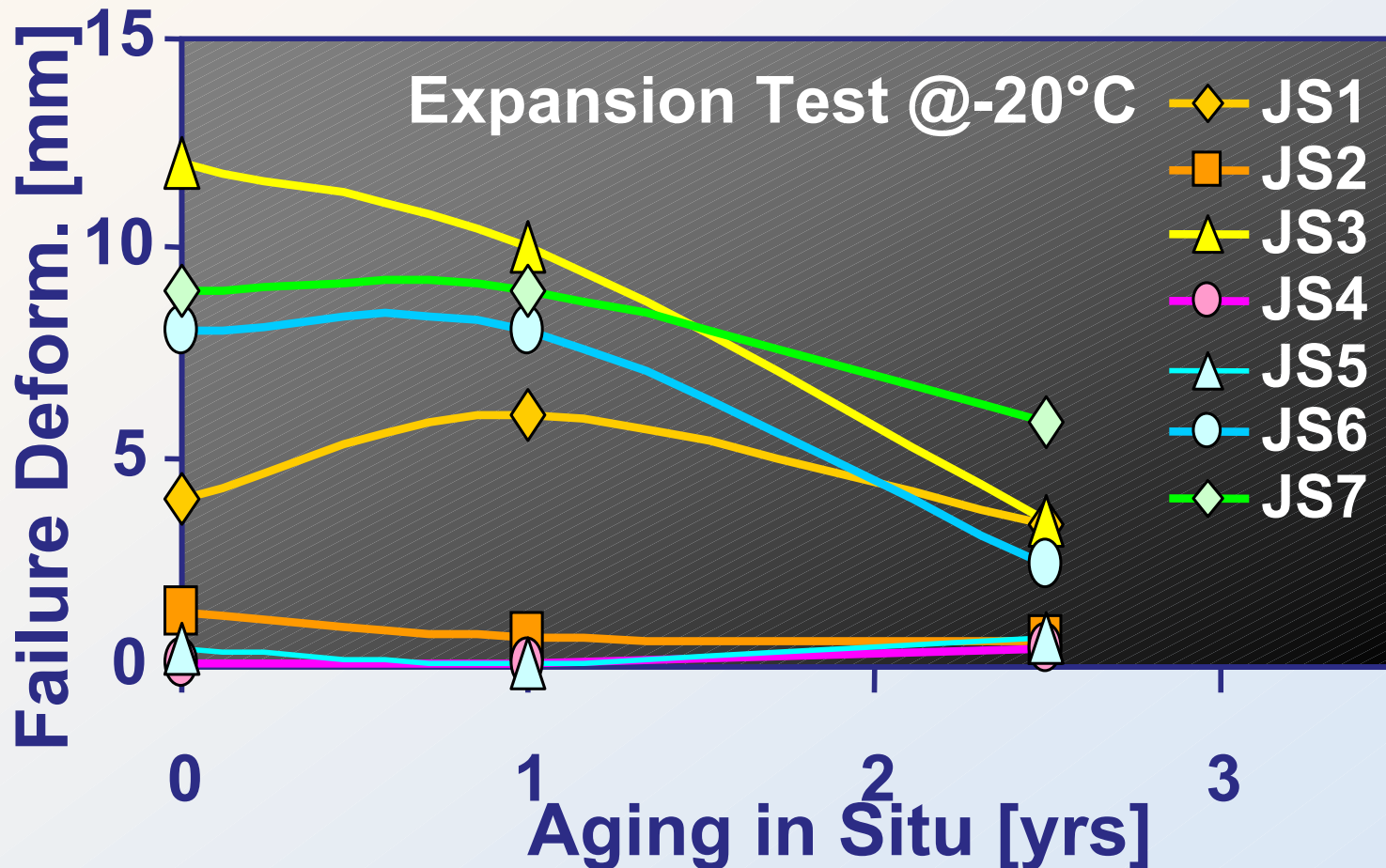


Joint: 150x13x20mm

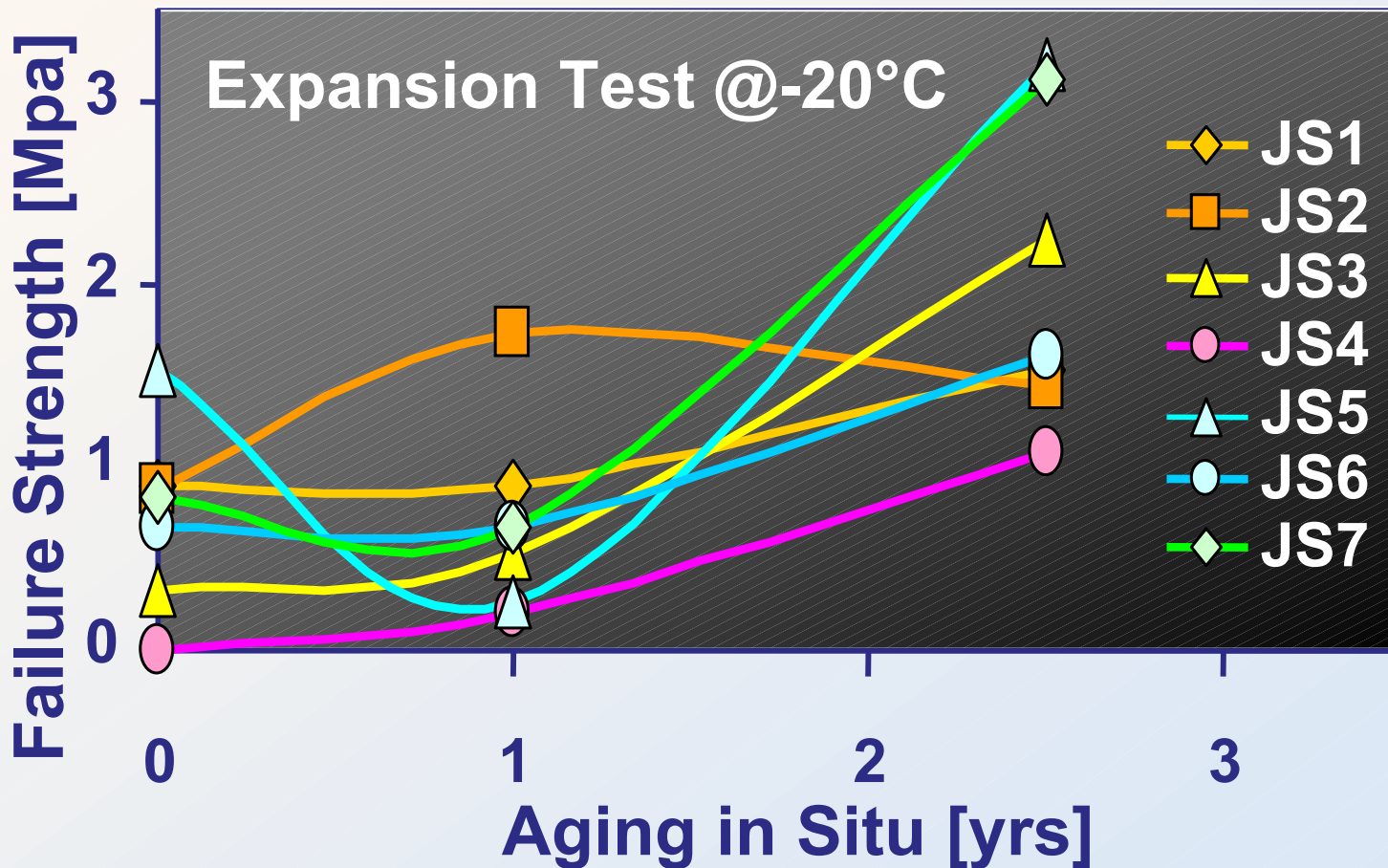
V=3mm/h

From 13mm to 28mm

Concrete Joints (1)

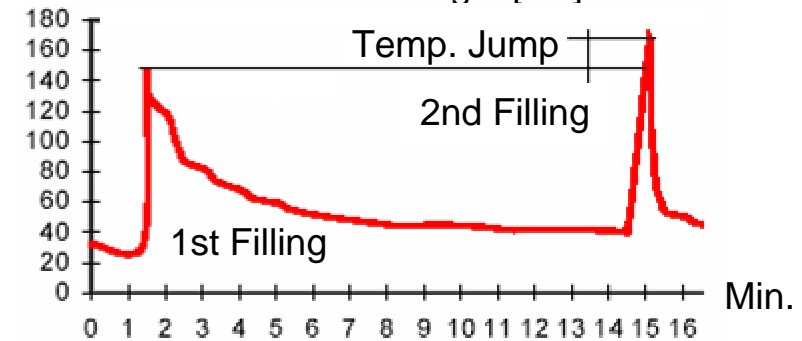
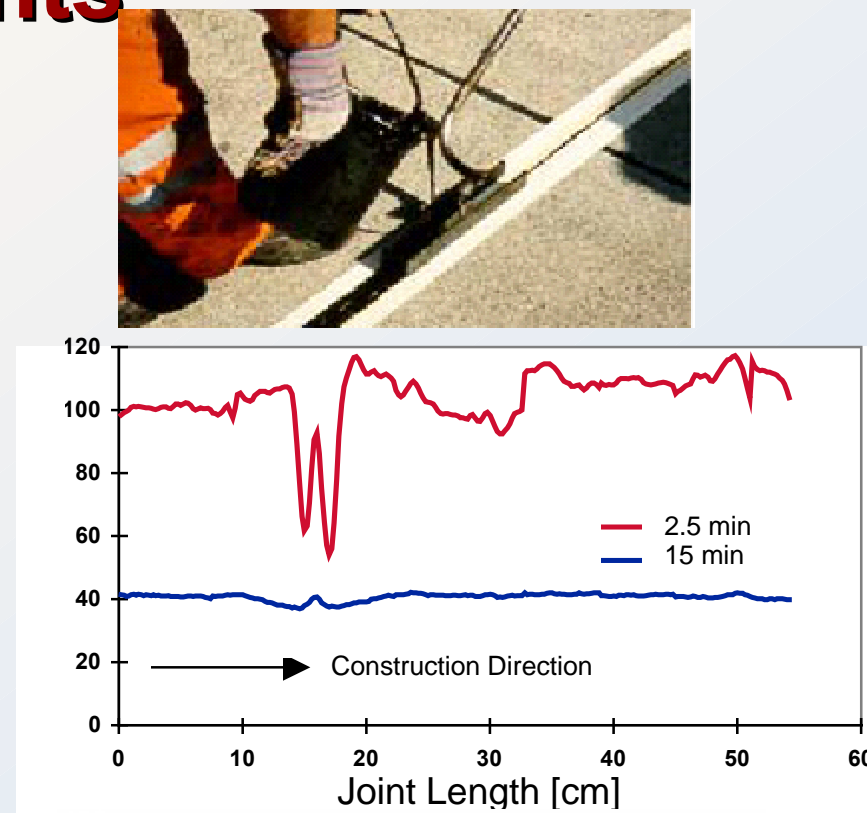
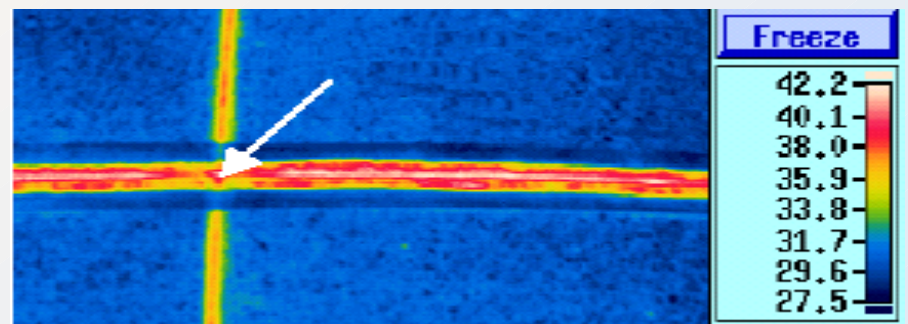
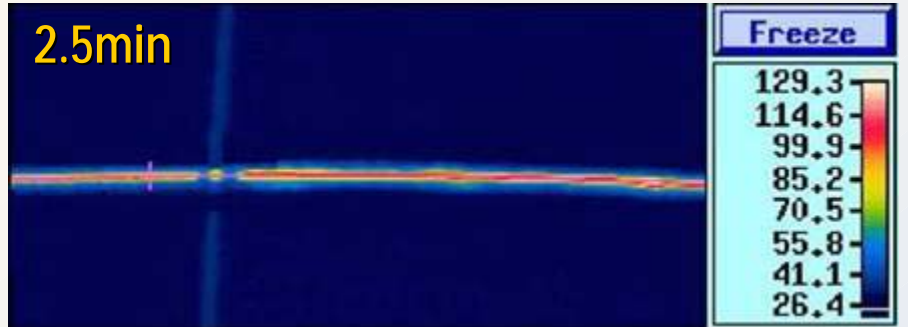
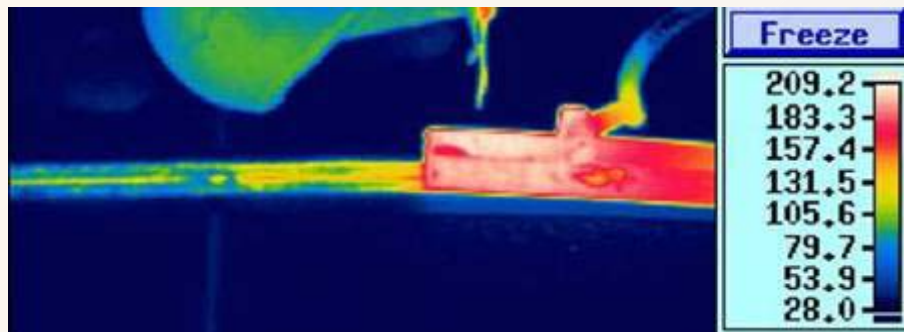


Concrete Joints (2)



Construction of Joints

COE Intensive Course, Hokkaido Univ. 16. Feb '05



Long-Term Prop. (Joint F4)

S. Hean

FM4. 1 Year



FM4. after 2.5 Years



FM4. after 2.5 Years

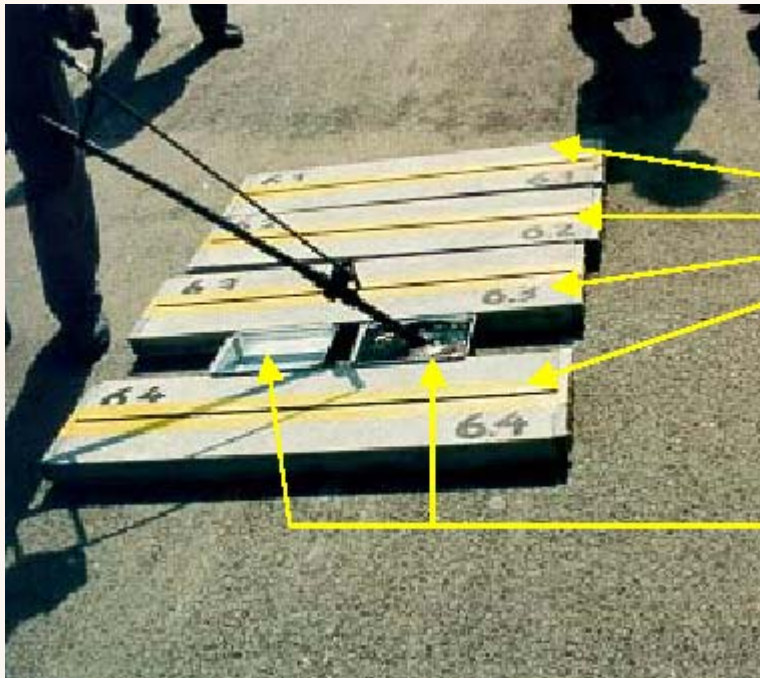


FM4. after 5 Years.

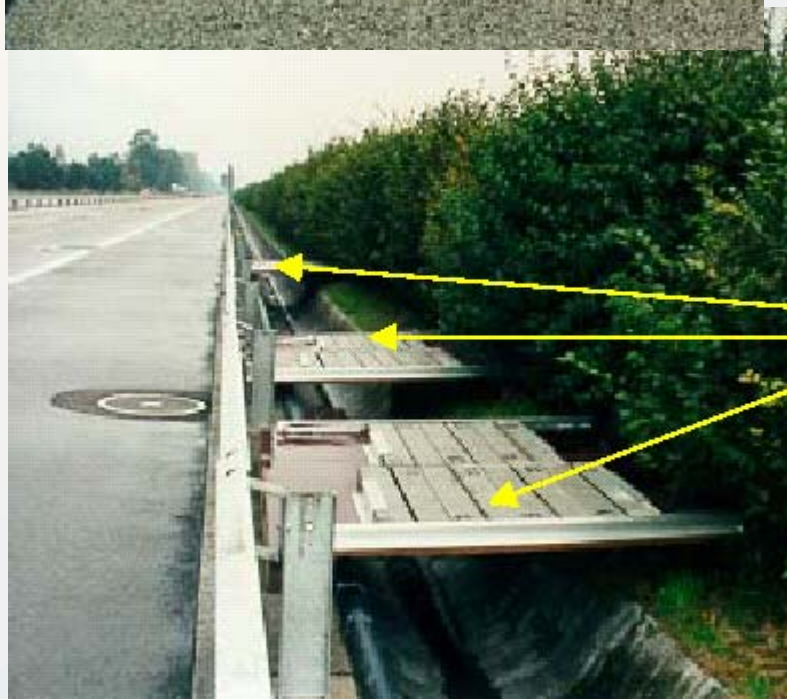


In-Situ Testing

Model Specimens



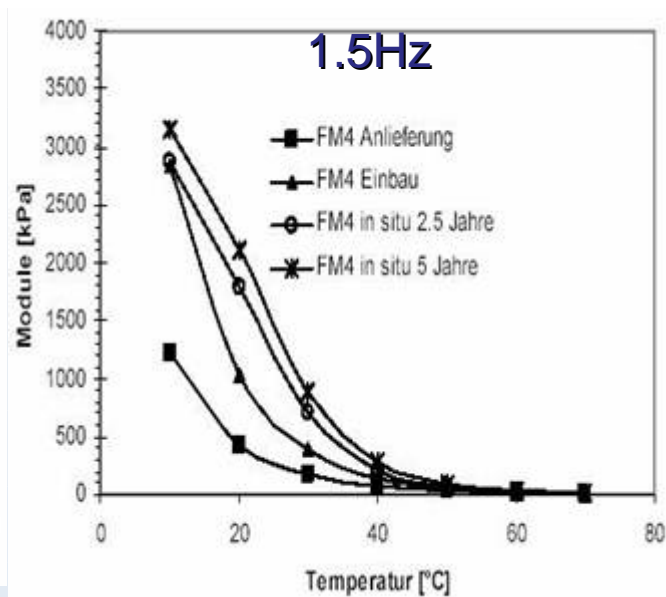
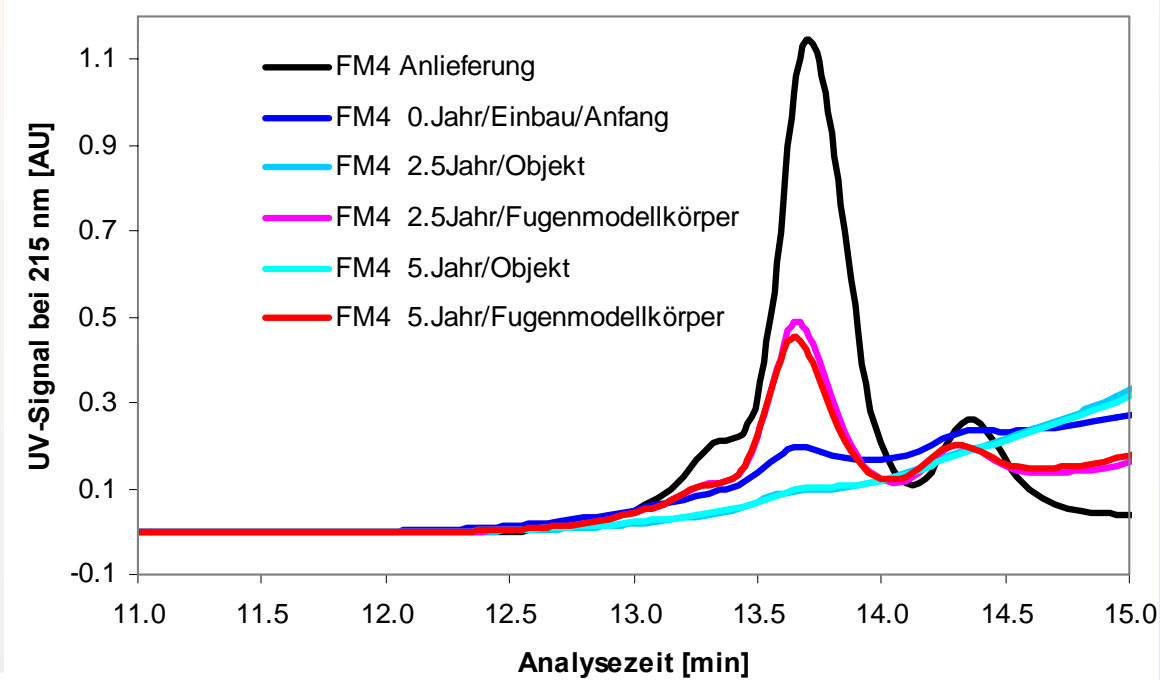
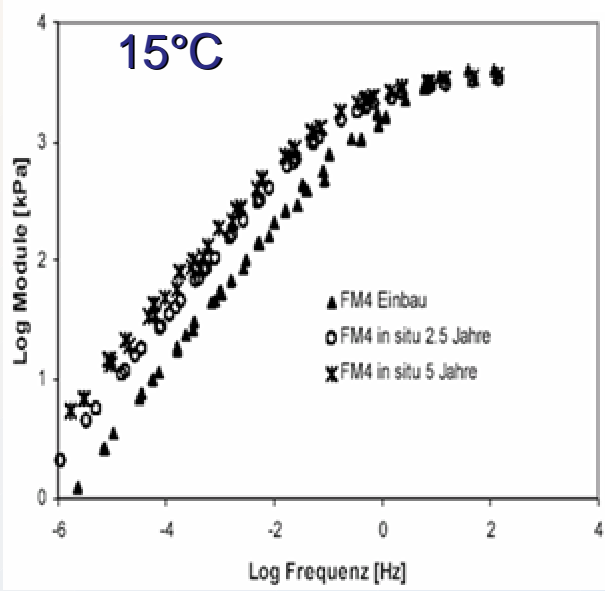
Lab Sampling



Installation of
Model Specimens

Long-Term Prop. (Joint F4)

S. Hean



Long-Term Prop. (Joint F6)

S. Hean

FM6. after 1 Year



FM6. after 2.5 Years



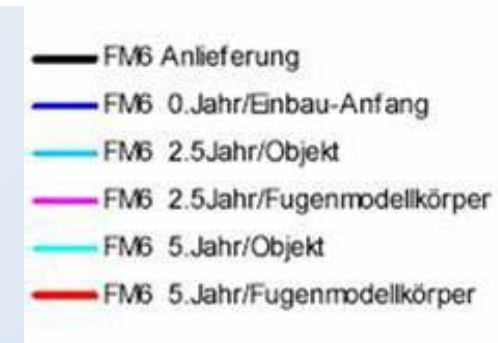
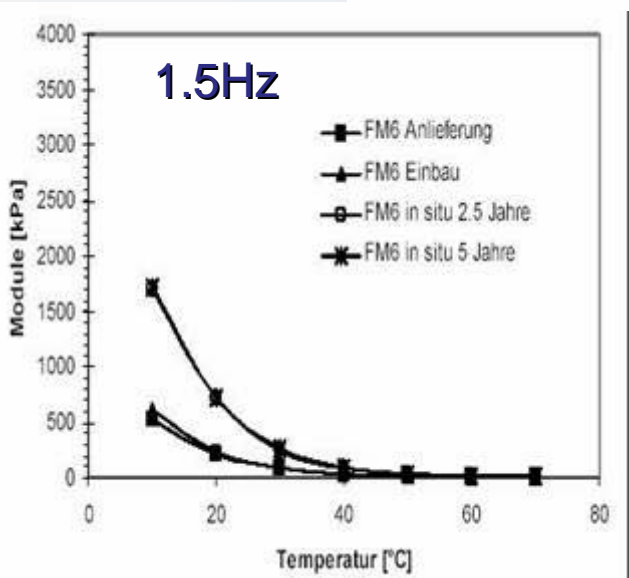
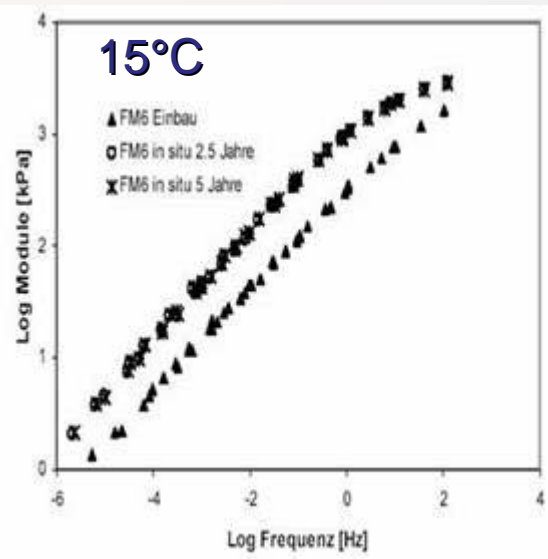
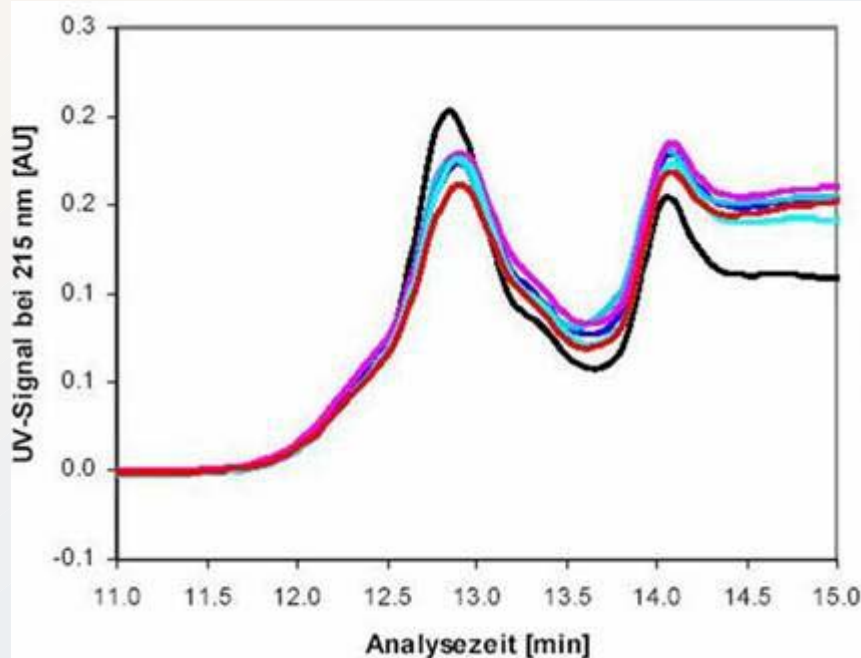
FM6. after 5 Years



Long-Term Prop. (Joint F4)

S. Hean

COE Intensive Course, Hokkaido Univ. 16. Feb '05



Thank You

